NASA CR — 152117

DEVELOPMENT, FABRICATION
AND TEST
OF A HIGH PURITY
SILICA HEAT SHIELD

By E. L. Rusert, D. N. Drennan and M. S. Biggs

Prepared by
MCDONNELL DOUGLAS ASTRONAUTICS COMPANY-ST. LOUIS
St. Louis, Missouri

for Ames Research Center
Moffett Field, California 94035

1 Report No CR-152117	2 Government Accession No	3 Recipient's Catalog No
4 Title and Subtitle DEVELOPMENT, FABRICATION AND TEST OF A HIGH PURITY SILICA HEAT SHIELD		5 Report Date APRIL 1978
		6. Performing Organization Code
7 Author(s) E.L. RUSERT, D.N. DRENNAN, AND M.S. BIGGS		8. Performing Organization Report No.
9. Performing Organization Name and Address MCDONNELL DOUGLAS ASTRONAUTICS COMPANY-ST. LOUIS P.O. BOX 516 ST. LOUIS, MISSOURI 63166		10. Work Unit No.
		11. Contract or Grant No. NAS 2-8895
12 Sponsoring Agency Name and Address NATIONAL AERONAUTICS AND SPACE ADMINISTRATION AMES RESEARCH CENTER MOFFETT FIELD, CALIFORNIA 94035		13 Type of Report and Period Covered CONTRACTOR REPORT
		14. Sponsoring Agency Code

15 Supplementary Notes

MR. J.C. BLOME - PROGRAM MANAGER FOR THIS CONTRACT RESIGNED HIS POSITION WITH MDAC-ST. LOUIS PRIOR TO THIS FINAL REPORT

16. Abstract

A highly reflective hyperpure (<25 ppm ion impurities) slip cast fused silica heat shield material previously developed and reported in NASA CR 137617 for planetary entry probes was successfully scaled up. Process development activities for slip casting large parts included green strength improvements, casting slip preparation, aggregate casting, strength, reflectance and subscale fabrication. Successful fabrication of a one-half scale Saturn probe (shape and size) heat shield was accomplished while maintaining the silica high purity and reflectance through the scale-up process. However, stress analysis of this original aggregate slip cast material indicated a small margin of safety (M.S. = +4%) using a factor of safety of 1.25. Therefore, the program was redirected to evaluate an alternate hyperpure material formulation to increase the strength and toughness for a greater safety margin. The alternate material incorporates short hyperpure silica fibers into the casting slip. The best formulation evaluated to date has a 50% by weight fiber addition resulting in an 80% increase in flexural strength and a 170% increase in toughness over the original aggregate slip cast materials with comparable reflectance. Further efforts toward evaluation of fabrication processing and material characterization is recommended for a 3D woven silica material since it offers even higher strength and toughness properties than that of the hyperpure silica grain/fiber reinforcements.

17. Key Words (Suggested by Author(s)) SILICA REFLECTIVE HEAT SHIELD ENTRY TECHNOLOGY JUPITER ENTRY PROBE PROJECT GALILEO	18 Distribution Statement

19. Security Classif. (of this report) UNCLASSIFIED	20. Security Classif. (of this page) UNCLASSIFIED	21. No. of Pages 108	22. Price*

77N 20255

CAT. 27

FOREWORD

TABLE OF CONTENTS

LIST OF FIGURES

LIST OF FIGURES (CONTINUED)

SYMBOLS

SAAS	Structural Analysis of Axisymmetric Solids (Computer Program)
SUAEP	Saturn/Uranus Atmospheric Entry Probe
ARC	Ames Research Center
IRAD	Independent Research and Development
cm	Centimeter
cc	Cubic Centimeters
MM	Millimeters
g or gm	Grams
Pa	Pascal - unit of stress or pressure quivalent to one Newton (force) per square meter (area)
kPa	Kilo-Pascals (10^3 Pascals)
MPa	Mega-Pascals (10^6 Pascals)
GPa	Giga-Pascals (10^9 Pascals)
µm	Micrometer
M	Meter
ppm	Parts per Million
°F	Degree Fahrenheit
°C	Degree Celsius
°K	Degree Kelvin
pH	Hydrogen Ion Activity in gram equivalents per liter
NH_4OH	Ammonium Hydroxide
HCl	Hydrochloric Acid
PCF	Pounds per Cubic Foot
AHS-1/2-2	Aggregate Cast Heat Shield - One-half Scale - Number Two
ASC	Aggregate Slip Cast
sc	Slip Cast
T	Toughness - area under the stress-strain curve
AR	Aspect Ratio
σ	Actual Stress (MPa)
E_c	Compression Elastic Modulus (GPa)
E_F	Flexural Elastic Modulus (GPa)
E_T	Tension Elastic Modulus (GPa)
F_{CU}	Ultimate Allowable Compression Strength (MPa)

F_{FU}	Ultimate Allowable Flexural Strength (MPa)
F_{SU}	Ultimate Allowable Shear Strength (MPa)
F_{TU}	Ultimate Allowable Tension Strength (MPa).
G	Modulus of Rigidity (GPa)
SEM	Scanning Electron Microscope
PSI	Pounds Force Per Square Inch
KSI	Kips (1000 pounds) Per Square Inch
MSI	Million Pounds Per Square Inch
MDAC-St. Louis	McDonnell Douglas Astronautics Company - St. Louis

1.0 INTRODUCTION

A probe entering the atmosphere of the outer planets such as Jupiter and Saturn will require heat shielding capable of withstanding convective and radiative heating environments considerably more severe than during an Earth entry. The success of an outer planet's probe mission is also highly dependent on the structural integrity of the forebody heat shield. The radiative heating arises from the bow shock wave accompanying the probe during entry. The high entry velocity of probes into the atmosphere of the outer planets produces extremely high temperatures as heating mode shifts from entirely convective to predominantly radiative. The heat shield must protect the payload and primary structure from these excessive high temperatures while remaining attached to the substructure during aerodynamic heating and peak deceleration phases of the mission. This is required to preclude center of gravity shifts that could cause possible perturbations to the probe's aerodynamic stability. For a Jupiter entry probe, as much as 30 to 50 percent of the probe's weight is the heat shield if conventional ablative heat shield material such as carbon phenolic is used.

A program to develop a reflective heat shield as an alternate to the carbon phenolic type heat shield was initiated at Ames Research Center in 1971 (Reference 1). The dissipation of the extreme heat fluxes during a Jupiter entry, primarily by reflection and by sublimation of an inorganic material (i.e., high purity silica) is desirable because:

1) These forms of heat dissipation remove uncertainties and assumptions made for resin matrix types of ablative materials, and,

2) The largest portion of the heat flux is radiative and is more efficiently dissipated by a reflective material.

During a recent program conducted at McDonnell Douglas Astronautics Company - St. Louis and funded by NASA-ARC (Contract 2-7897) silica materials of various forms were evaluated as well as various processing methods for fabricating the heat shield (Reference 2). Silica was selected as a promising candidate material because it has a high reflectance to incident radiation, is a good ablator, has excellent resistance to thermal stress and is readily available in various forms for heat shield construction. During this program, purity and morphology were identified as key properties affecting the reflectance of the silica material. Purity was shown to be a particularly important variable in the ultra violet wavelength region which is most critical for a Jupiter entry. The most reflective silica material evaluated was high purity slip cast grains. A process was developed for slip casting synthetic high purity fused silica. The impurity level of this hyperpure slip cast material was estimated at < 25 ppm (of metallic ions), while the best commercially pure slip cast fused silica has an impurity level of $\sim$ 3700 ppm. Subsequently additional NASA-ARC funding was provided to further characterize the hyperpure slip cast material from the standpoint of high temperature reflectance and high temperature mechanical properties (Reference 3).

The goal of this program was to scale-up the technology for slip casting hyperpure fused silica for a full-scale 88.9 cm dia. (35" dia) Jupiter Probe heat

shield. Early in the program, the material was modified slightly by the addition of coarse aggregate hyperpure silica grains to control drying shrinkage. The addition of the aggregate grains did not reduce the reflective properties of the material.

Scale-up of the aggregate cast material was accomplished by fabricating one-sixth scale and one-half scale (44.5 cm dia X 2.54 cm thick) aggregate cast heat shields. The necessary tooling was completed and hyperpure slip was prepared for casting a full-scale shield. However, analysis of strength data for the aggregate cast material revealed low margin of safety for the then current Jupiter Probe heat shield design. Therefore, the goal of the program was changed to develop a tougher and stronger silica reflective heat shield material. The slip cast hyperpure material was modified by the addition of chopped Suprasil (1 ppm impurities) silica fibers as a reinforcement. A fiber reinforced slip cast material was developed with higher toughness (170% increase) and strength (80% increase) than the aggregate cast material while maintaining its high reflectance.

2.0 PROGRAM SUMMARY

The purpose of this program was to scale-up the hyperpure fused silica slip casting technology developed under Contract NAS 2-7897 (Reference 2), with the ultimate goal being to fabricate a full-scale silica heat shield for the Jupiter Planetary Entry Probe. The plan was to scale-up the heat shield in three phases, fabricating one-sixth scale models, a one-half scale model, followed by a full-scale heat shield. The majority of the development work was conducted in a specially established clean room area shown in Figure 2-1 which was dedicated solely to the processing of hyperpure silica.
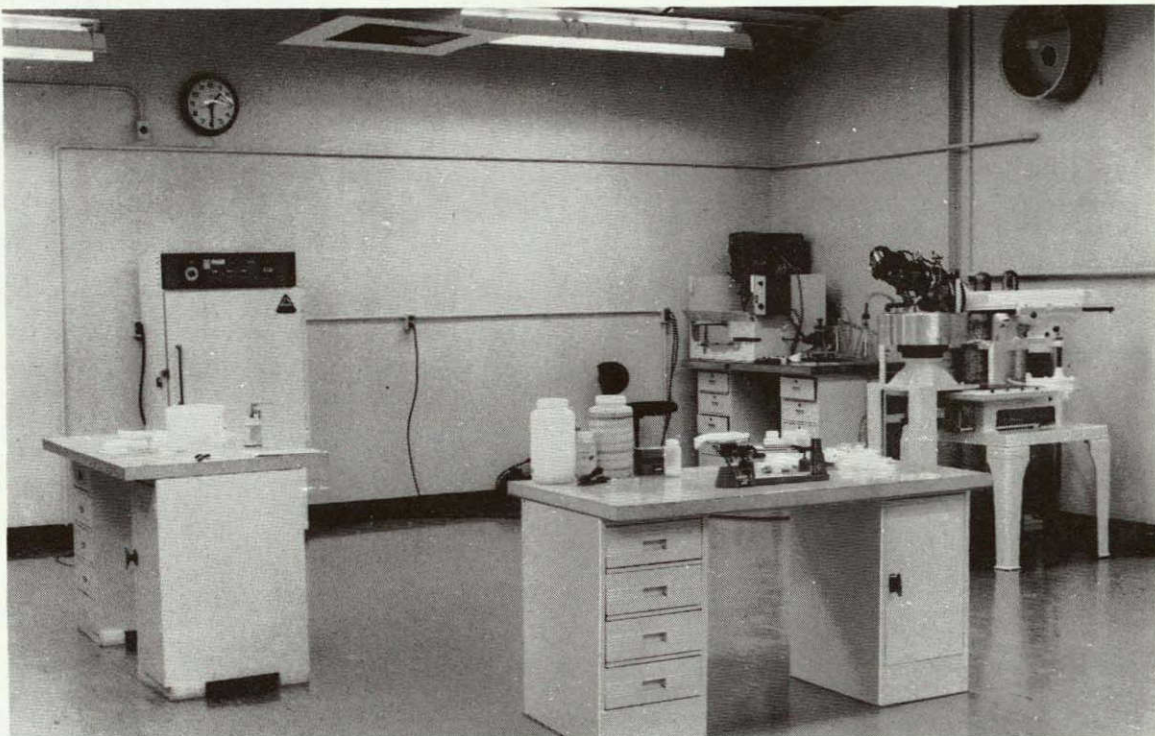
FIGURE 2–1 DEDICATED CLEAN ROOM FOR HYPERPURE SLIP CAST FUSED SILICA

During scale-up, several key improvements were made in the slip cast material. Green strength of hyperpure silica castings was increased over two-fold. This was done primarily by increasing the concentration of very fine particles in the material. The size of the ball milling containers, for hyperpure slip preparation, was increased from 1.8 liters, (1/2 gallon) to 7.6 liters, (2 gallon) and finally, 19 liters (5 gallon). Larger milling containers increased milling efficiency and rheological properties of the milled slip. Slips milled in the larger containers were thixotropic, having a high apparent viscosity for low shear levels. Therefore, grain settling in the slip during casting was reduced. Subsequently, it was learned that the rheology was interrelated with the purity, pH level, and particle size of the slip, and that the rheology could be shifted from dilatant to thixotropic and vice versa by changing the pH level of the slip.

3

Mr. Joe N. Harris, (technical consultant) of the Georgia Institute of Technology, suggested that in order to fabricate a 2-3 inch thick full-scale heat shield coarse aggregate particles were necessary to reduce drying shrinkage. Various size and amounts of hyperpure aggregate particles were added to the 10 μm slip. It was determined that 15% aggregate particles (-40 mesh) reduced the drying shrinkage of the material nearly 50% and did not lower the radiative properties. The aggregate material also had the benefit of a lower firing shrinkage and faster casting rate.

During the first phase one-sixth scale model heat shields were rotational drain casted and were largely unsuccessful due to problems with pumping the slip into the rotating mold. Improvements were made to include developing a thixotropic slip, aggregate casting development, and the elimination of a rotating mold. These shields were used to gain information about the effect of slip rheology on the castings, the use of vibration during casting, and the drying and firing shrinkage problems involved with heat shield configurations.

Three attempts were made at casting a one-half scale heat shield, the first two being unsuccessful. The first one-half scale shield was not processed into the drying stage because of problems removing the male mandrel, which caused the part to deform. A modified mandrel design allowed us to successfully cast the second one-half scale shield, using the slip reclaimed from the first shield. This shield was cracked due to rapid drying which resulted in excessive shrinkage gradients. It was, however, taken through the drying and firing stages and valuable processing experience was gained. The third one-half scale heat shield was successfully cast, dried, and fired and is shown in Figure 2-2. Extensive visual and radiographic analysis indicated that this shield is totally crack-free.

FIGURE 2—2 OUTER PLANETS ENTRY PROBE

1/2 Scale
Hyperpure Silica
Heat Shield
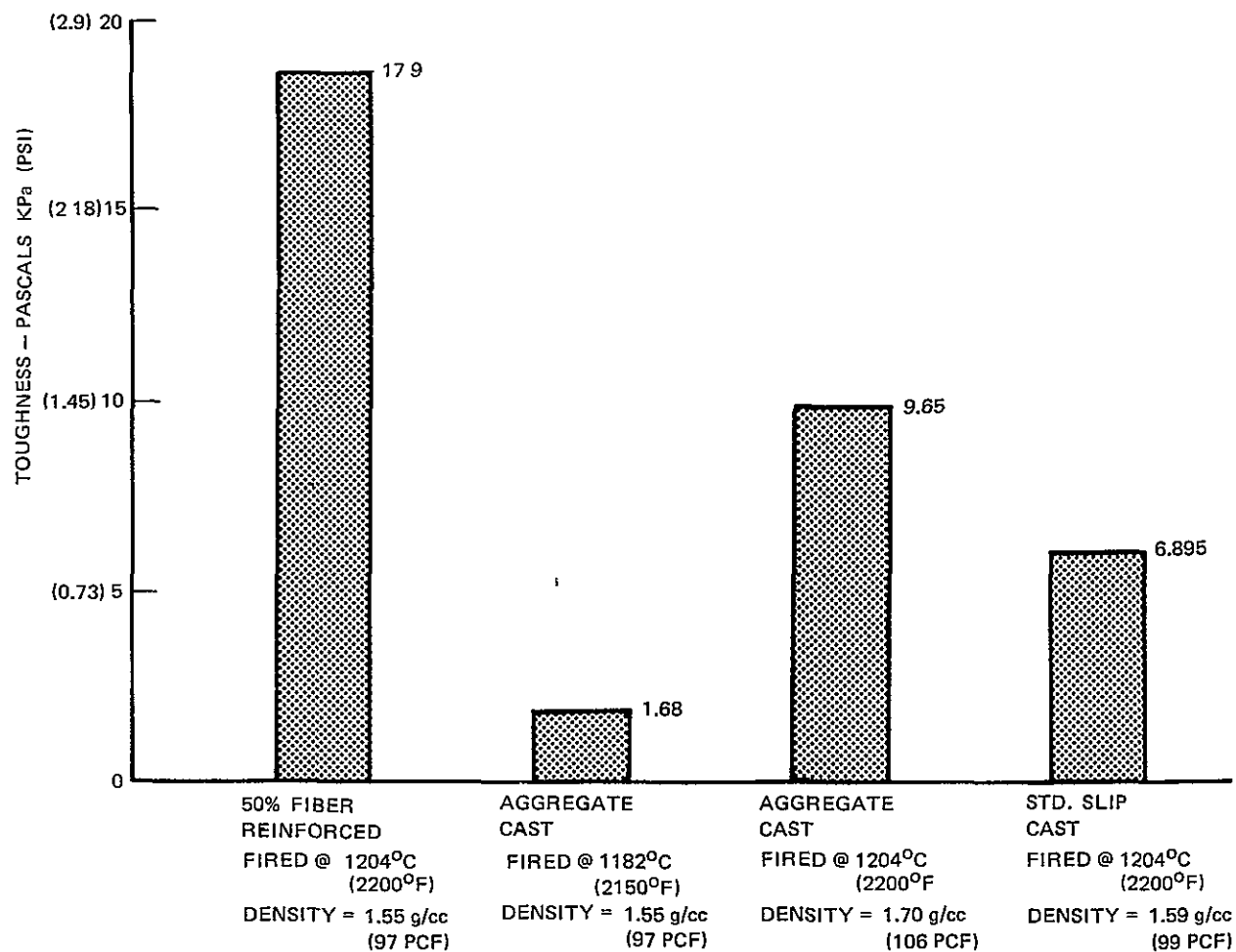
FIGURE 2–3 TOUGHNESS OF HYPERPURE FUSED SILICA SLIP CAST MATERIALS

6

3.0 MATERIAL AND PROCESS DEVELOPMENT PREPARATORY TO SCALE-UP

This section deals with the modifcations made in the hyperpure fused silica slip casting techniques for the first phases of the scale-up operation. The unfired strength of the earlier slip cast materials was improved, by two-fold, by increasing the amount of very fine particles in the material. Also, it was necessary to scale-up the size of the ball mills for slip preparation. Larger size milling containers yielded a larger percentage of fine particles. This helped the green strength improvement and also resulted in improved rheological properties of the slip. The thixotropic rheology of the improved slip produced more uniform castings as grain settling was reduced. Use of the aggregate particles in the casting slip reduced the drying shrinkage thus making it possible for fabrication of a thick full-scale shield.

3.1 BALL MILL SCALE-UP

In order to produce enough slip for half-scale and full-scale heat shield fabrication, scale-up from 1.9 liter (½ gallon) ball mill containers to 7.6 liters (2 gallons) and subsequently 19 liters (5 gallons) polypropylene containers was necessary.

The milling speed for each container was 70% of critical speed as given by

$$W = \frac{54.19}{\sqrt{R}}.$$

where W = critical speed (rpm)

R = radius of milling container (feet)

A 65% solids content was used for each size container and the silica charge was -40 mesh. A summary of the pertinent data for each size ball milling container is given in Figure 3.1-1.

MILLING JAR SIZE (LITERS)	DIA. OF GRINDING MEDIA (CM)	SIZE OF -40 SILICA CHARGE (Kg)	MILLING SPEED (RPM)	MILLING TIME (HRS)	SLIP BATCH	AS MILLED pH	pH AFTER AGING
1.9 (1 GAL)	1.9	.95	90	100	8	3.8	3.2
7.6 (2 GAL)	2.54	4.08	62	89	9	3.8	3.4
19.0 (5 GAL)	2.54	9.70	57	85	10	4.0	3.6

FIGURE 3.1—1 BALL MILL SIZE VERSUS MILLING TIME

A problem was encountered with the use of larger size mills as a large amount of organic contaminates were introduced into the slip. About 0.2% of the solid weight was plastic material removed from the milling container for slips milled in 1.9 liter jars, while the contaminates from 7.6 liter and 19 liter batches was measured at 0.9% and 0.6%, respectively.

The organic material introduced during milling does not affect the purity level of the fired silica product because the polypropylene burns away totally during firing. When present in large quantities, however, it caused nonuniformities during slip casting and in the fired product. A simple procedure for removing a large amount of the organic solids (plastic ball mill liner material) was initiated which required skimming off the top of the liquid phase of the slip (inorganic solids float on the surface) after silica solids are allowed to settle out. The small amount of silica (0.2%) which is entrapped and removed along with the plastic, does not alter the slip properties.

The milling times shown in Figure 3.1-1 are the hours required to achieve an average particle size of 10 μm. In the case of the 19 liter jars, a 65-hour milling time was required for the first batch. With each subsequent milling batch a slightly longer time was required to achieve the 10 μm average size. After 5 milling runs a time of 85 hours was required. It was concluded that the grinding media was eroding at a significant rate. The SiO_2 grinding material was therefore weighed before and after selected milling runs. A weight loss of about 2% for each run was noted in the grinding media. This is equivalent to a reduction in diameter of 0.7%. Therefore, additional fresh grinding material is added before each run so that the mass of grinding media is consistent (∿ 10.1 Kg). A constant milling time of 85 hours was established to achieve the proper particle size distribution for the 19 liter ball milling container.

A typical particle size distribution curve for slip prepared in each size milling container is shown in Figure 3.1-2. Although, it is not evident from
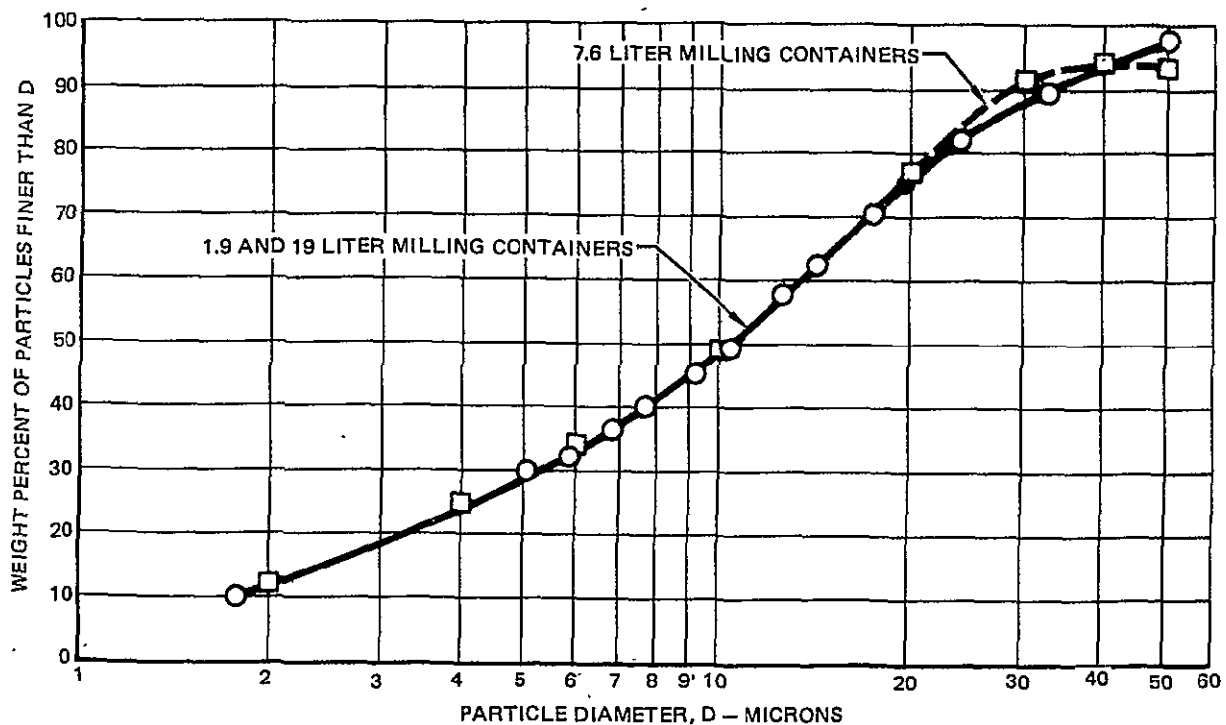
FIGURE 3.1—2 PARTICLE SIZE DISTRIBUTION OF HYPERPURE FUSED SILICA SLIPS

8

these curves, the larger milling containers produce slip with a higher concentration of very fine particles. This results in slip with thixotropic properties which offer certain processing advantages and will be described in Section 3.4.

Quality control specimens were cast routinely from slips milled in 7.6 and 19 liter milling container. These specimens verified that the physical and optical properties of these slips were comparable to the material as developed by milling in 1.9 liter container.

3.2 GREEN STRENGTH IMPROVEMENT

A necessary part of the effort to scale-up the slip casting of hyperpure fused silica for large parts was to improve the unfired or "green" strength of the material. Handling strength of the green material was marginal and was known to be less than that of castings made with commercial silica casting slips of lower purity. Green strength was evaluated quantitatively by measuring the compressive strength of the unfired material.

The age of the casting slip was one key factor identified that effects green strength. The effect of slip aging on green strength is shown in Figure 3.2-1 for two different mill batches of slip. The more rapid aging of Slip 11 is believed to be the presence of a greater number of very fine particles (2 μm) than that present in Slip 10. After ball milling, the solid content of Batch 10 was raised from 65% to 78% by decanting liquid which contained some fines, thereby reducing the quantity of fines. The solid content of Slip 11 was raised by evaporating the required amount of liquid, thereby retaining all the fines.

The pH was known to be a key property effecting slip rheology and will be discussed in Section 3.4. Changes in pH noted with aging of slip batches have been observed as follows:

Slip Batch	As Milled pH	pH after aging
8	3.8	3.2
9	3.8	3.4
10	4.0	3.6

As noted the presence and quantity of very fine particles effects the aging time of hyperpure silica slips. The quantity of very fine particles also has a great effect on the green strength after aging, the finer particles (larger surface area) acts as a binder to improve the strength. Figure 3.2-2 shows a photograph taken with a scanning electron microscope (SEM) of a casting which had low green strength compared to a casting in which the quantity of fines was intentionally increased thereby increasing green strength from 5.52 MPa to 15.17 MPa.
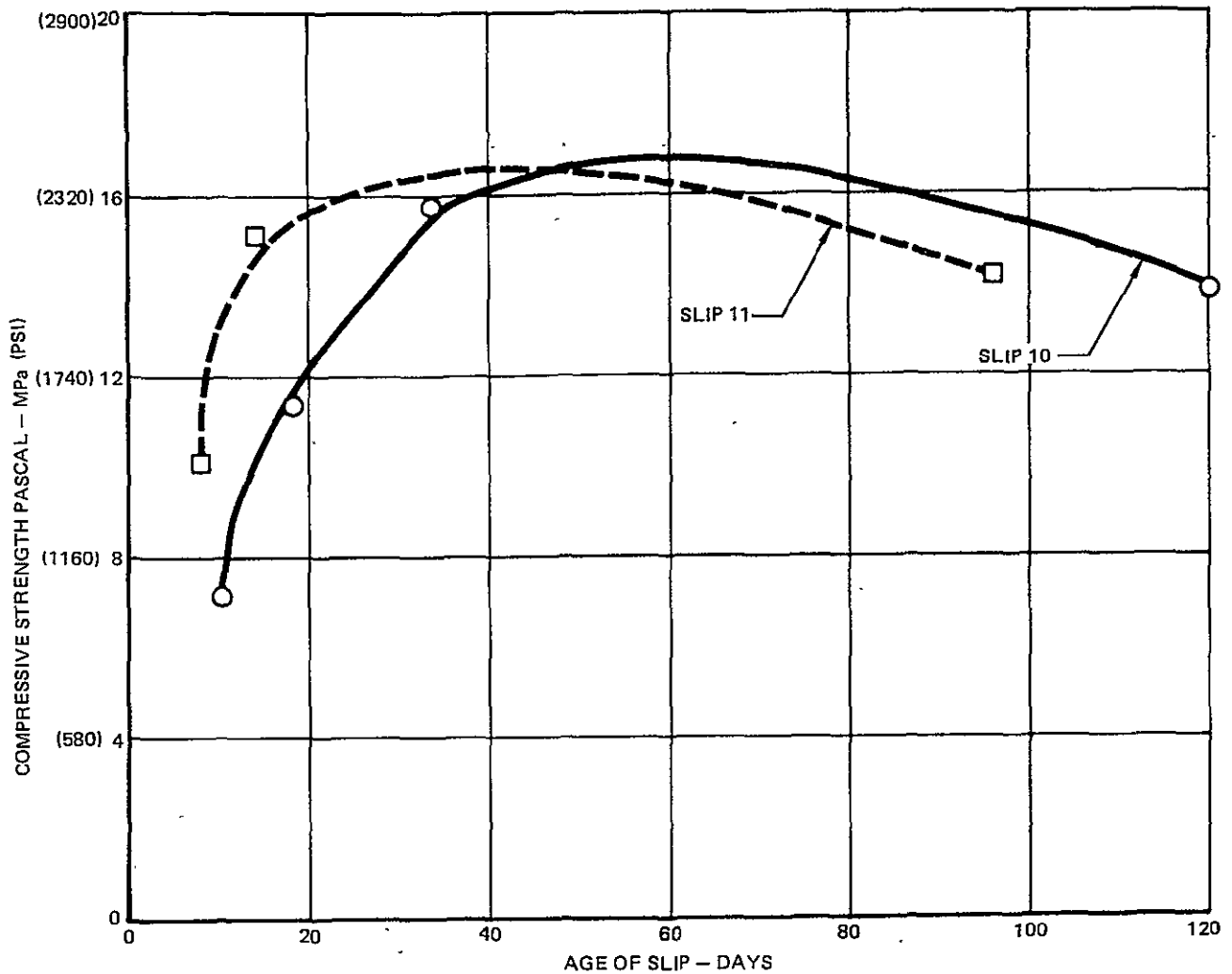
FIGURE 3.2—1 EFFECT OF SLIP AGING ON CASTING GREEN STRENGTH

The large difference in the concentration of fine particles is shown in Figure 3.2-2. The particle size distribution curves for the batches of slip used to make these two castings are very similar, both batches of slip having an average (by weight) particle size of 10 μm. Therefore, the SEM was established as a particle size quality control and characterization tool, as well as use of Stokes Law (ASTMDH422), to generate particle size distribution curves for each batch of slip prepared.

The difference in the quantity of very fine particles as shown in Figure 3.2-2 was achieved primarily by changing the particle size distribution of the mill charge. . Batches with low green strength were made with powder prepared by a manual crushing technique. Mill batch charges of -40 mesh powder, which had higher concentration of fines and therefore better green strengths, were made by a crushing apparatus developed specifically for crushing silica without intro-ducing metallic impurities. The crushing apparatus utilizes organic materials

10
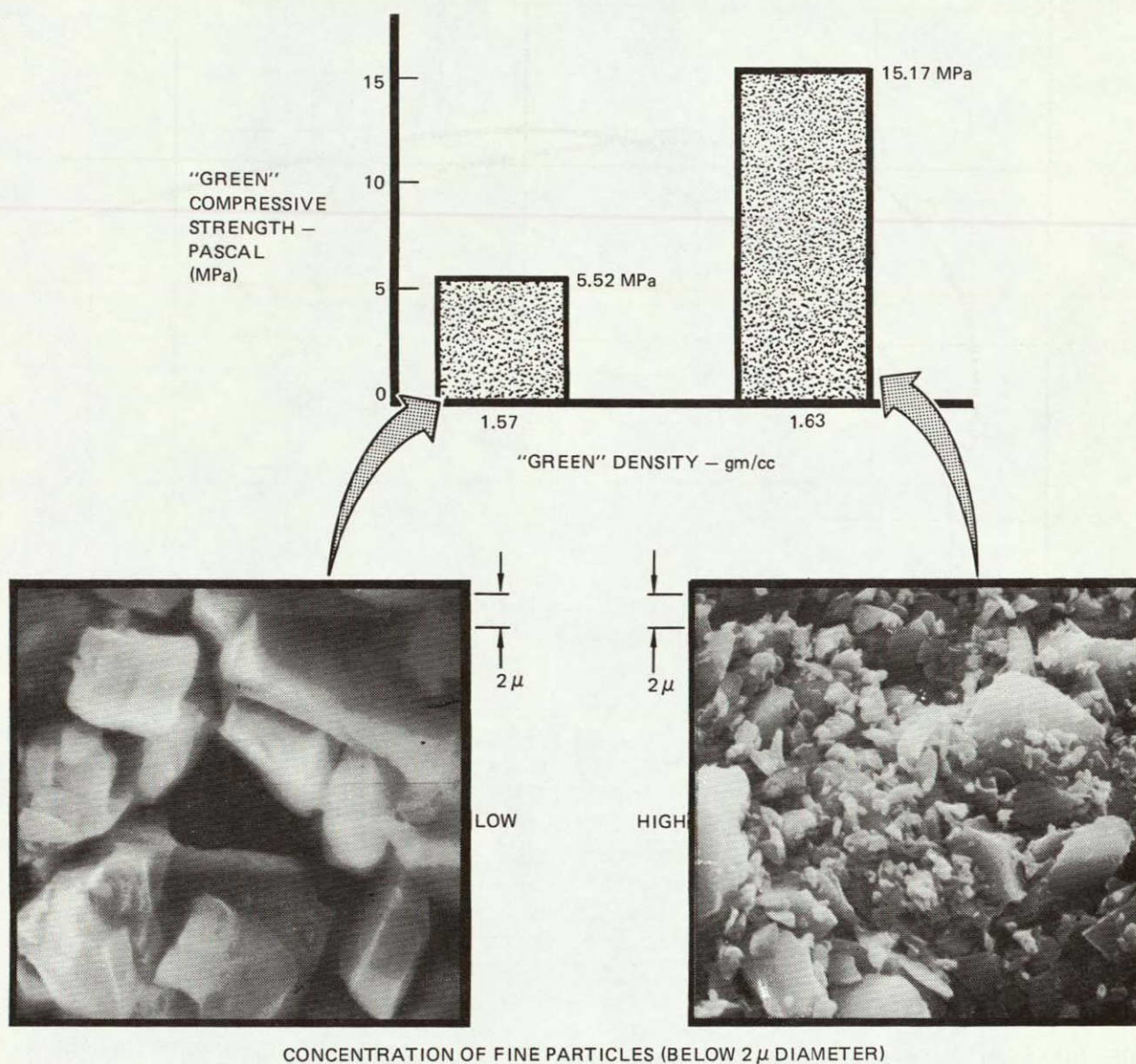
FIGURE 3.2—2 STRENGTH IMPROVEMENT IN DRY, SLIP CAST,
HYPERPURE FUSED SILICA

which may be subsequently removed by heat cleaning. The particle size distri-
bution of mill charges prepared manually and with the crushing apparatus are
shown in Figure 3.2-3. The distribution of the -40 material prepared in the
crusher can be controlled by altering the number of cycles and the crushing
pressure.

11

WEIGHT PERCENT OF PARTICLES FINER THAN D

60

40

MANUALLY
PREPARED

PREPARED IN
CRUSHING FIXTURE

20

0

10   20   40   60   80   100

PARTICLE DIAMETER, D — MICRONS
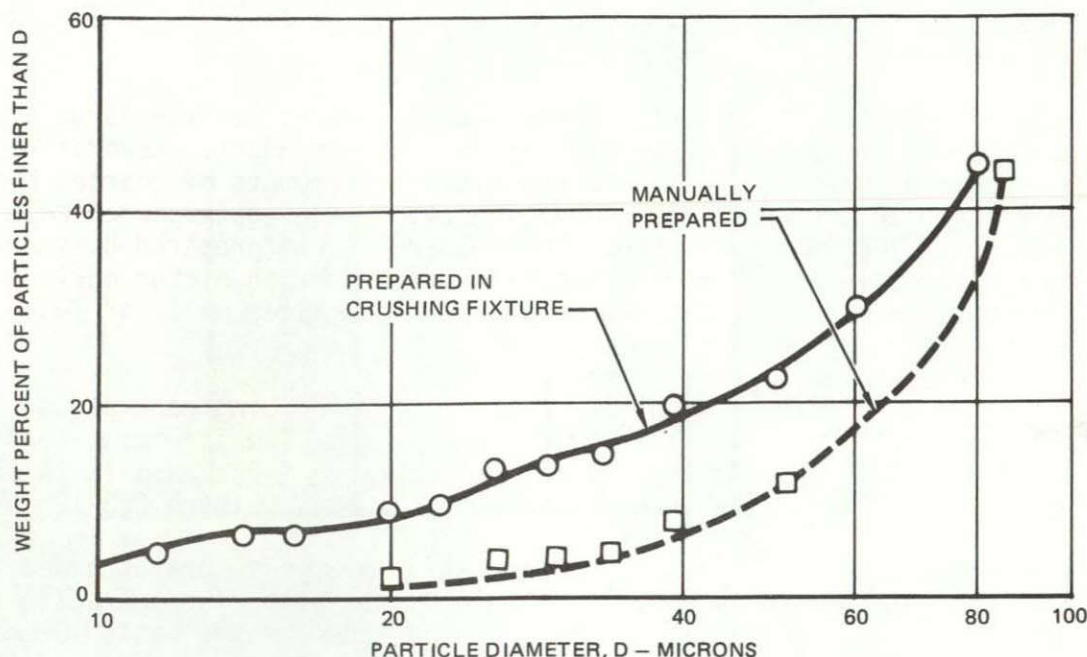
**FIGURE 3.2–3 PARTICLE SIZE DISTRIBUTION OF –40 MESH HYPERPURE
SILICA BALL MILL CHARGE**

3.3 AGGREGATE CASTING DEVELOPMENT

MDAC has been successful in developing a hyperpure slip cast fused silica mater-
ial which is highly reflective (Reference 2). Slip casting of this material,
at the beginning of this program, was limited to simple and small shapes. To
minimize scale-up problems associated with slip casting large parts (similar
to the Jupiter heat shield), a technical consultant, Mr. Joe N. Harris of the
Georgia Institute of Technology, was employed. For a number of years, the
Georgia Institute of Technology has been doing work which involves the slip
casting of large shapes (primarily missile radome shapes) using a less pure
grade of fused silica slip.

Mr. Harris was advised that the goal of the scale-up program was to cast a full-
scale Saturn Probe heat shield which could be 5 to 7.6 cm thick. He was very
apprehensive about slip casting a part with the wall thickness required because
it would be difficult to dry a full-scale heat shield without shrinkage cracks.
The problem of shrinkage cracks is discussed in Reference 1 and will also be
discussed in Section 4.0.

Because of the severe drying shrinkage problem, Mr. Harris advised that the
feasibility of aggregate slip casting be investigated. Aggregate casting is
a variation of slip casting wherein (-20 mesh to -100 mesh) silica grains are
added to normally processed fused silica slip, forming a very viscous fluid
or slip. The aggregate slip is cast in a porous plaster mold in a manner simi-
lar to normal slip casting. Vibration of the mold is employed to ensure proper
filling of the mold and to remove entrapped air.

12

The advantages of aggregate casting are lower drying shrinkage, lower firing shrinkage, and more rapid casting rate.

A major concern regarding aggregate casting was the effect of the large aggregate particles on the optical properties of the final product. Accordingly, a series of specimens were made with various sizes and amounts of coarse, hyperpure powder added to the normal 10 μm casting slip. Aggregate powder mesh sizes of -40, -60, and -100 were evaluated. These powders were prepared by screening with nonmetallic screens to minimize metallic contamination pickup during processing. The amount of aggregate powder added varied between 11 and 18.5% (based on the weight of 10 μm slip used).

A total of eight specimens were made in this study, including control specimens made by conventional 10 μm particle size slip casting. The specimens were cast, dried, fired at 1230°C and checked for reflectance with a Beckmann DC 2A spectroreflectometer. The results of this study are shown in Figure 3.3-1.

As shown in Figure 3.3-1, the lower the precentage of coarse grains added (all three sizes) the higher the reflectance (.225 to .350 μm). The aggregate casting formulation with 15% coarse grains (-40 mesh) added to the basic 10 μm hyperpure casting slip was chosen for the heat shield scale-up program. It had the least effect on reflective properties and a lower shirnkage than the formulations with -60 and -100 mesh powders. Also, the -40 mesh powder is the same size material required for the standard ball mill charge and is less expensive to produce than -60 or -100 mesh powders. A reflectance vs wavelength curve for a typical aggregate cast specimen of this formulation is shown in Figure 3.3-2. The reflectance data shown in Figure 3.3-1 indicates that the key factor governing the degradation of optical properties by the coarse powder additions is the surface area of the powder added. A 12% addition of -100 mesh powder reduces the reflectance at all wavelengths while a 15% addition of -40 mesh powder is not detrimental to the reflectance.

SPEC NO.	COARSE POWDER ADDED (SIZE/AMOUNT)	FIRING SHRINKAGE (%)	FIRED DENSITY gm/cc	REFLECTANCE @.225μm	@.250μm	@.275μm	@.300μm	@.350μm
SC-113	NONE	2.4	1.6	89	90.5	96.5	98	98.5
SC-126	NONE	2.5	1.6	87	92.5	97	99	98.5
ASC-1	-40/15%	1.5	1.62	89	92	97	98.5	98.5 SELECTED
ASC-14	-40/18.5%	1.5		80.5	87	93	97	97.5
ASC-7	-60/13/5%	1.8	1.6	91	93	97.5	98.5	98.5
ASC-15	-60/15%	2.0		83	89	94	97	97.5
ASC-5	-100/11%	1.6	1.59	89	90.5	95.5	98	98
ASC-16	-100/12%	2.0	1.59	83	89	94	97	97.5

**FIGURE 3.3—1 REFLECTIVE PROPERTIES OF HYPERPURE SILICA
WITH VARIOUS AGGREGATE GRAINS ADDED**
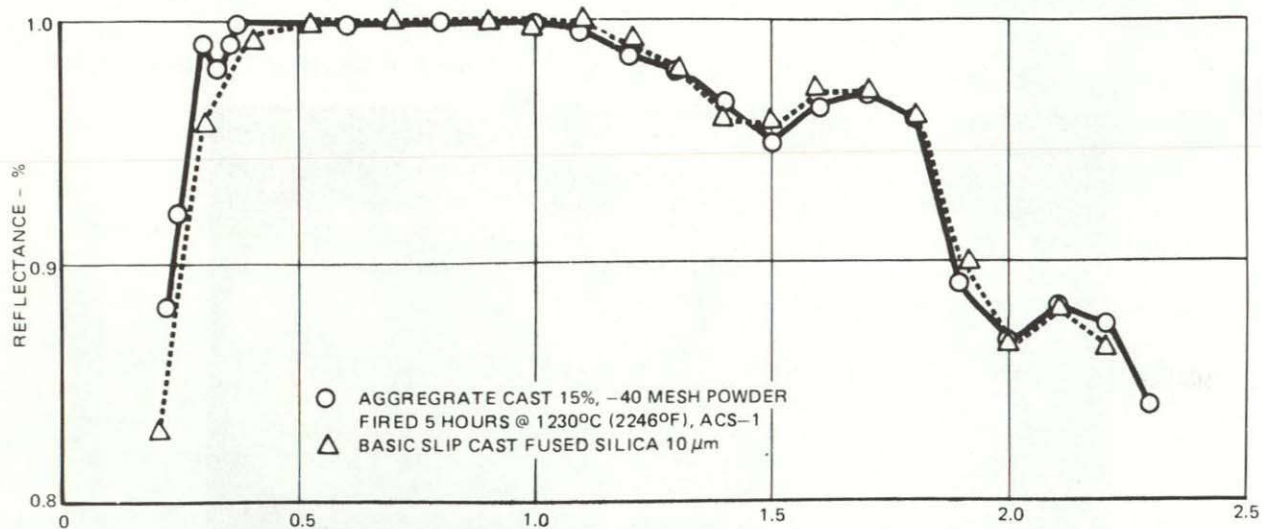
FIGURE 3.3–2 REFLECTANCE VS WAVELENGTH, AGGREGATE CAST VERSUS BASIC SLIP CAST FUSED SILICA

Drying shrinkage for various slip cast silicas are shown in Figure 3.3-3. The drying shrinkage of the commercial material is greater than the hyperpure material because it has a higher concentration of very fine particles and a higher green density, 1.76 gm/cc vs 1.52 gm/cc.
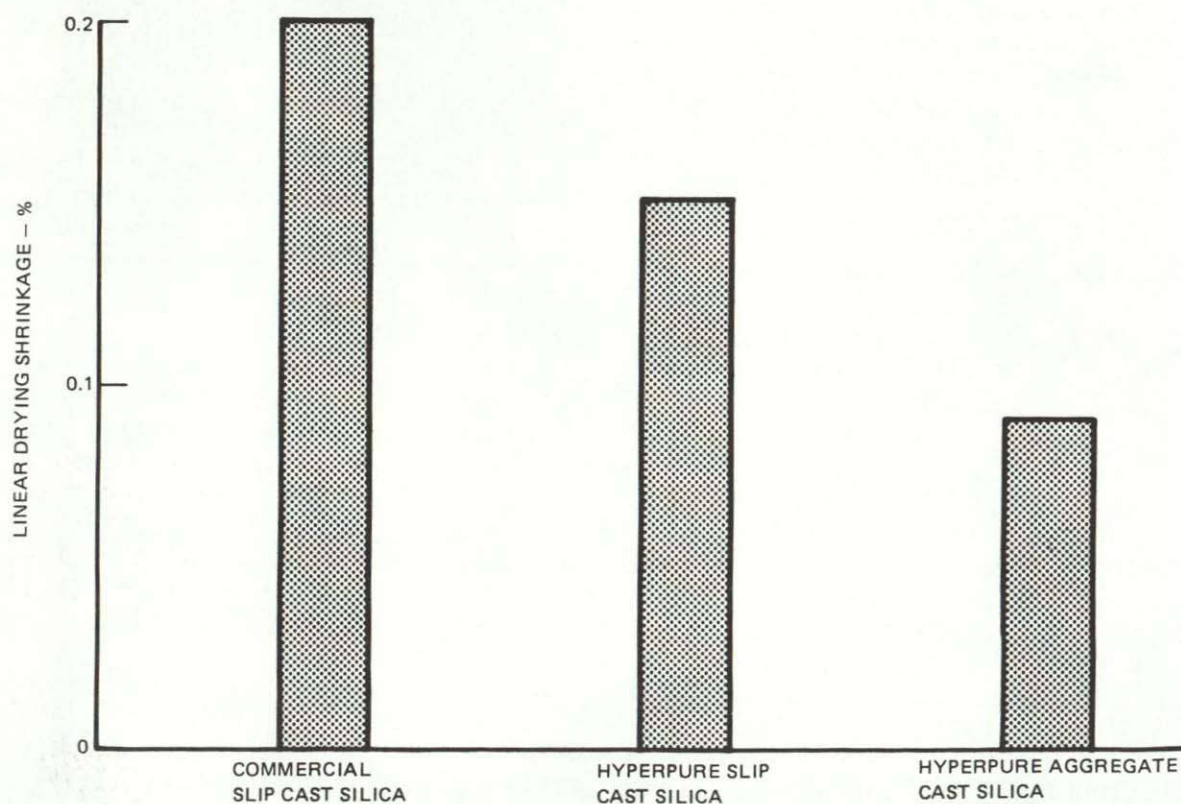
FIGURE 3.3–3 DRYING SHRINKAGE OF VARIOUS SLIP CAST SILICA MATERIALS

The advantage of aggregate casting as compared to the basic slip casting is demonstrated by the photograph shown in Figure 3.3-4. This photograph shows a basic slip cast and an aggregate cast billet of similar size which were sub-
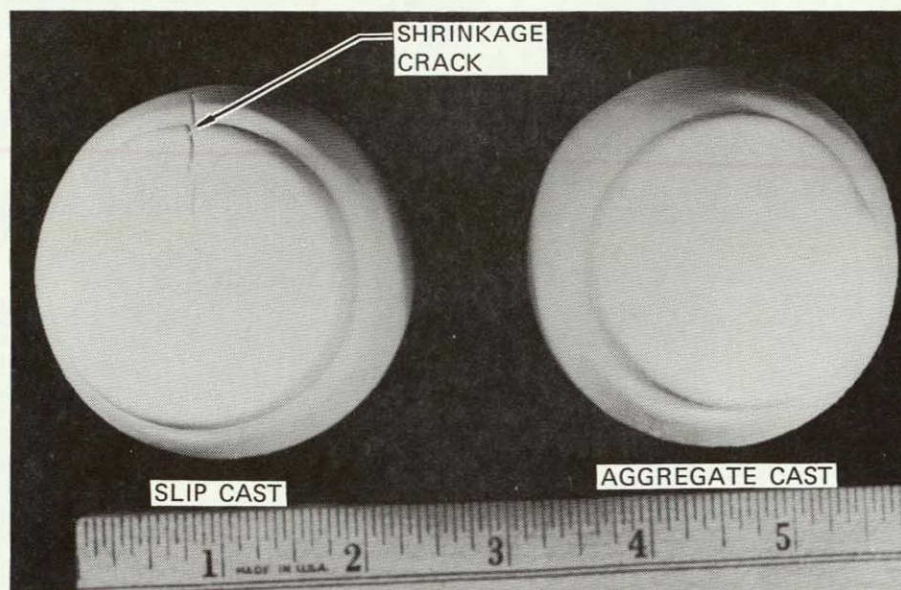
FIGURE 3.3—4 SLIP CAST AND AGGREGATE CAST RAIN EROSION TEST MODELS

jected to identical drying and firing histories. Both specimens shown in Figure 3.3-4 were cast in the form of cylinders 6.1 cm diameter and 7.0 cm thick. Immediately after casting, both specimens were dried in a controlled humidity environment for 13 days to prevent shrinkage cracks. The humidity drying cycle was followed by room temperature and oven drying. Each specimen was sanded to the approximate shape required prior to firing at 1343°C for 5 hours to reduce the subsequent machining time. Two basic slip cast billets were fabricated. Both of these developed large shrinkage cracks, as shown in Figure 3.3-4. A total of 4 aggregate cast billets were made, none of which developed shrinkage cracks.

3.4 THIXOTROPIC SLIP DEVELOPMENT

Among the key properties routinely measured for hyperpure fused silica slip are solids content, particle size distribution, pH and rheology (viscosity). The rheological properties of the slip are determined by taking viscosity measurements with a Brookfield Model LVT rotating spindle viscometer. By using different spindle sizes and spindle rotating speeds, changes in slip viscosity with different shear levels are indicated. The aluminum spindles of the viscometer were coated with Teflon (DuPont Teflon S) to prevent metallic contamination of the slip being tested. It was determined that the Teflon coated spindles did not change the viscometer readings.

Hyperpure slip prepared by milling in 1.9 liter polypropylene containers consistently exhibited dilatant rheological properties at the shear levels measured by the Brookfield viscometer. Dilatancy is the condition of increasing apparent viscosity with increasing shear levels. Batches of slip prepared in 7.6 and 19 liter milling containers were thixotropic. Thixotropy is the condition of

decreasing viscosity at increasing shear levels. Typical viscosity data for the two types of slip are shown in Figure 3.4-1.
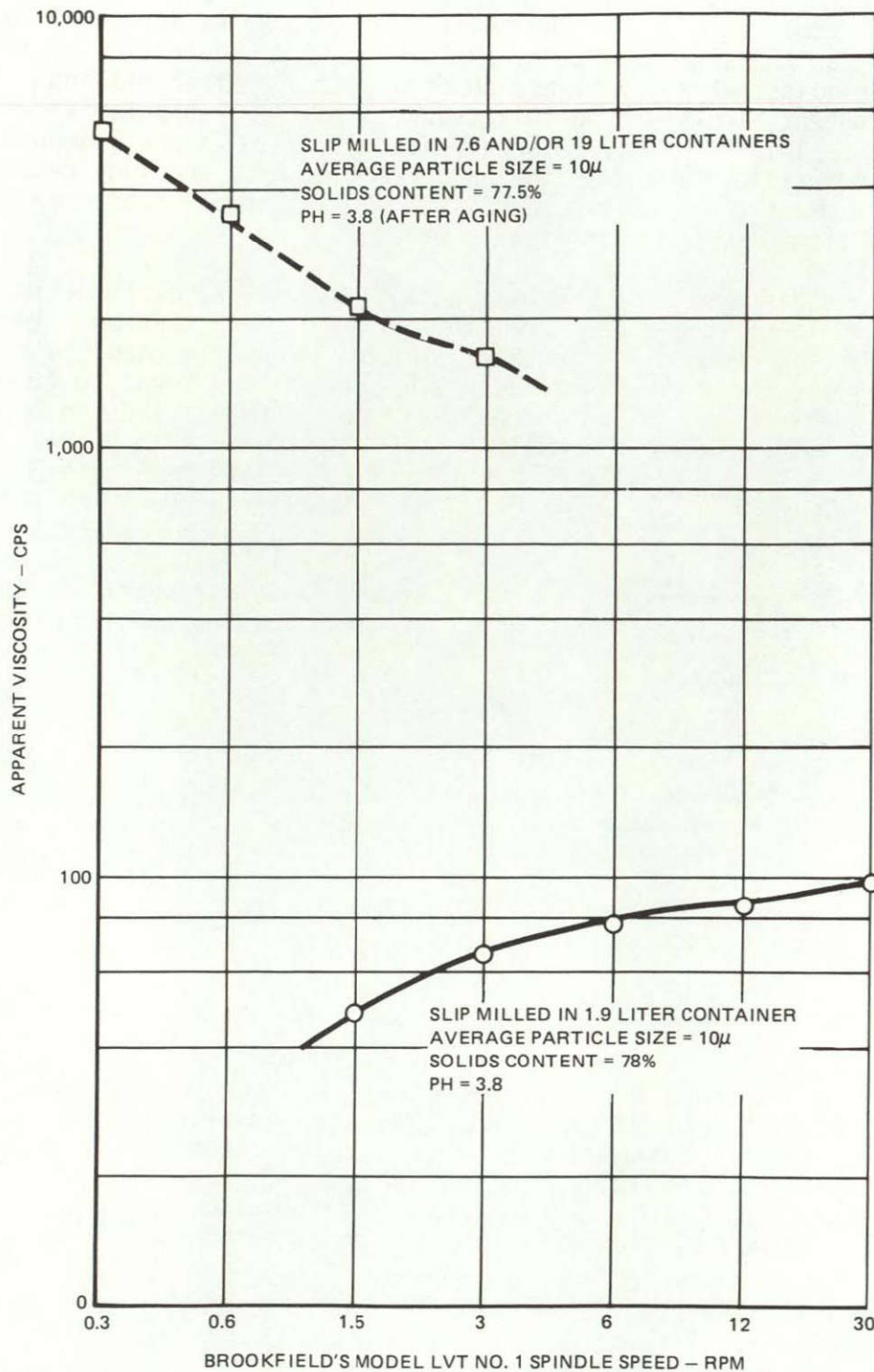
FIGURE 3.4-1 RHEOLOGICAL PROPERTIES OF HYPERPURE FUSED SILICA SLIPS

Immediately after milling and solids content adjustment, the slips milled in the larger size containers have dilatant rheologies similar to those prepared in 1.9 liter containers. The shift to thixotropy is observed after the slips were aged. The time required for the shift to occur varies between 2 to 30 days, depending on the solids content, pH level, and concentration of fine particles. The slips generally have a pH of 3.4 to 3.9 after milling. For a given solids content, the shift to thixotropy generally occurs faster with lower pH values. This shift may be accelerated by adding a small amount of HCl solution to artificially lower the pH. The change in rheology caused by lowering of the pH is shown in Figure 3.4-2. The shift to thixotropy occurs within minutes after the acid addition is made.

The particle size distributions, as measured by ASTM DH242, of the slips milled in 1.9 liter and larger containers are similar. The pH of the as-milled slips are similar, varying between 3.4 and 3.9. The difference in rheology is apparently due to the concentration of very fine particles. When the fines (<2 μm) are a small weight percentage of the total size distribution of particles they are not measured accurately by the Stokes Law (ASTM DH 242) procedure; but they can be detected by SEM photographs as shown in Figure 3.4-3. The additional fine particles result from the use of larger grinding media, 2.54 cm versus 1.9 cm, and from the larger diameter containers. The finer particles, together with the lower pH of the hpyerpure slip, produce the thixotropic properties. The low pH of the milled slip is a result of the high purity maintained during slip processing. As shown in Figure 3.4-3, commercial silica slips have a higher concentration of fines, yet they have a much higher pH and are consequently dilatant. The higher pH of the commercial slip is apparently due to the large amount of aluminum oxide contamination (∿ 2000 ppm) resulting from the high alumina milling jars and grinding media. The rheology of the hyperpure slip may be changed from thixotropic to dilatant by adjusting the pH upward. This effect, which is shown in Figure 4.4-4, is accomplished by the addition of a small amount (drops per gallon) of NH_4OH. For heat shield fabrication, the use of hyperpure slip in its thixotropic form is preferred because of processing advantages which are discussed below.

Although the apparent viscosity of the thixotropic slip, as shown in Figure 3.4-2, is much higher than that of the dilatant slip, it becomes fluid during normal handling, such as pouring from one container to another, indicating a lower viscosity at these shear levels. The thixotropic material does resist very vigorous agitation or stirring, indicating that it becomes dilatant at very high shear levels. The thixotropic nature of the more recently developed slip is important because it offers several processing advantages which are summarized in Figure 3.4-5. The thixotropic slip exhibits extremely slow settling of the silica solids due to its high viscosity at low shear levels. This resistance to settling is an advantage in producing uniform castings, particularly aggregate castings. As discussed in Section 3.3 aggregate casting slip is made by adding 15% of -40 mesh powder (particles up to 420 μm in diameter) to the 10 μm average diameter casting slip. The silica solids of aggregate casting slips made with the thixotropic slip are held in complete suspension (no layer of solids observed at the bottom of the holding container) for as long as 24 hours. Aggregate castings made with dilatant slip show evidence of settling within minutes. According to Joe Harris, Georgia Tech, must use 50% aggregate grains
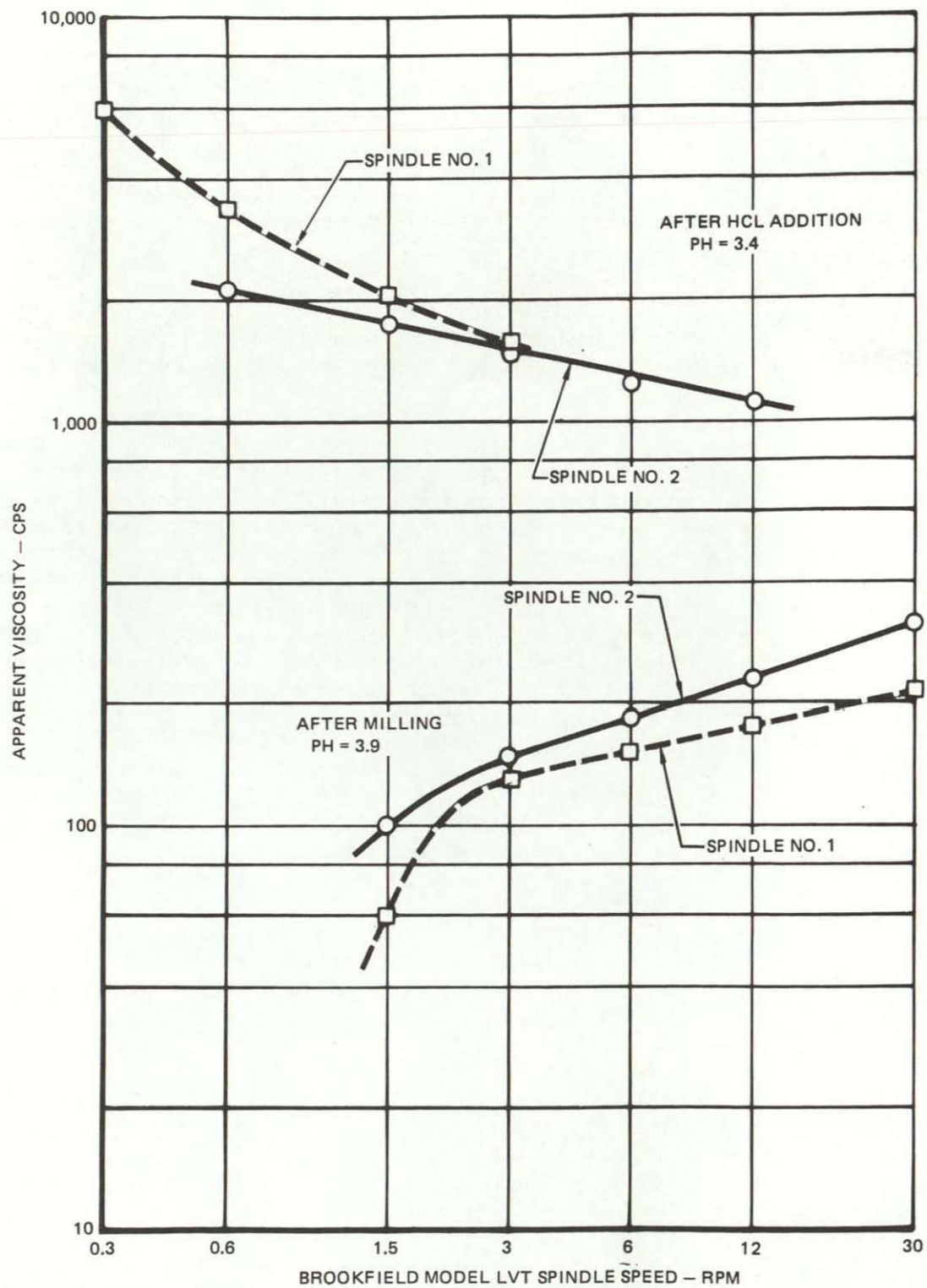
FIGURE 3.4—2 SHIFT FROM DILATANCY TO THIXOTROPHY ACCELERATED
BY HCL ADDITION

18
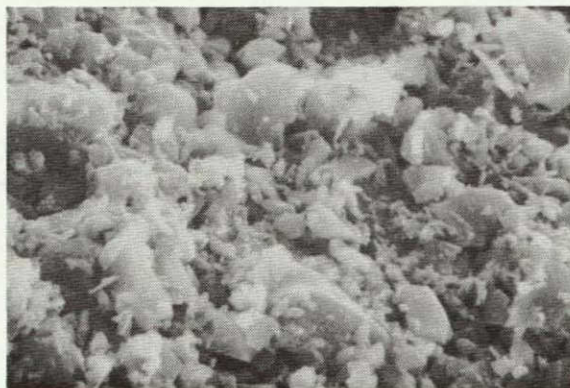
HYPERPURE

COMMERCIAL
HIGH PURITY
(GLASROCK)

PH = 3.8

PH = 6.0
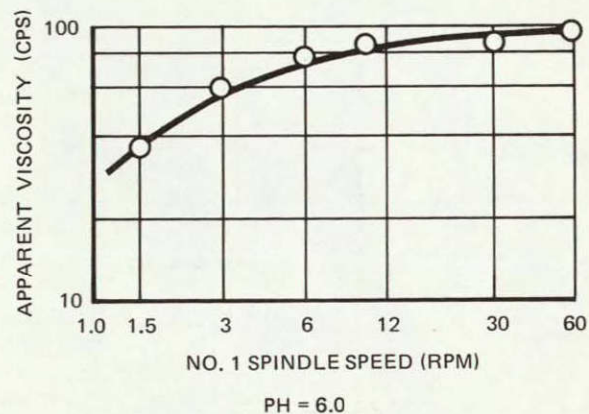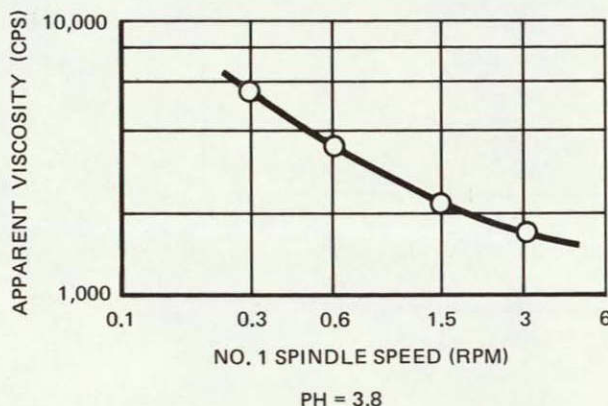
**FIGURE 3.4—3 RHEOLOGY OF HYPERPURE SLIP AND
COMMERCIAL HIGH PURITY SLIP**

to produce a viscous mixture whereby the particles are kept in suspension during casting. As previously indicated, the quantity of aggregate grains added must be limited in order to maintain a high reflectance in the fired product.

Another advantage of the thixotropic slip versus dilatant slip castings is a lower bulk density. The reduction in density is about 8% in both the green and sintered state, the firing shrinkage being nearly the same. The lower density has no apparent effect on the reflectance of the material as measured on the Beckman DK-2A. The lower cast density also results in a higher casting rate due to a lower filtration resistance to the moisture withdrawal by the plaster mold. An advantage to a higher casting rate is maintaining uniformity in castings of considerable wall thickness such as a full-scale Jupiter Probe reflective heat shield.

19
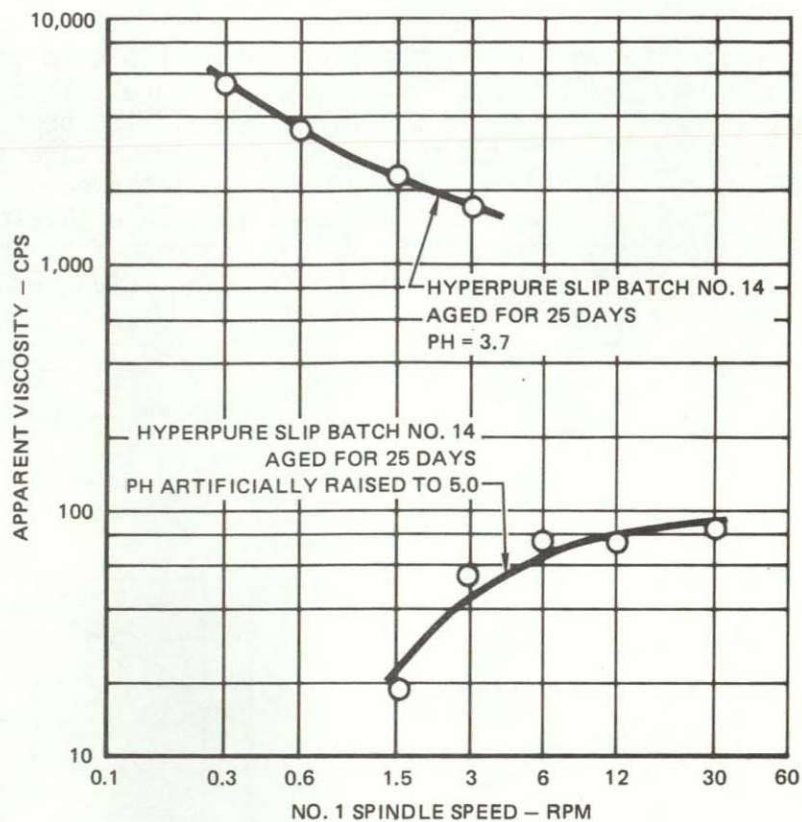
**FIGURE 3.4—4 RHEOLOGY OF HYPERPURE SLIP MAY BE
CHANGED BY ADJUSTING PH LEVEL**

- MUCH LOWER SETTLING RATE — MOVE UNIFORM CASTINGS — ESSENTIAL FOR AGGREGATE CASTING OF HEAT SHIELDS
- MORE RAPID CASTING RATE — ALONG WITH NEW SETTLING RATE — MAKING ROTATIONAL CASTING UNNECESSARY
- LOWER GREEN AND FIRED DENSITIES WITH COMPARABLE STRENGTHS — WEIGHT SAVING
- PROCESSING FLEXIBILITY — CASTINGS MAY BE SINTERED TO A WIDER RANGE OF DENSITIES
- MORE FLUID DURING NORMAL HANDLING — LESS AIR ENTRAPMENT

**FIGURE 3.4—5 PROCESSING ADVANTAGES OF THIXTROPIC SLIP VERSUS
DILATANT SLIP**

4.0 SCALE-UP OF HEAT SHIELD SLIP CASTING

This section describes the work performed to scale-up the slip casting proce-
dures, the goal being to fabricate a full-scale hyperpure silica heat shield
by slip casting. A design drawing of the full-scale silica heat shield is
shown in Figure 4.0-1. The plan was to scale-up in three stages: casting one-
sixth scale shields, casting one-half scale shields, followed by casting the
full-scale model. The initial work on the one-sixth scale shields was done in
parallel with the material improvement. A one-half scale heat shield was
successfully cast, dried, and fired. Tooling was fabricated for a full-scale
shield prior to program redirection to improve the toughness of the material.

4.1 ONE-SIXTH SCALE HEAT SHIELDS

This section describes the first phase of the scale-up of the aggregate slip
casting process.

4.1.1 COMMERCIAL GRADE SLIP CASTING STUDIES

Prior to this contract some experimental miniature heat shield shapes were slip
cast using a commercially available silica slip (Glasrock's High Purity Slip).
This work is described in Reference 2.

Although these miniature heat shields were not a direct scale-down of the probe's
shield they were about the size of one-sixth scale model, being approximately
15 cm in diameter and 2.5 cm thick. The plaster of paris mold used to cast
these shields is shown in Figure 4.1-1. The male mandrel shown in Figure 4.1-1
was also made of plaster of paris, so that casting of the shields took place
from two directions. It was later learned that casting shapes from both sides
can result in void areas near the center of the part. Therefore, all subsequent
heat shield molds had metallic male mandrels.

A total of five miniature heat shields (Figure 4.1-2) were processed before a
crack-free part was successfully dried and fired. Shrinkage problems asso-
ciated with drying and firing slip cast fused silica were identified during
this study.

After slip casting a part in a porous plaster mold, about 15% of the water
remains within the material with a thin layer of water present between the
grains. During the early stages of drying, the casting shrinks as the water
layer between the grains evaporates. Drying shrinkage rates of commercial
grade and hyperpure slip cast fused silica are presented in Figure 4.1-3. The
shrinkage of the commercial grade material is higher because of the greater
percentage of very fine particles. A slow drying cycle, as discussed in
Reference 2, must be used to assure uniform drying during which the casting is
kept in a high humidity environment. Drying shrinkage control is critical to
the scale-up effort because uniform drying becomes more important and increas-
ingly difficult with larger and particularly thicker parts. An eleven day
drying cycle was used for the commercial grade miniature heat shields.

FIGURE 4.0–1 FULL SCALE SILICA HEAT SHIELD DRAWING
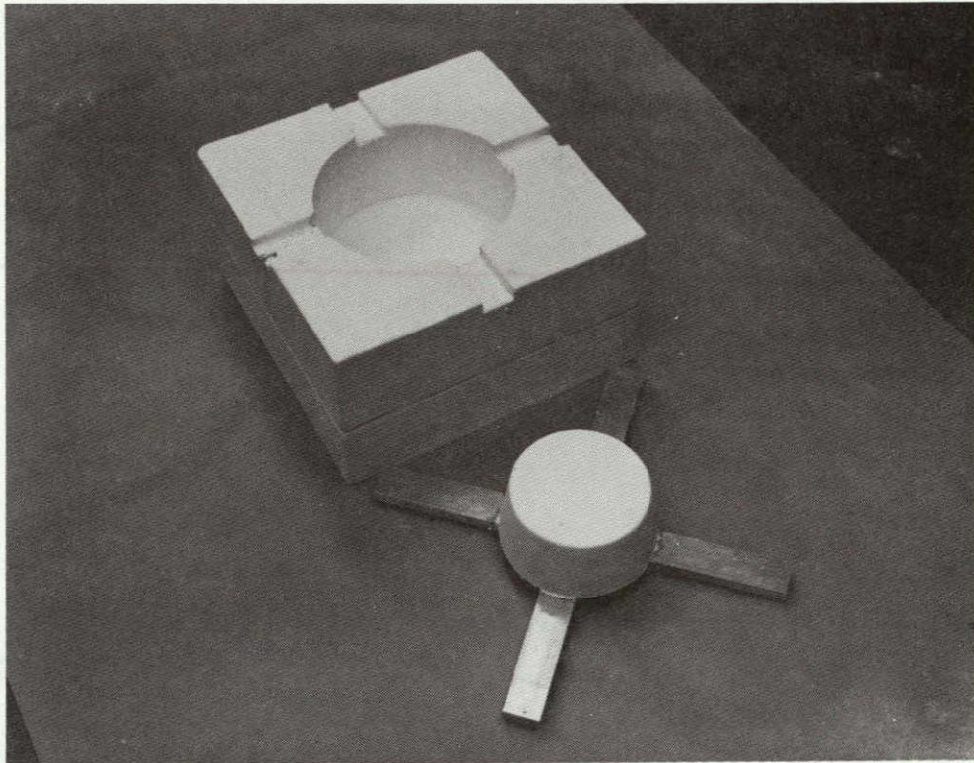
DISASSEMBLED
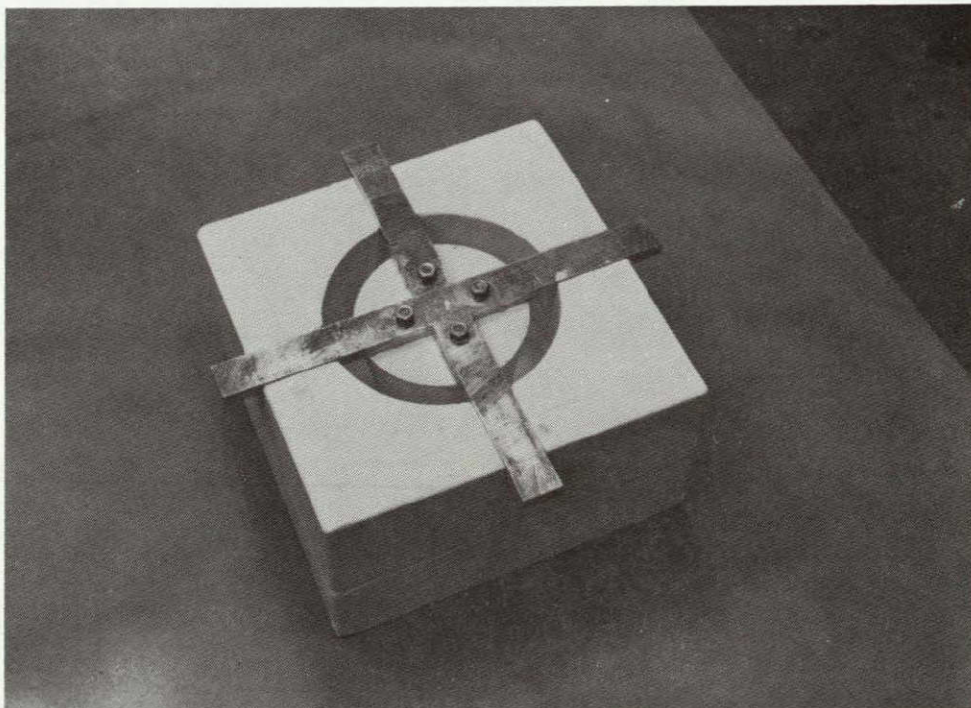
ASSEMBLED FOR CASTING

FIGURE 4.1–1 PLASTER OF PARIS MOLD USED TO CAST MINIATURE HEAT SHIELDS
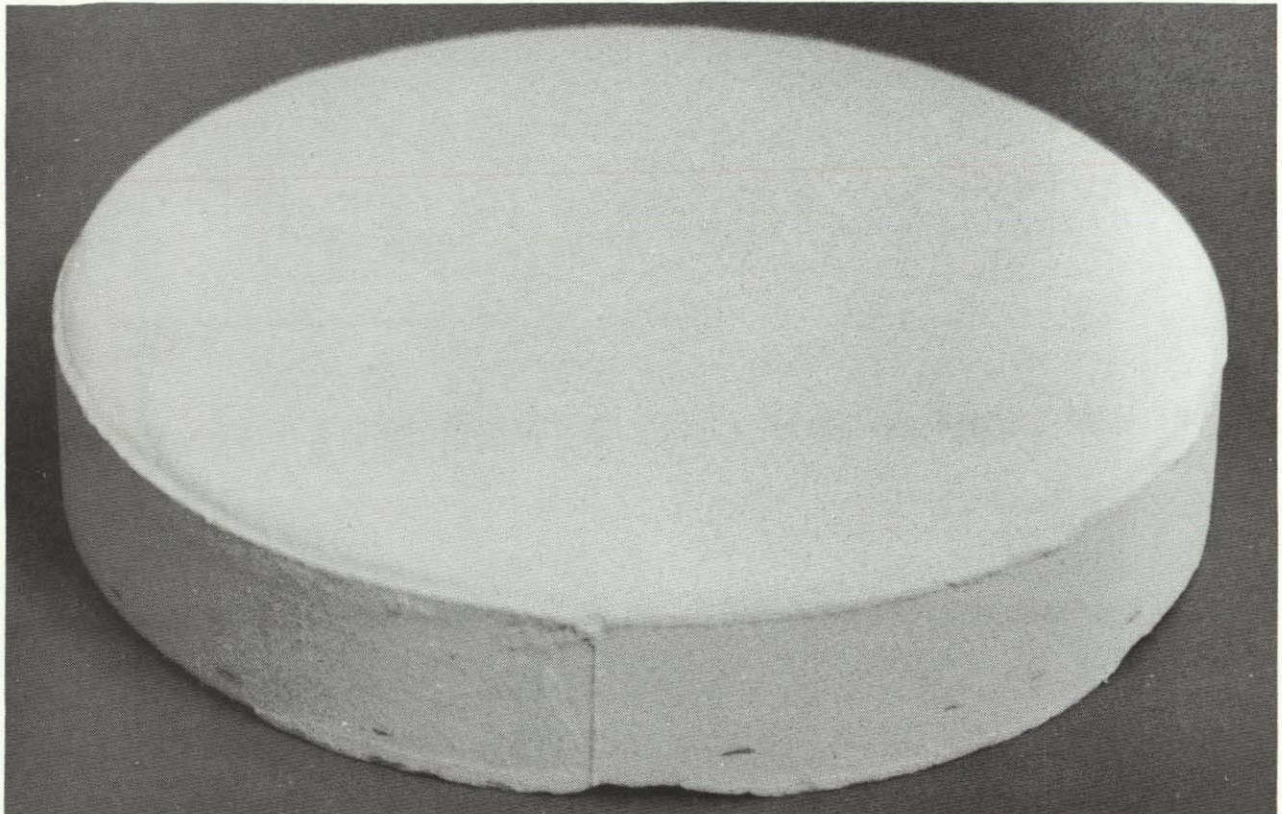
TYPICAL HEAT SHIELD AS REMOVED FROM MOLD
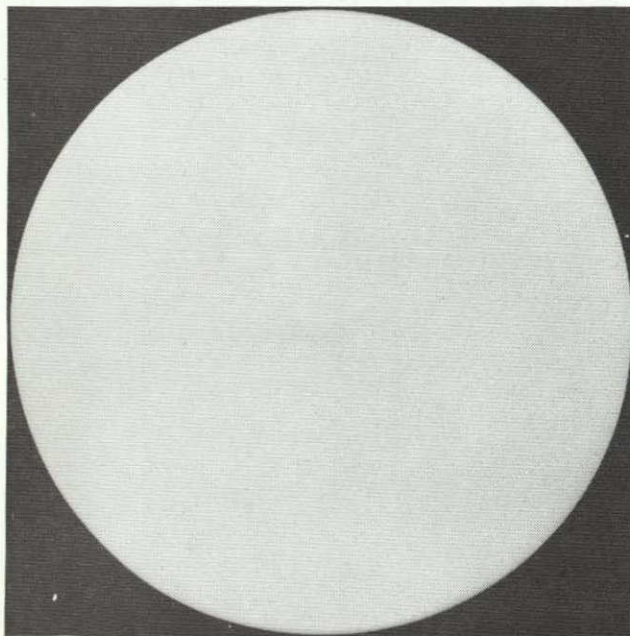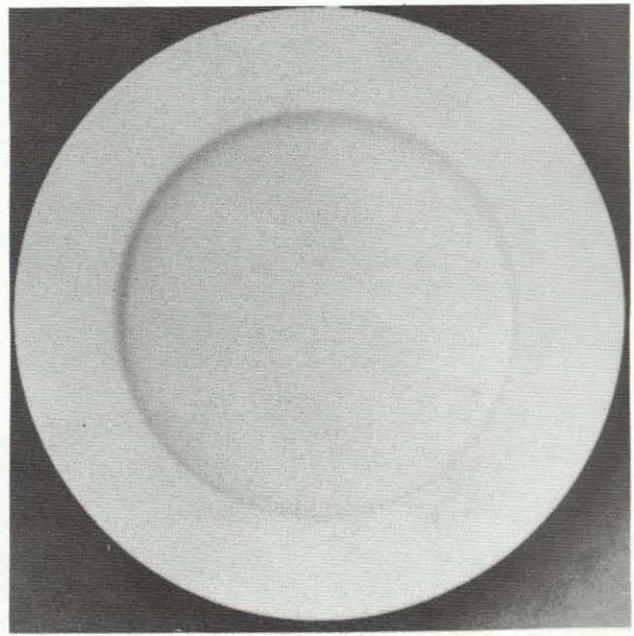
AFTER FIRING

FIGURE 4.1–2 MINIATURE SLIP CAST FUSED SILICA HEAT SHIELD
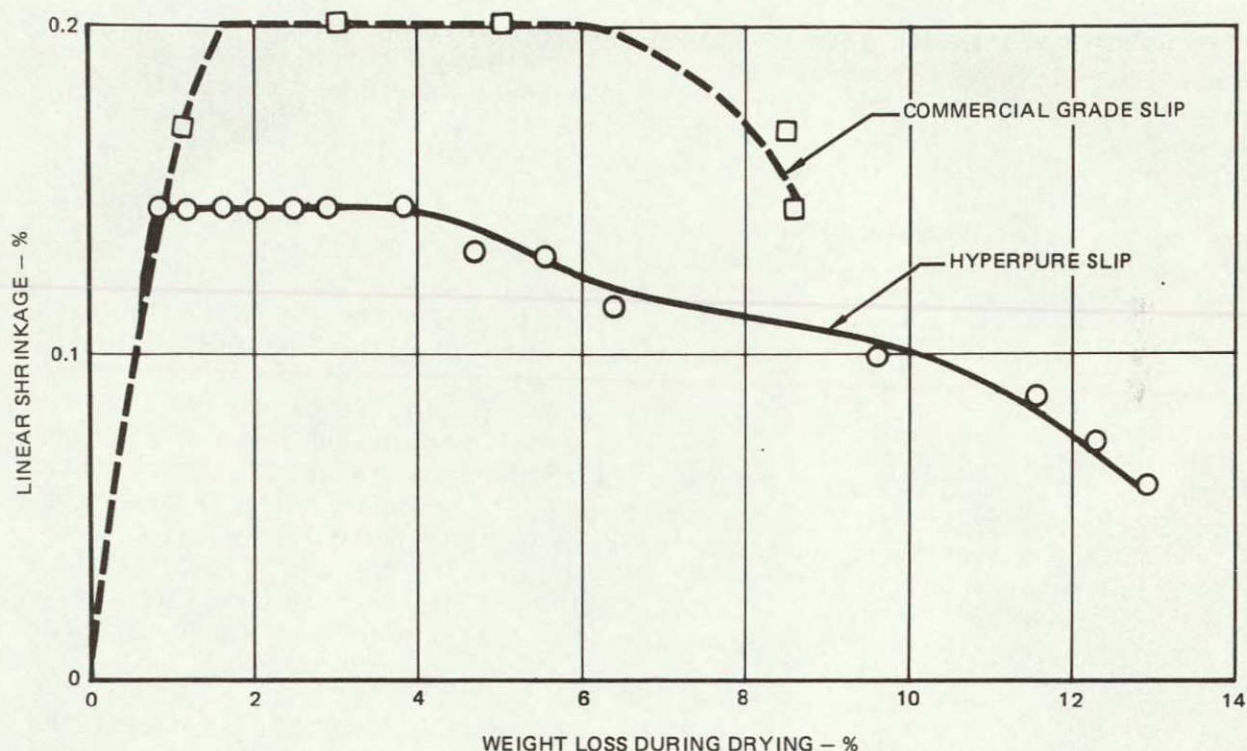
FIGURE 4.1–3 DRYING SHRINKAGE OF SLIP CAST FUSED SILICA

In a manner similar to drying shrinkage, differential firing shrinkage can also cause cracks in slip cast fused silica. Large parts must be heated slowly to assure uniform shrinkage. A heating time of four hours from room temperature to 1150°C was used to successfully fire the miniature heat shield shown in Figure 4.1-2.

4.1.2 ROTATIONAL DRAIN CAST OF ONE-SIXTH SCALE HEAT SHIELDS

The original plan was to slip cast hyperpure fused silica heat shields by drain casting using a rotating mold in a manner similar to that described for slip casting commercial grade fused silica radome shapes in Reference 4. Drain casting refers to a method of slip casting in which an excess of slip is maintained in the mold cavity. Proper wall thickness is controlled by casting time and the remaining excess slip is drained from the mold cavity. The cast wall thickness build-up for a given casting slip at a given casting pressure is predicted by the relationship.

$$W = K\sqrt{T}$$

where W = cast wall thickness (cm)
      T = casting time (min)
      K = proportionality constant

The constant K may be determined for the casting slip in question by making small test castings of varying thickness and measuring the casting time.

25

A rotating mold was anticipated to be required for casting heat shields because of the nature of the silica slip and the full-scale heat shield thickness (∿ 5 to 7.5 cm). Casting time for a full scale heat shield was calculated to be in excess of ten (10) hours. Grain settling in the slip during the long casting time would result in unacceptable density gradients.

Accordingly a rotating mold setup was designed and fabricated which provided for the drain casting of a one-sixth scale (15 cm diameter) probe heat shield. A design drawing of the rotating mold is shown in Figure 4.1-4. The mold was equipped with a stainless steel sealing plate with a mandrel for slip displacement which provided for a casting thickness of 2.54 cm. The internal surfaces of the cover plate and mandrel were Teflon coated to prevent slip contamination. The rotating mold was equipped with a slip reservoir outside of the mold cavity with an electrical centrifugal pump to transfer slip from the reservoir to the mold cavity. The slip was recycled from the mold to the reservoir, being raised to a higher level to ensure a slight positive pressure on the slip in the mold cavity. An air driven mixer agitated the slip in the holding reservoir and kept the solid particles in suspension. The reservoir, the centrifugal pump, and all the lines and fittings which provided for fluid transfer and recycling were plastic materials to prevent metallic contamination of the hyperpure silica slip.

A total of four unsuccessful attempts were made to rotational cast a one-sixth scale heat shield. Failure of the slip transfer pump resulted in aborted casting runs. Two attempts were made using an electrical centrifugal pump. One casting run was made with an air driven centrifugal pump and another with a peristaltic type pump with water diluted slip for lower viscosity and pumpability, without success. Two problems with pumping the silica slip were maintaining the very high purity and the induction of very high shear rates on the dilatant slip.

The problems of pumping slip to the rotational mold could have been solved by using a gravity feed system in which the slip reservoir was above the mold and rotating the transfer lines to the mold. However, the cost to scale-up the rotating mold was high and the properties of the recently developed thixotropic aggregate slip made a rotating mold unnecessary.

During the rotation casting investigation, the size of the ball milling containers were being scaled-up (Section 3.1). The slip prepared in larger containers had notably different rheological properties and the slips could be controlled by pH adjustment (Section 3.4). The resulting thixotropic slips had a high viscosity at low shear, therefore, the solid particles remained in suspension for much longer times. Also, the thixotropic slips cast to a lower green density (1.49 g/cc vs 1.60 g/cc), which resulted in faster casting time due to lower filtration resistance to moisture withdrawal by the plaster molds.

Also during this scale-up it was discovered that aggregate casting was necessary because of the high shrinkage problems anticipated on the 5-7.6 cm thick full-scale heat shields. (See Section 3.3).
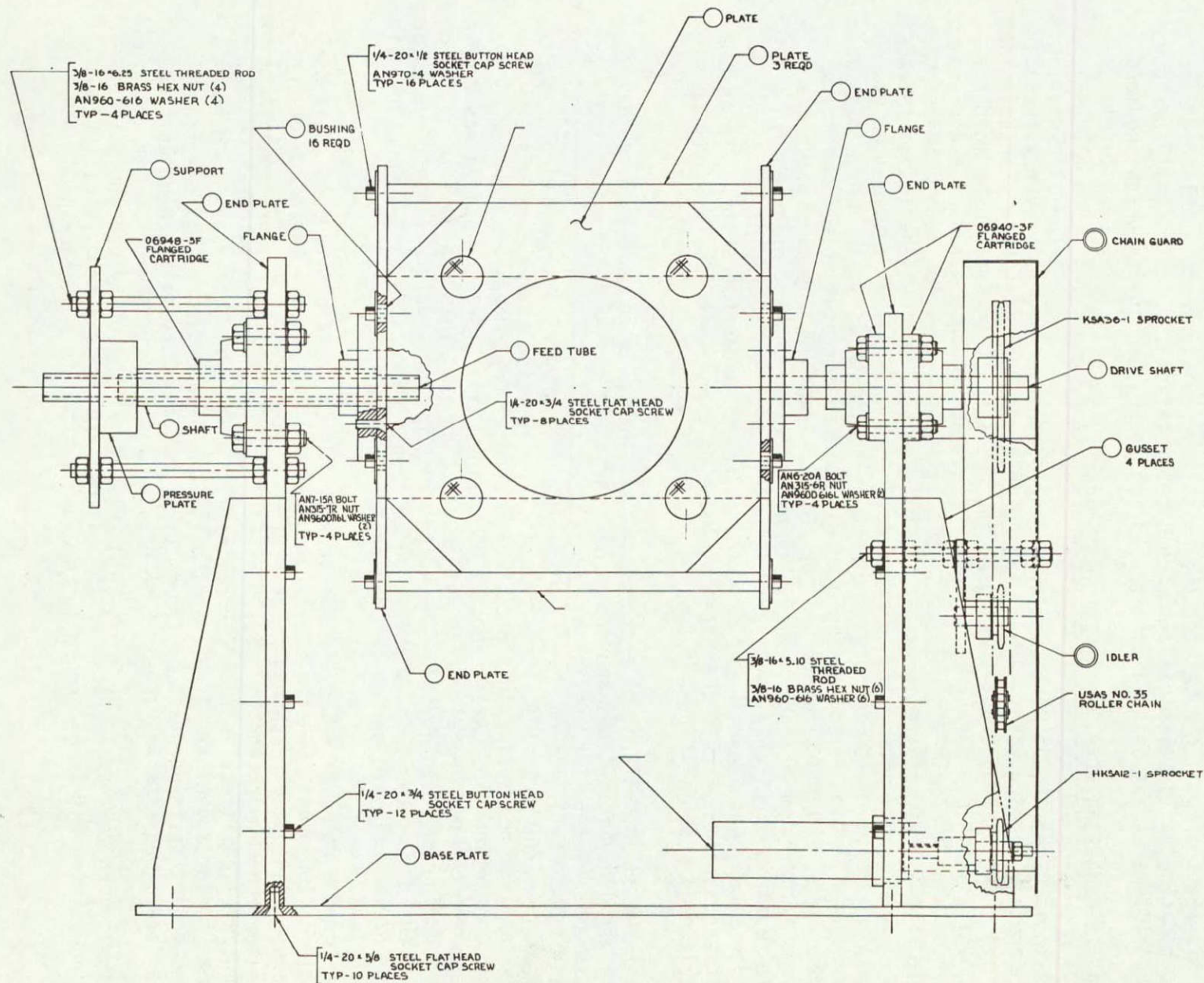
FIGURE 4.1—4 DESIGN DRAWING ROTATING MOLD FACILITY

27

Calculations showed that casting 5-7.6 cm thick heat shield from the thixotropic aggregate type slip would take less than 3 hours rather than 10-20 hours for the dilatant continuous particle size (nonaggregate) slip initially considered. This reduced casting time, together with the resistance to settling of the thixotropic materials, eliminated the need for rotational casting. All subsequent heat shields were cast using aggregate casting techniques in a nonrotating mold.

4.1.3 AGGREGATE CAST ONE-SIXTH SCALE HEAT SHIELDS

A total of eight one-sixth scale heat shields were made with hyperpure silica aggregate casting slip. A nonrotating mold was used for these shields. The mold shown in Figure 4.1-1 was used for AHS-1/6-1 (aggregate heat shield - one-sixth scale - number 1). Figure 4.1-5 shows a photograph of a 4 piece mold along with the male mandrels and a plexiglass spacer which were fabricated especially for aggregate casting. The male mandrel defines the inside surface of the shield and controls the casting wall thickness. The disassembled view of the mold shows two male mandrels, one made of tooling plastic (Eppolite 30) and one made of aluminum. The plastic mandrel was used for heat shield numbers AHS-1/6-2 through 6, and the aluminum one for AHS-1/6-7 and 8. The plexiglass spacer allows for an excess amount of slip to be initially poured into the mold cavity to maintain the liquid level as moisture is absorbed by the plaster. A similar size spacer was added to the plastic mandrel in order to maintain the shield thickness at 2.54 cm. The external shape of a one-sixth scale aggregate heat shield is shown in Figure 4.1-6.

The initial one-sixth scale aggregate cast shields were used to determine the required drying methods and the drying shrinkage characteristics of the aggregate material in the heat shield configuration. AHS-1/6-1 was successfully dried and fired with no shrinkage cracks. The shield, after casting, was dried slowly in a high humidity environment. The humidity environment was achieved by sealing the casting in a plastic container. Drying was accelerated by cracking the sealed lid. After about a 4% drying weight loss the shield was removed from the chamber and air dried with a cloth cover. This was followed by exposed air drying and oven drying. The weight loss of the sample was monitored throughout the drying cycle and diameter measurements were taken with a vernier caliber. The drying rate and shrinkage data are shown in Figure 4.1-7.

The drying rate for AHS-1/6-2 was accelerated in an effort to gain additional information about the effect of drying rate on shrinkage. Shrinkage cracks were evident in this shield after firing. Since the two shields (AHS-1/6-1 and -2) were made with the same batch of slip and subjected to nearly identical firing cycles (5 hours at 1230°C (2250°F) with a 3.5-hour heat-up) it was concluded that the drying of AHS-1/6-2 was too rapid. Also shown in Figure 4.1-7 is the drying shrinkage rate of the material based on the moisture weight loss as determined from AHS-1/6-1. The greater slope of this line as compared to the corresponding one for AHS01/6-1 indicates the more rapid drying of AHS-1/6-2. The shrinkage cracks on this shield are evident from visual examination but are not large enough to be clearly shown in a photograph.
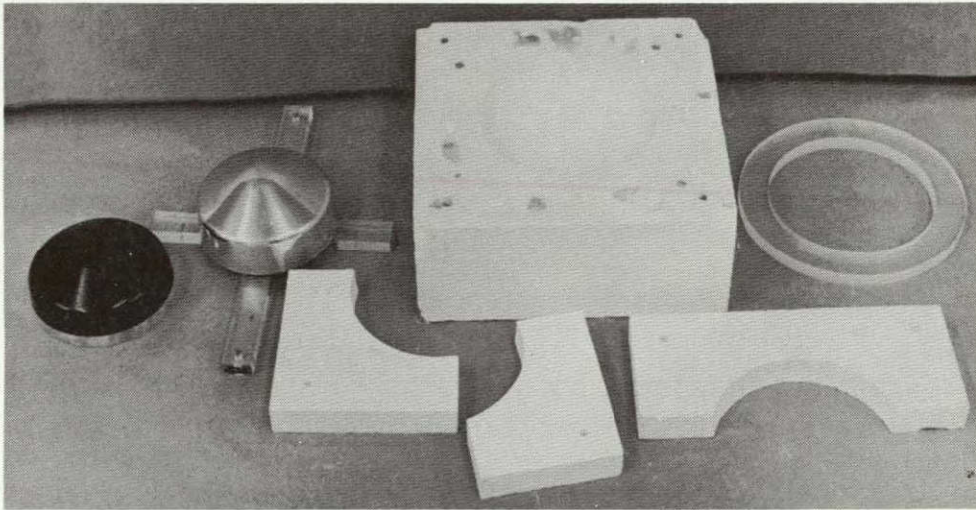
DISASSEMBLED
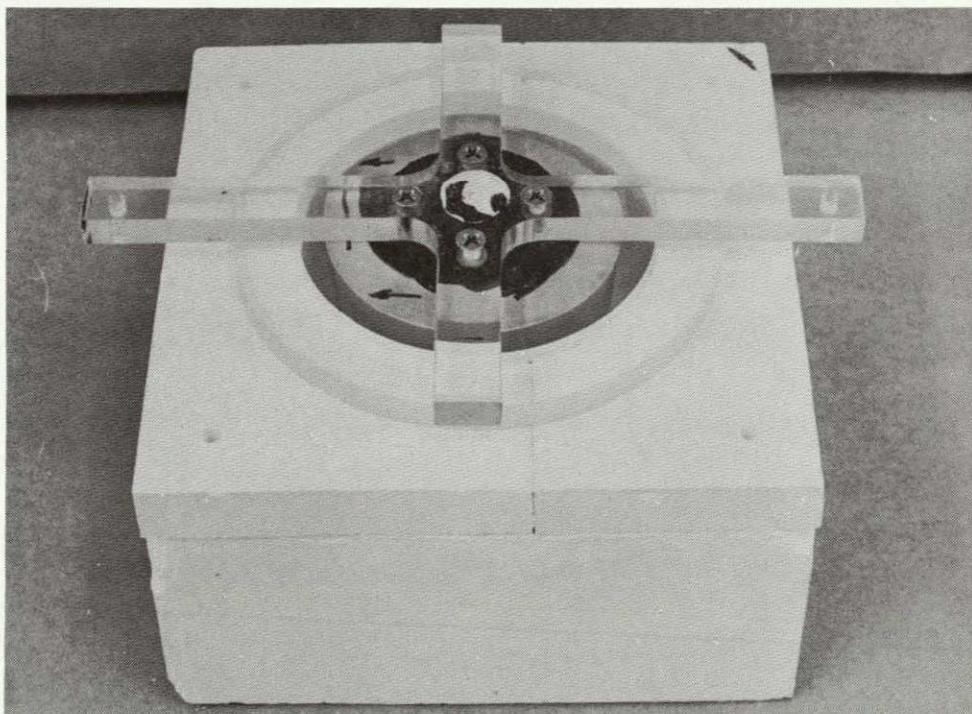
ASSEMBLED FOR CASTING

FIGURE 4.1–5 PLASTER OF PARIS MOLD FOR AGGREGATE CASTING
1/6 SCALE HEAT SHIELDS

29
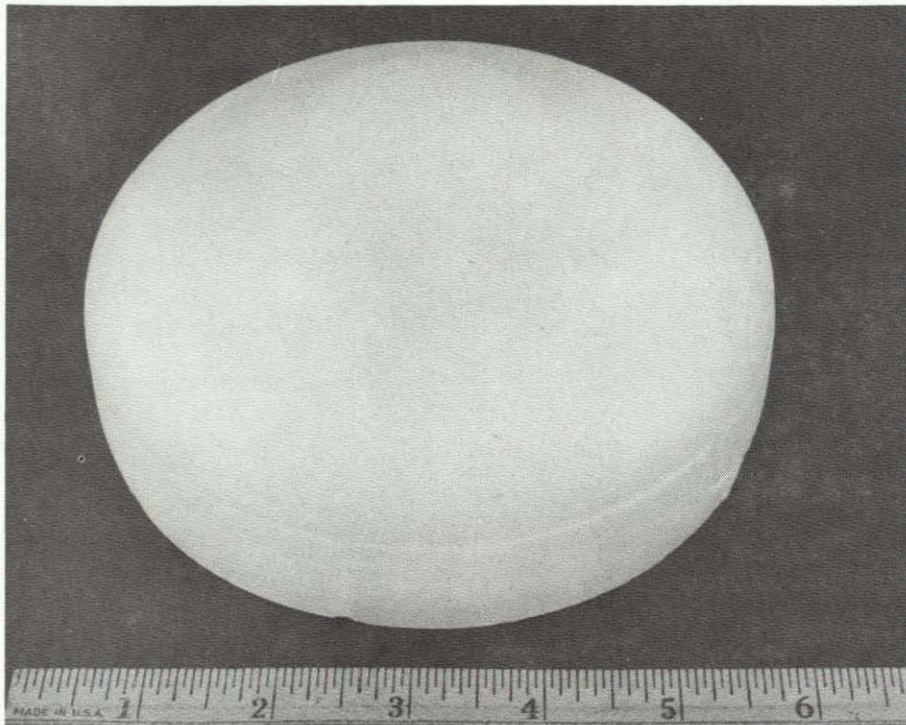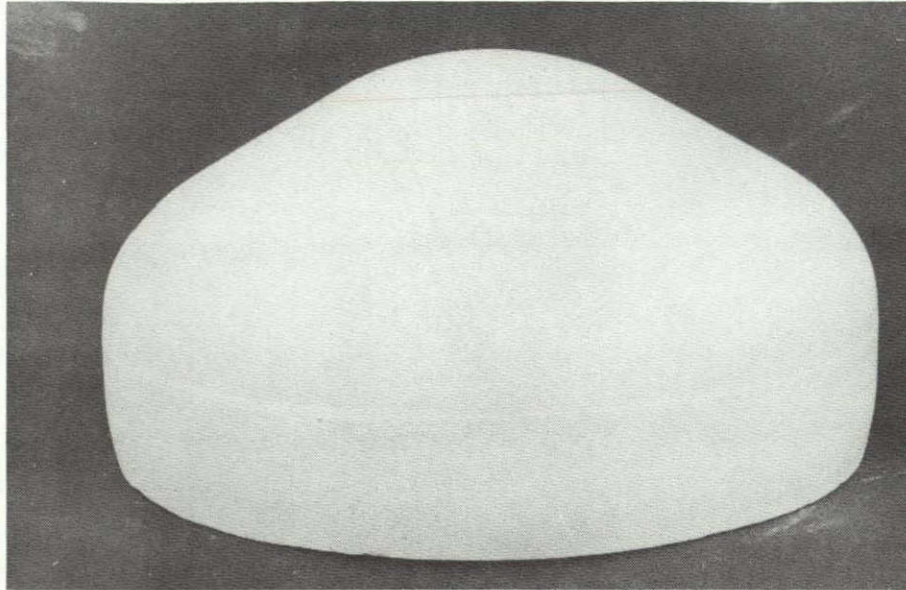
FIGURE 4.1–6   TYPICAL 1/6 SCALE AGGREGATE CAST HYPERPURE
FUSED SILICA HEAT SHIELD
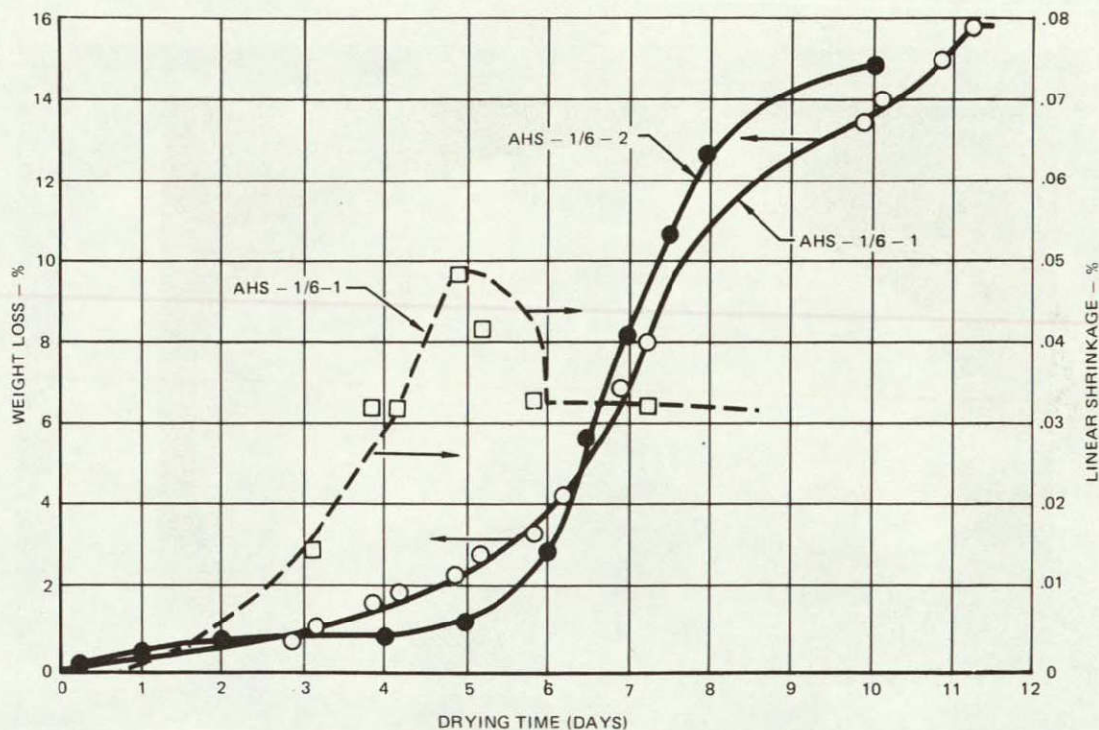
FIGURE 4.1–7   DRYING RATE AND DRYING SHRINKAGE RATE FOR AHS–1/6–1 AND 2

In the case of AHS-1/6-3 and -4, problems were encountered in removing the male mandrel after casting.   Therefore, humidity drying could not be started immediately and the shields were intentionally dried very rapidly.   AHS-1/6-3 and -4 was dried in 4 days and 2 days respectively.   As expected, AHS-1/6-3 had very large shrinkage cracks after firing.   The cracks on this shield, as well as on AHS-1/6-2, seem to start from the lip edge of the part.   This is the most exposed area of the shield where shrinkage would be expected to begin.   Therefore, before firing AHS-1/6-4, about 0.3 cm of this edge was removed by lightly sanding with fine grain SiC sand paper.   AHS-1/6-4 had no cracks after firing.   A photograph comparing AHS-1/6-3 and AHS-1/6-4 is shown in Figure 4.1-8.

As noted above, difficulty was encountered in removing the male mandrel from AHS-1/6-3 and -4.   The problem seemed to be one of slip adherence to the mandrel rather than tightening due to shrinkage.   The plastic mandrel was coated with a silicone lubricant for AHS-1/6-5 casting.   Because the mandrel was inadvertently pulled before the silica was completely set or cast, a good test of the release material was not obtained.   The silicone release material was repeated on AHS-1/6-6 and it seemed to act as an adhesive rather than a release material.

At this point, fabrication of tooling for the one half scale shield was in process.   Since the one half scale mandrel was made of aluminum and adherence of the cast wall to the mandrel was a problem, an aluminum mandrel was made for the one sixth scale mold setup.   AHS-1/6-7 was cast using the aluminum mandrel coated with RAM 225, which was a recommended release agent. The mandrel stuck very tightly to the casting, but it was finally removed with a great deal of force.

31
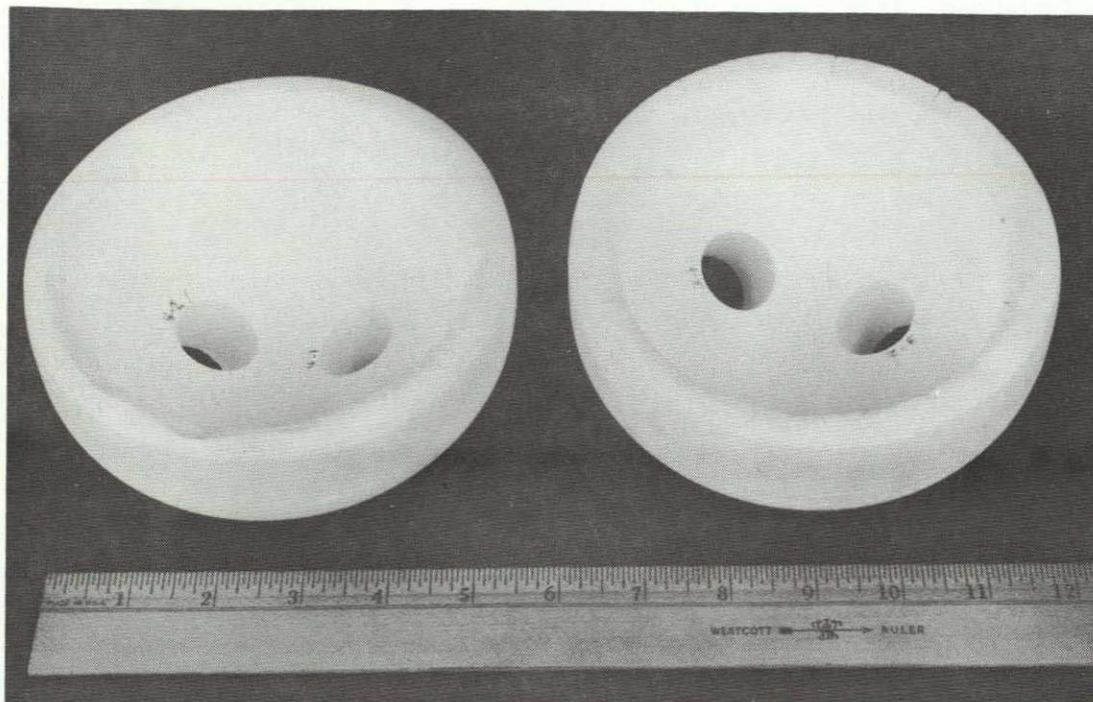
FIGURE 4.1–8 FIRED 1/6 SCALE AGGREGATE CAST HEAT SHIELDS WITH AND WITHOUT SHRINKAGE CRACKS

A series of tests were performed on several candidate release agents using very small (1.5" diameter) aluminum mandrels and small plaster molds to minimize material usage. The following release materials were tested: silicone grease, Partall 10, RAM 225, CAMIE 1000, CAMIE 666, and Mold Whiz. AHS-1/6-8 was successfully cast using the aluminum mandrel coated with CAMIE 1000 release lubricant. The CAMIE 1000 was judged to be a suitable release for the aluminum mandrel.

A problem encountered in varying degrees with all of the one-sixth scale aggregate cast shields was that of entrapped air, particularly on the inside surface (mandrel surface) of the castings. The flaw was either in the form of spherical voids or bubbles or in extreme cases large randomly shaped void areas where slip failed to flow around the mandrel. Some form of vibration was used for all of the one-sixth scale shields. For AHS-1/6-1, vibration was supplied by a Syntron 110V vibrator clamped to the table on which the mold was sitting. For AHS-1/6-2 through AHS-1/6-8 more sophisticated vibration equipment was employed, as shown in Figure 4.1-9, with eqiupment to monitor the frequency and amplitude of the vibration. For AHS-1/6-2, vibration of the entire mold was used and for AHS-1/6-3 through -8 vibration of the mandrel directly was used. Vibration of the mandrel was generally done for the first few minutes of casting or until no escaping air (bubbles) was observed to ensure that damage was not done to the cast wall. Vibration of the mandrel resulted in slip displacements of 0.025 to 0.05 cm.

Analysis of the vibration employed and the resulting gas voids in the various shields indicated that the rheology of the slip is the variable most responsible

32
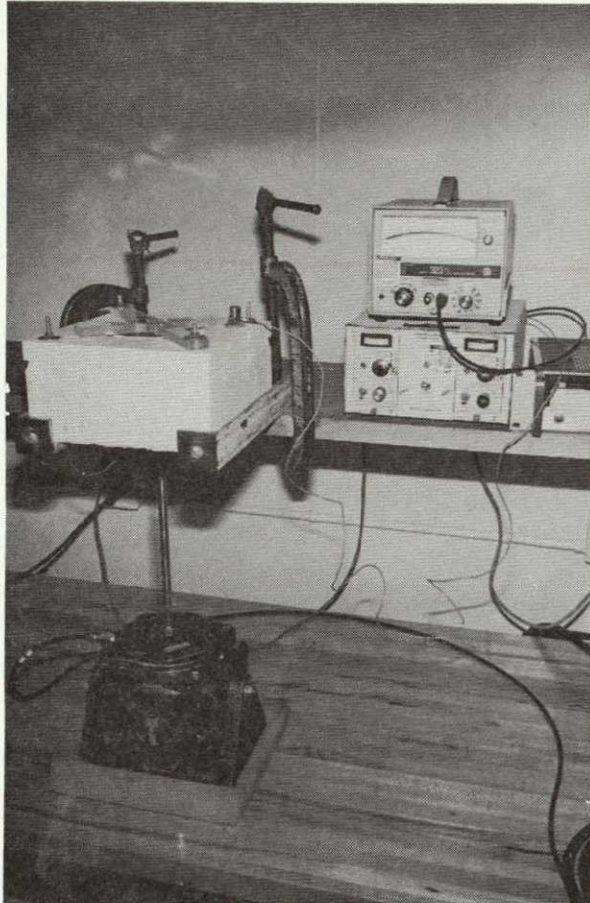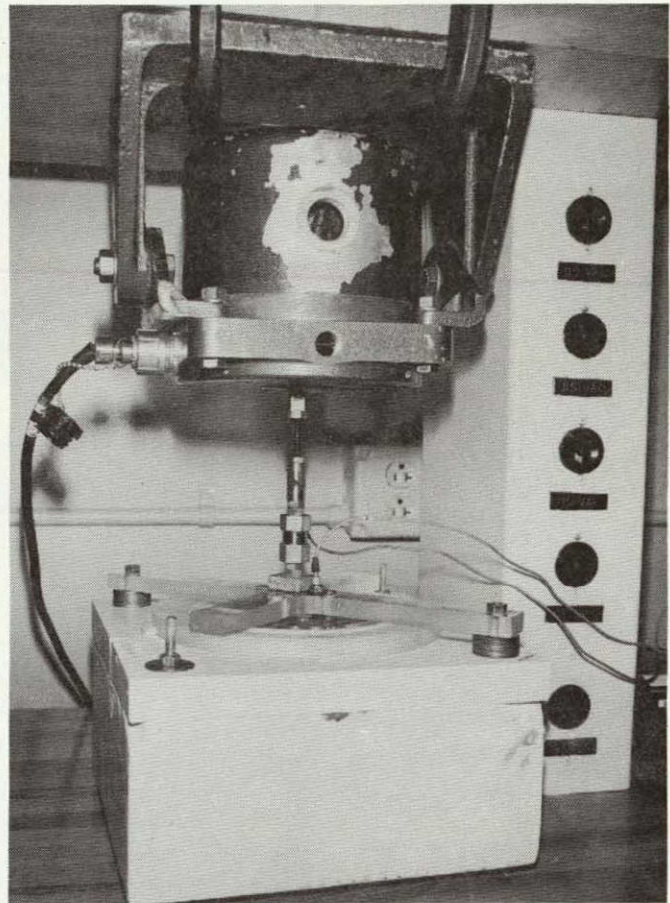
VIBRATION OF MOLD   VIBRATION OF MANDREL

FIGURE 4.1–9 ELECTRODYNAMIC EXCITER FOR VIBRATION CASTING

for the air entrapment problem. The shields with the most severe and least
severe air entrapment had similar vibration histories. AHS-1/6-4 was the best
casting from this standpoint with no void area and only a few very small bubbles.
AHS-1/6-7 had a very large void area on the inside surface because slip did not
flow around the mandrel. Viscosity data for the two aggregate slips are shown
in Figure 4.1-10 along with curves for the slips before the aggregate particles
were added. The slip used for AHS-1/6-4 was very thixotropic and as a result
poured in a very fluid manner with little air entrapment and offered little
resistance to flow around the mandrel. The slip used for AHS-1/6-7 had a more
dilatant character which was reflected in stiffness during pouring, more air
entrapment, and resistance to flowing around the mandrel. The results of all
the shields follow this trend in that the more thixotropic the slip the fewer
gas voids in the casting as determined by visual inspection and radiographic
analysis. As discussed in Section 3.4, slight adjustments in the pH level of
the hyperpure slip produces the desired thixotropic rheology.
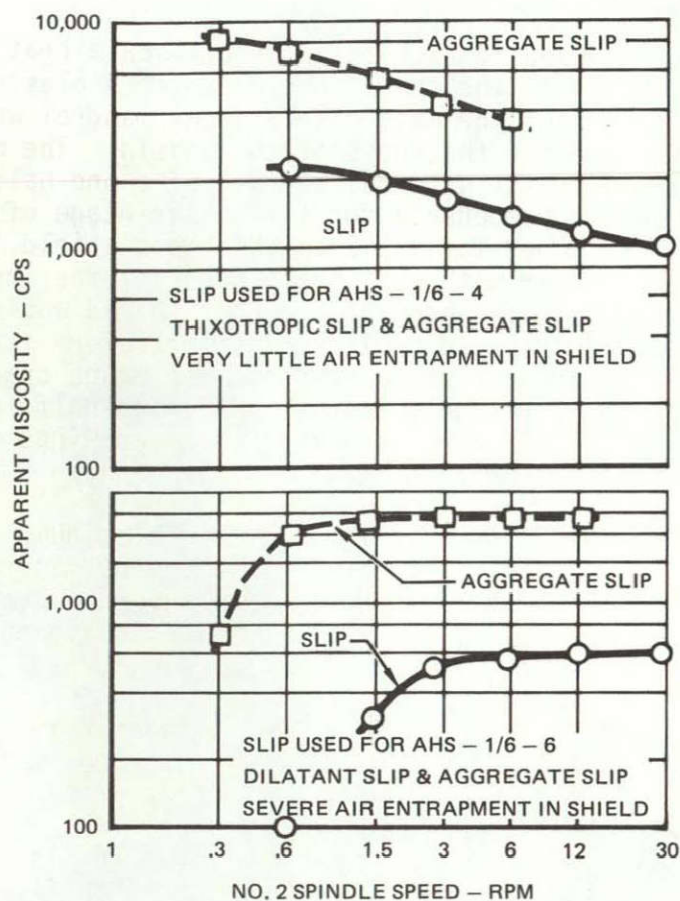
FIGURE 4.1–10   RHEOLOGY OF SLIPS – AIR ENTRAPMENT STUDIES

4.2 ONE-HALF SCALE HEAT SHIELD FABRICATION

This section describes the aggregate slip casting of one-half scale hyperpure fused silica heat shields, including the fabrication of the mold and the tooling required. A total of three one-half scale shield castings were made. Problems were encountered during the casting of the first shield. Therefore, the material was converted back into aggregate slip and reused for the second attempt. The second shield was cast successfully but developed cracks during drying and was broken in handling between drying and firing. Sections of this shield were fired in order to gain experience with the use of the firing facility. A new batch of aggregate slip was prepared for the third half-scale shield which was successfully cast, dried, and fired. It was determined to be crackfree by extensive visual and radiographic analysis. This shield was also machined (edges only) in the machining facility which was especially designed and fabricated for hyperpure fused silica heat shields.

34

4.2.1 ONE-HALF SCALE TOOLING FABRICATION

The first step in fabricating tooling for the one-half scale heat shield was the design of the master model of the shield around which a plaster of paris mold was poured and the design of the male displacement mandrel which defines the inside surface contour and the thickness of the shield. The master model was designed to be identical to the external surface of a one-half scale shield and 1.5% larger in diameter to compensate for firing shrinkage of the silica casting. The mandrel was designed for a 2.5 cm thickness shield, again allowing the 1.5% firing shrinkage and with a 5% draft angle at the inside edge. The tooling was designed so that the edge of the cast shield would be oversize in height. This edge would be rounded by light sanding before firing (to minimize the chances of formation and/or propagation of shrinkage cracks) and machined to size after firing. Design drawings of the one-half scale master model and mandrel are not included here because similar drawings of the corresponding full-scale parts are included in Section 4.3.

Both the master model and mandrel were fabricated from aluminum. A coating of CAMIE 1000 dry release lubricant was planned for use on the mandrel during the actual casting of shields. The coating was to serve the dual purpose of preventing contamination of the shield, attack of the aluminum by the low pH slip, and preventing adhesion of the cast wall to the mandrel.

In order to minimize the amount of aluminum material and machining time required for the master model and mandrel, 3.8 cm thick aluminum rings were cut and stacked rather than using a solid billet of metal. Photographs showing the cut rings for the two parts are shown in Figure 4.2-1. The rings were bonded together with American Cyanamid FM-123-2 adhesive as shown in Figure 4.2-2. A photograph showing the machined master model is presented in Figure 4.2-3.

The plaster of paris mold was made from U.S. Gypsum Number 1 pottery plaster, which is the recommended material for slip casting fused silica (see Reference 4).

A mold frame was fabricated which provided for seating of the male mandrel during casting of the heat shield. Precision tooling pins were used to aid in location of the parts of the five-piece mold. The raw plaster was combined in water in the ratio of 100 parts plaster to 70 parts water. Mixing and pouring of the plaster was done according to methods recommended for ceramic mold making (see Reference 5). Photographs showing the one-half scale mold with and without the mold frame are shown in Figure 4.2-4.

4.2.2 ONE-HALF SCALE AGGREGATE CAST HEAT SHIELD NO. 1

The batch of hyperpure fused silica slip used for aggregate casting slip for AHS-1/2-1 (aggregate cast heat shield - one half scale - number 1) was prepared in a 5 gallon milling container. The milling time for this batch was 65 hours and it had the normal 10 µm average particle size distribution as shown in Figure 3.1-2. After milling and adjustment of the solids content, viscosity measurements were taken and the slip was observed to be dilatant. The pH of the slip was lowered from 3.9 to 3.4 by addition of
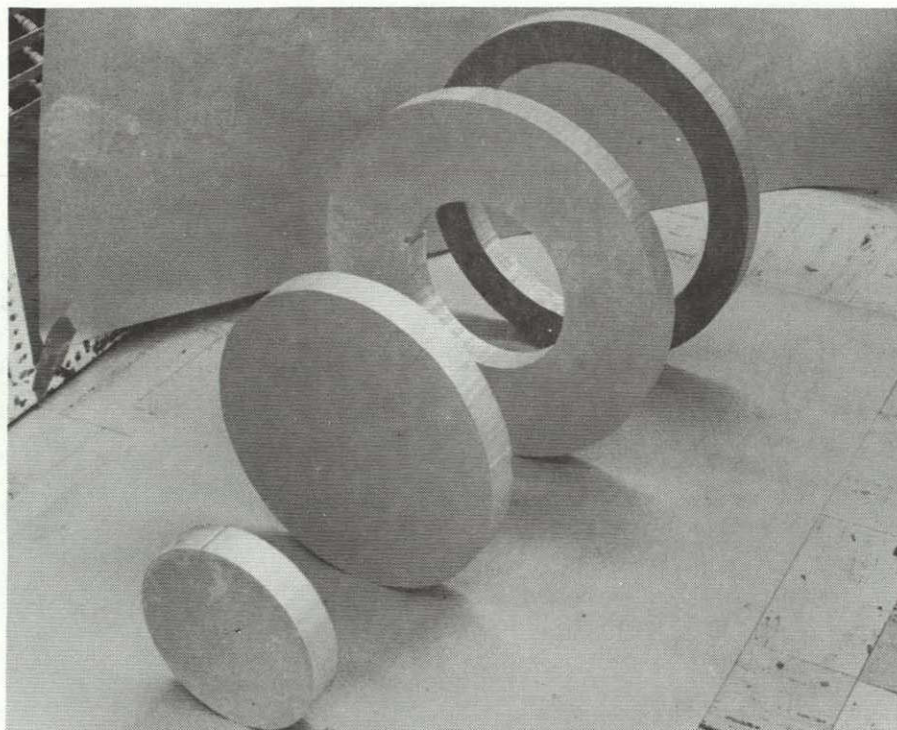
RINGS FOR MANDREL
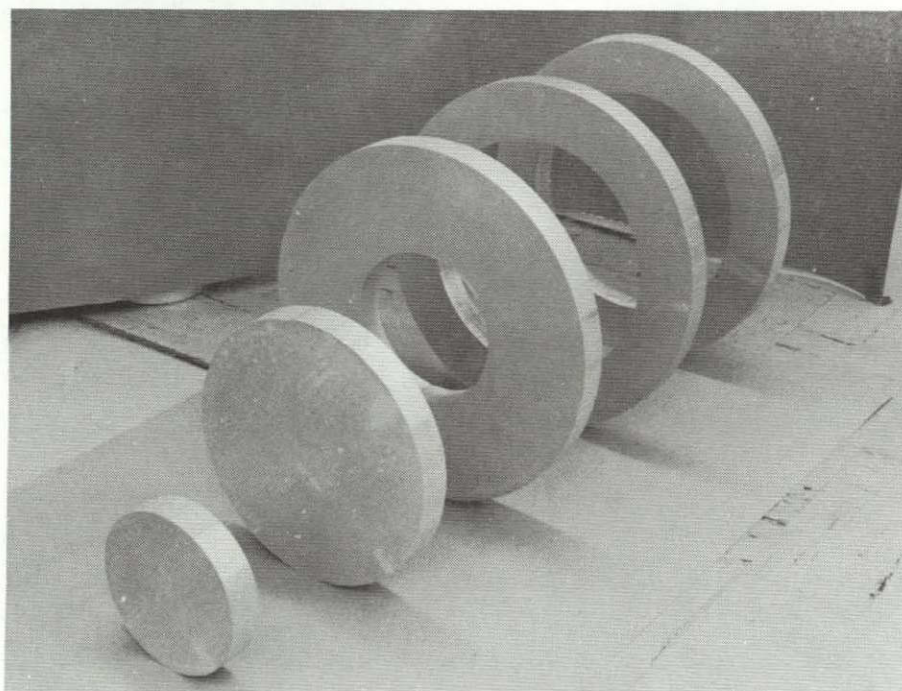
RINGS FOR MASTER MODEL

FIGURE 4.2–1 ALUMINUM RINGS FOR 1/2 SCALE MASTER MODEL AND MANDREL

36
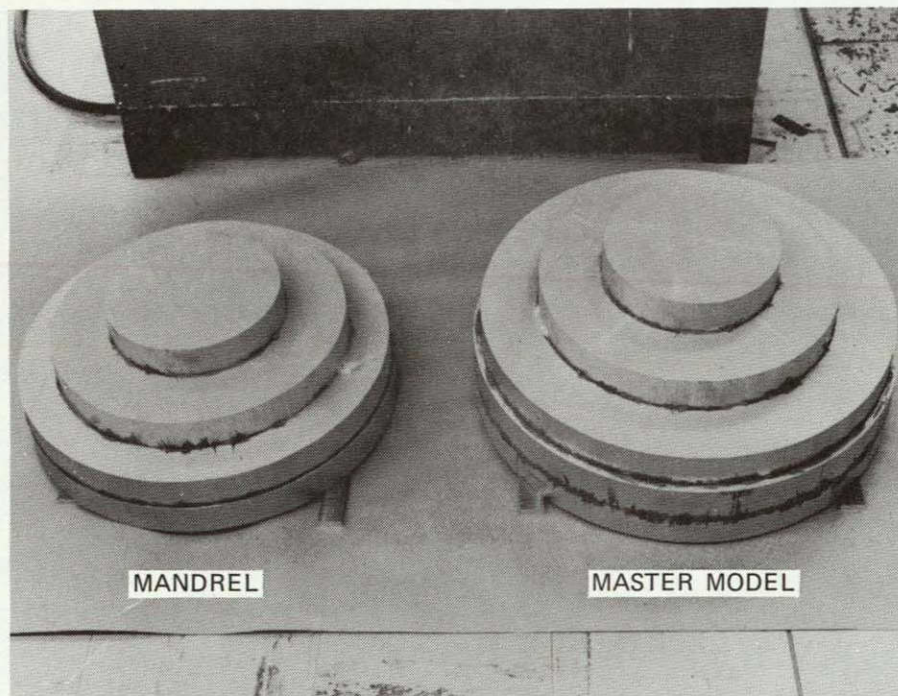
FIGURE 4.2—2   FM-123-2 BONDED ALUMINUM RINGS FOR 1/2 SCALE
MASTER MODEL AND MANDREL
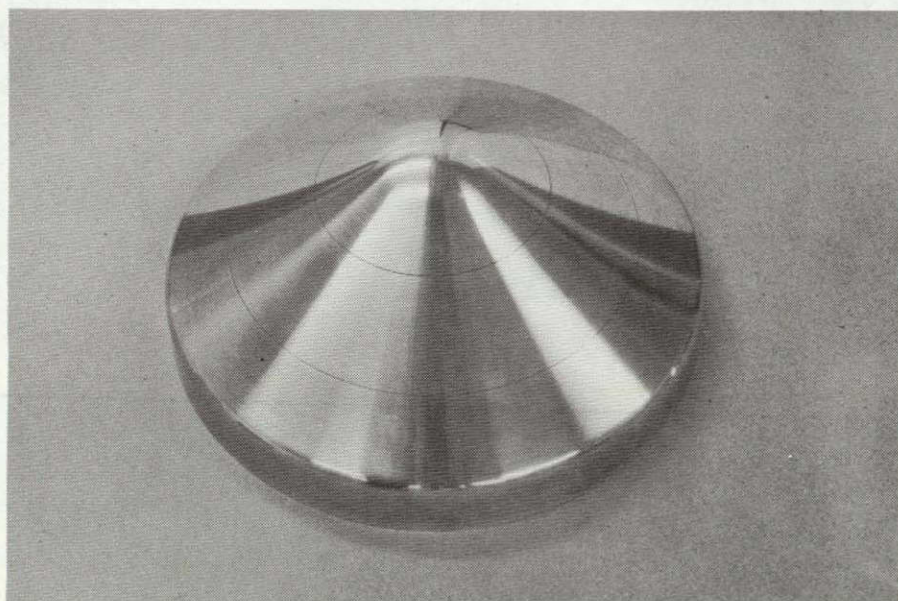
FIGURE 4.2—3   MASTER MODEL FOR 1/2 SCALE HEAT SHIELD
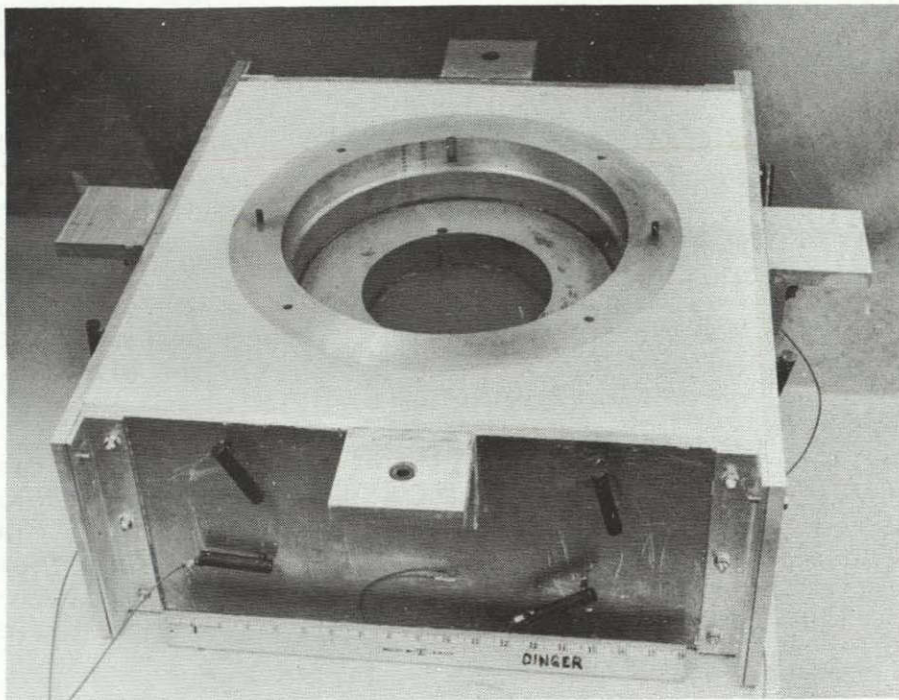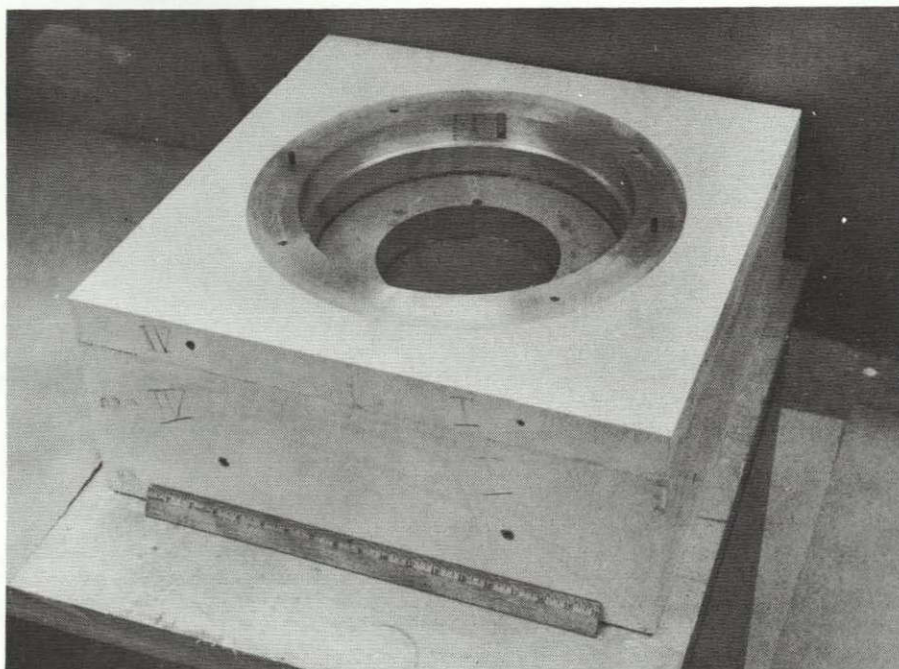
WITH MOLD FRAME

WITHOUT MOLD FRAME

FIGURE 4.2–4 PLASTER OF PARIS MOLD – 1/2 SCALE HEAT SHIELDS

dilute HCL to obtain a thixotropic material. The total batch size was 11.56 kg, of which 8.18 kg were solids and the acid addition consisted of 4 drops of a 5% HCL solution. Curves showing the rheology of the slip before and after the pH adjustment are shown in Figure 4.2-5. The shift in viscosities took place over a period of ten days.

The batch of slip weighed 10.07 kg and had a solids content of 77.5% or 7.80 kg. The conversion to aggregate slip was made by adding 1.51 kg of -40 mesh hyperpure silica powder. The coarse powder addition was made one day before the heat shield was cast and the slip was allowed to turn slowly on the ball mill overnight to completely disperse the powder (with no grinding media and a very slow milling speed, any particle size reduction is negligible). Before the heat shield was cast, viscosity measurements were taken on the aggregate slip. As shown in Figure 4.2-5 the slip had the desired thixotropic rheology.

Before casting the heat shield four quality control samples were cast. These were 3.8 cm diameter specimens cast on a flat plaster mold using plastic cylinders as forms. The 2.5 cm thick specimens cast in about 35 minutes, as expected. The specimens were removed from the mold and the plastic cylinders within 15 minutes after casting (50 minutes after pouring) and were observed to be firmly cast or set. The time to cast and completely set was evaluated
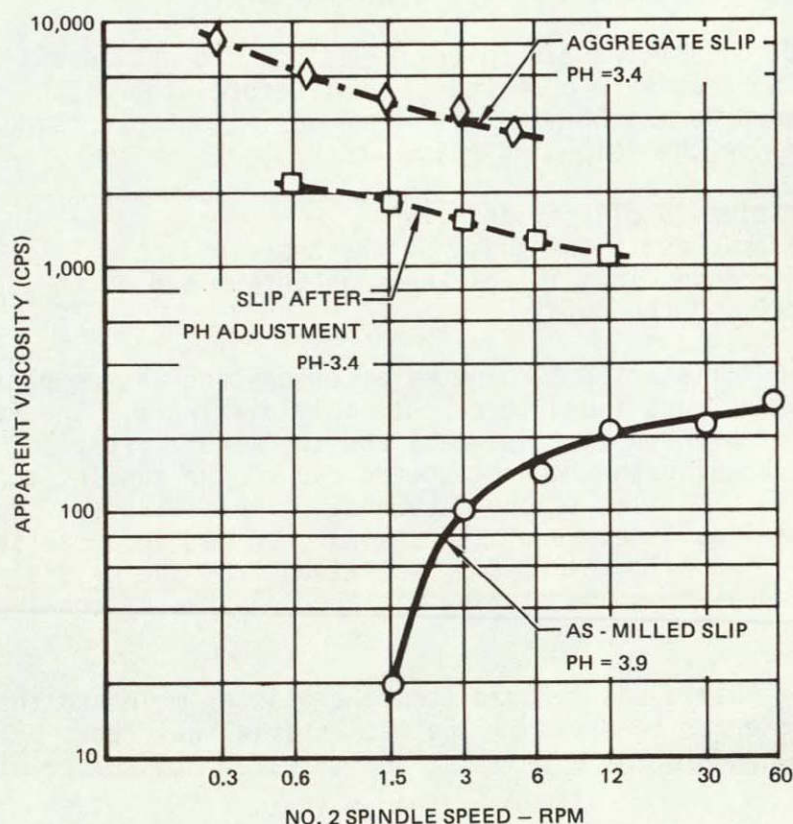
FIGURE 4.2–5 RHEOLOGY OF HYPERPURE SILICA SLIP FOR ONE HALF SCALE AGGREGATE HEAT SHIELD NO. 1

carefully because a false setting problem had been noted with very thixotropic slips in which the material appears to be cast but then deforms when support is removed from the cast wall. This problem was observed when the mandrel was removed too early during casting of AHS-1/6-5 (see Section 4.1.3).

The one-half scale plaster of paris mold was dried to constant weight to ensure a reproducible condition of dryness. One day before casting AHS-1/2-1 the mold was coated with ammonium alginate film (Superloid), to provide a contamination barrier. The male mandrel was given a high polish and three spray coatings of CAMIE 1000 dry release lubricant. Vibration was employed directly to the mandrel using the same 22.7 kg rated electrodynamic exciter as was used for the one-sixth scale coatings. The mold with mandrel in place along with the vibration equipment are shown in Figure 4.2-6.

The top 1.25 cm interior mold surface was coated with a nonabsorbing material to act as a reservoir as the liquid level dropped during casting. Aggegate slip was introduced into the mold cavity, the mandrel was immediately lowered into place, the vibration equipment connected and started. Vibration was continued for one minute and very few bubbles, indicating entrapped air, were observed to escape. Maximum force of the vibrator induced an amplitude of .127 mm in the mandrel.

The time required to cast the 2.5 cm thick heat shield wall was less than one hour. Certain areas were observed to cast before others, the actual time varying between 45 and 55 minutes. Some variation in casting rate is to be expected for the following reasons:

- o Irregularities in plaster density
- o Small differences in thickness of the Superloid mold film
- o Small differences in wall thickness as determined by the contour of the mandrel and the mold.

Raising of the mandrel started 20 minutes after casting was completed. Removal of the mandrel was found to be extremely difficult. The large area of intimate contact between the cast wall and the mandrel resulted in large adhesive forces. Forcing the mandrel upward caused the casting to deform. It sagged in a manner similar to the occurence of the false set experience earlier. The semi-liquid nature of the silica resulted in a partial vacuum between it and the mandrel, which made separation from the mandrel difficult. Removal of the mandrel from the casting was accomplished by cooling it with dry ice.

The resulting heat shield was removed from the plaster mold and the silica material reclaimed prior to drying. The wet material was reconverted to aggregate slip by addition of a small amount of water and tumble milling slowly overnight.

Additional design work was done in an effort to solve the problem of releasing the mandrel from the cast heat shield. The major factors affecting this problem were:
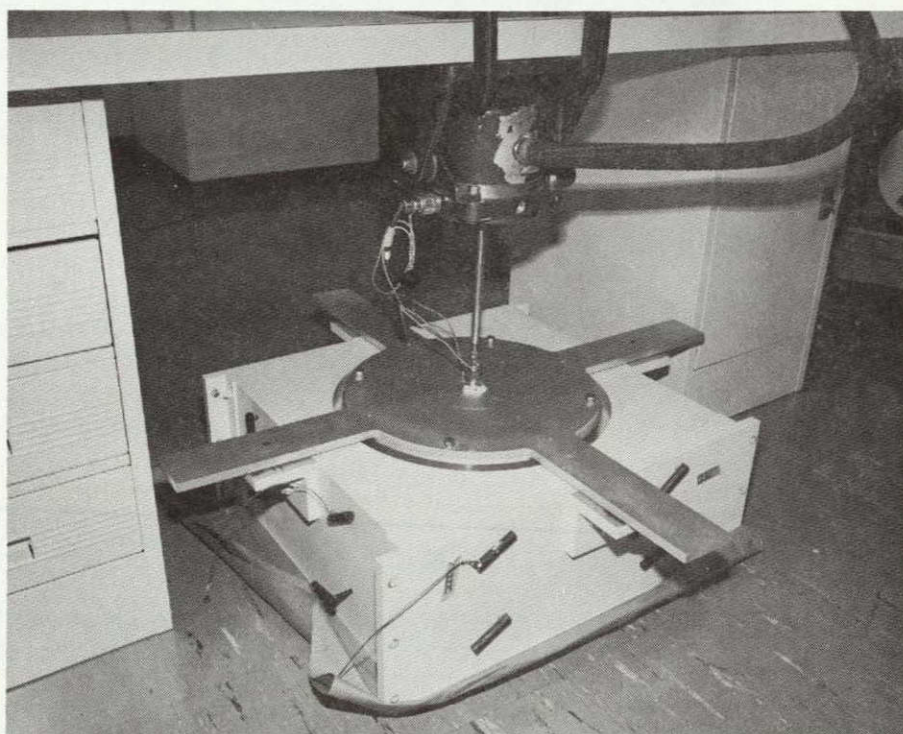
FIGURE 4.2–6 MOLD SETUP FOR CASTING 1/2 SCALE HEAT SHIELD NO. 1

o The mandrel must be removed soon after casting to prevent cracking of the shield by shrinking against the mandrel.

o Support must be maintained against the cast wall until it is fully set or cast.

o Considerable adhesive forces develop due to intimate contact of the wet casting and the mandrel (partial vacuum).

4.2.3 ONE-HALF SCALE AGGREGATE CAST HEAT SHIELD NO. 2

The one-half scale male mandrel was modified (see Figure 4.2-7) to provide for release from the casting slip. It consists of a layer of low modulus foam rubber attached directly to the mandrel followed by a double layer of cloth and a thin nonpermeable bladder. The foamed rubber acts as a strain relief material, for the heat shield-mandrel interface, if any drying shrinkage occurs before the mandrel is raised. The double layer of dry cloth provides for release of the mandrel and the nonpermeable bladder keeps the cloth layers dry and also prevents contamination of the hyperpure slip by the foam rubber and the mandrel.

The rubber material was 1.57 mm (.062") thick AM3195 GW1000 foam rubber. This material was cut into strips and attached to the entire mandrel surface using a silicone pressure sensitive adhesive, Dow Corning's DC282. Two layers of No. 120 fiberglass cloth were stretched over the rubber, each cloth layer being .127 mm (.005") thick. The nonpermeable bladder was previously prepared by stretching a layer of No. 120 cloth over the mandrel and brush coating with 5 layers of DC92-009 silicone dispersion coating. Thickness of the bladder was .254 mm. Before final installation, the bladder was tested for water penetration and reactivity with the hyperpure silica slip and found to be nonpermeable and compatible with the silica slip. Total thickness of the mandrel and modification including the foam rubber, cloth layers, and bladder was 2.08 mm. The resulting heat shield would, therefore be about 8% thinner than the intended 2.5 cm..
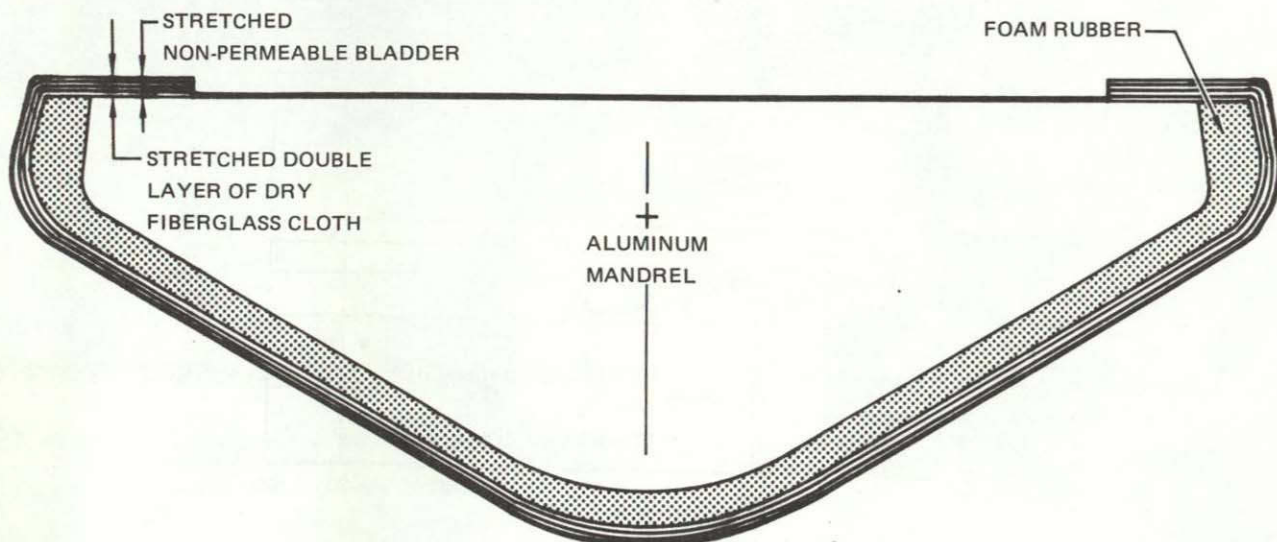
FIGURE 4.2–7 MODIFIED ONE HALF SCALE MALE MANDREL

The aggregate slip reclaimed from AHS-1/2-1 was known to be contaminated from contact with the mold and mandrel. The contaminated slip retained a thixotropic rheology but the absolute viscosity numbers were much higher than before reclaimation. The material was adjusted to a slightly lower solids content (79.9% including the aggregate particles) but the viscosity remained higher than for AHS-1/2-1 casting as shown in Figure 4.2-8. The slip was noticeably stiffer than before reclaiming. Any additional lowering of the solids content would affect other processing variables such as casting time and drying shrinkage.

The casting method for AHS-1/2-2 were altered from that used for AHS-1/2-1. Vibration was not used and the casting was not "topped off", meaning additional slip was not added as the liquid level of the slip dropped during casting. The failure to top off caused several problems with AHS-1/2-2. Large void areas formed on the inside surface of the shield between the cast wall and the mandrel as the liquid slip available was depleted. It was difficult to judge the actual casting time as the top area of the casting was thin (no topping off) and appeared to be cast in about 20 minutes. Rapid drying of the thin upper portion of the shield resulted soon after casting. After 2 hours the mandrel was raised and it released without any problems. At this point, the cracking was observed.

Despite the poor quality of the inside surface and the visible cracks, it was decided to humidity dry AHS-1/2-2 to gain experience with this process. The specially fabricated humidity drying chamber shown in Figure 4.2-9 was placed over the mold containing the heat shield and sealed to the floor. The baffles in the chamber were left closed and the relative humidity in the chamber raised to virtually 100% in about 2 hours. A hygrometer placed inside the chamber read a maximum of 93%, but the actual humidity was at or near 100% based on the condensation formation on the inside walls. The humidity readings drop from the 93% to about 45% (normal ambient conditions) in 10 days by gradually opening the baffles. The rate of humidity drying is shown in Figure 4.2-10.
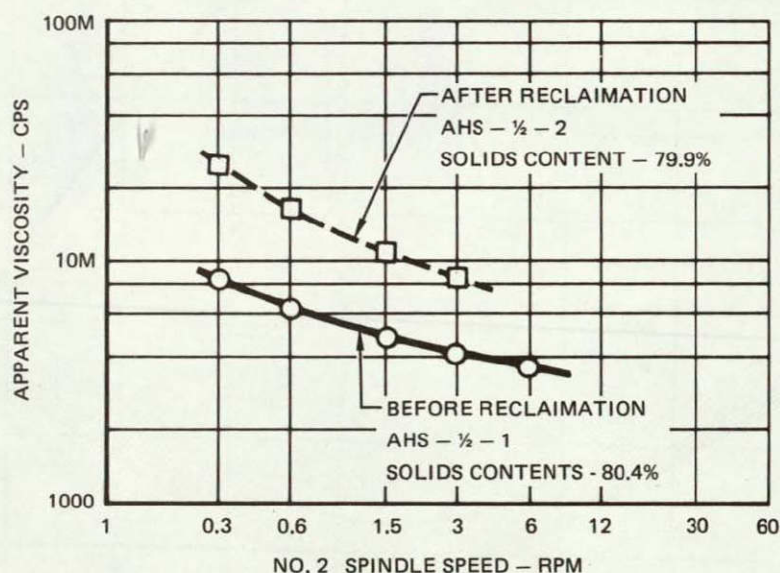
FIGURE 4.2—8 RHEOLOGY OF RECLAIMED AGGREGATE SLIP
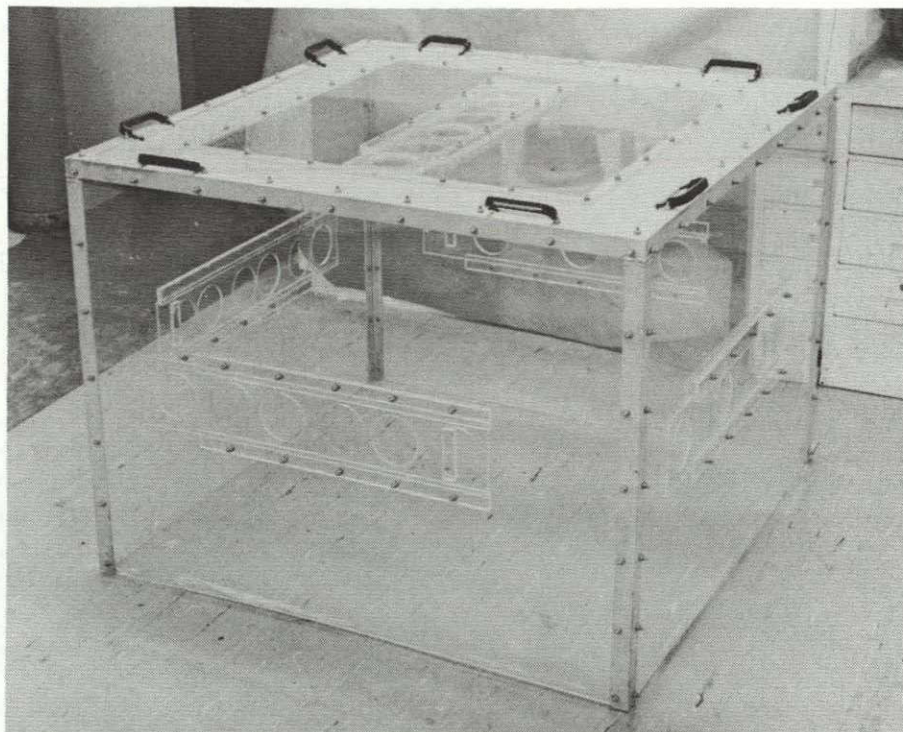
FIGURE 4.2—9 HUMIDITY DRYING CHAMBER

DAYS AFTER CASTING
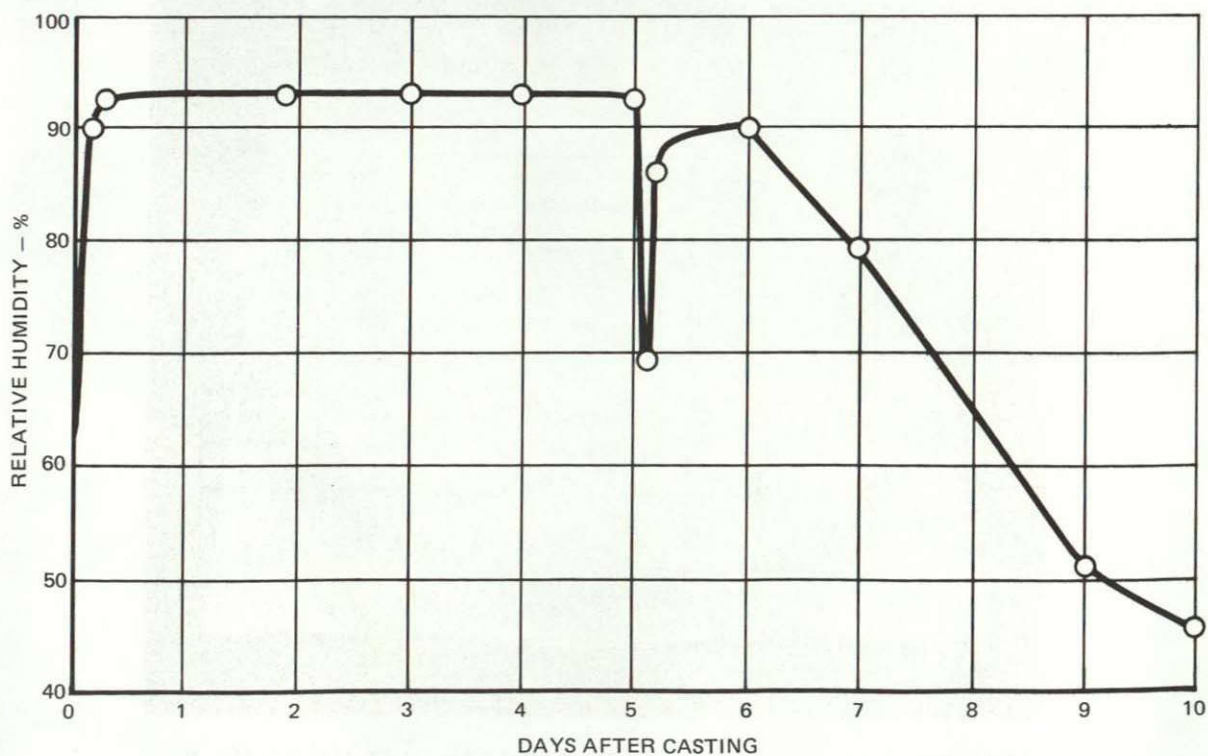
FIGURE 4.2—10 HUMIDITY DRYING RATE — HALF SCALE HEAT SHIELD NO. 2

The downward spike in the humidity curve on day 5 occurred during the inside surface repair of the shield as the baffles were opened. Several large air bubbles were present on this surface due to air entrapment in the highly viscious slip. These voids were filled with the reclaimed aggregate slip from which the shield was cast. An attempt was made to repair cracks by removing material around the crack and refilling it with slip. After the shield was removed from the humidity drying chamber it continued drying in the mold at room temperature. After three days it was removed from the mold and placed in a firing setter fabricated from fused silica foamed blocks lined with Astroquartz cloth. The edge of the shield was cleaned with a high speed grinding tool and smoothed with SiC sand paper. A photograph of AHS-1/2-2 at this stage is shown in Figure 4.2-11.

The green strength of hyperpure silica castings is known to decrease during drying and is at a minimum when totally dry. As drying of this shield continued several additional large cracks were noted. These cracks propagated and widened as the shield dried and the green strength was lowered. The shield, when completely dry, was literally full of cracks and broke into several pieces during handling.

A study of the processing of AHS-1/2-2 lead to the following list of items which may have caused or contributed to the formation and/or propagation of cracks.

1) Not topping off the shield during casting - the upper part of the shield cast and dried early causing differential shrinkage.
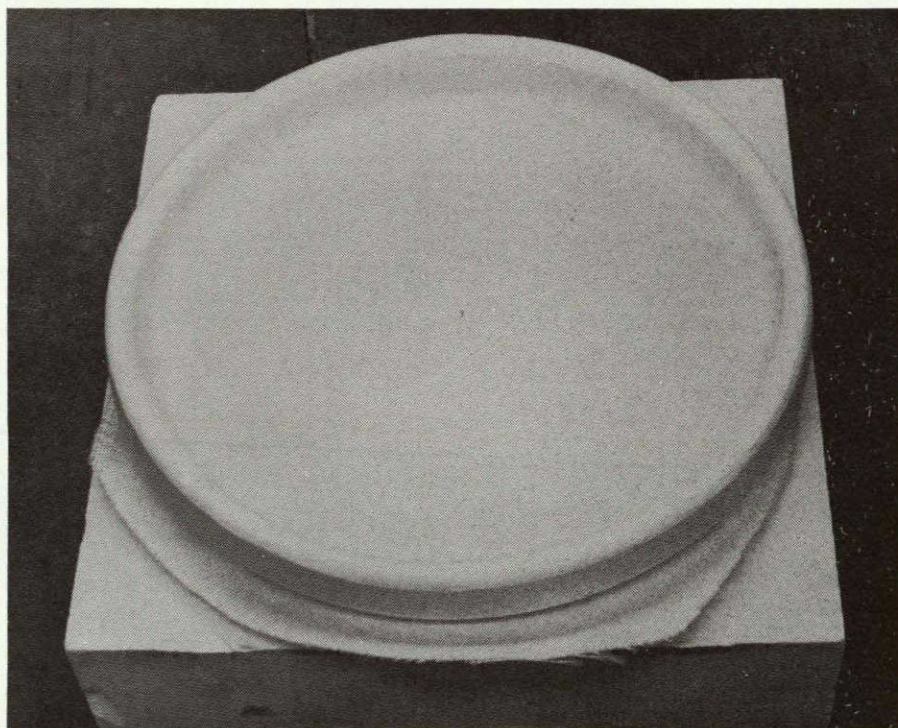
FIGURE 4.2-11 1/2 SCALE AGGREGATE CAST HEAT SHIELD NO. 2 — ROOM TEMPERATURE DRYING

45

2) Waiting too long to remove the mandrel from the shield-stresses may have developed in spite of low modulus foam rubber.

3) Too rapid drying after removing the mandrel - it took 2 hours for the humidity chamber to reach maximum humidity.

4) Repairing the shield after it had partially dried for 5 days creating stresses due to shrinkage of the patched area.

5) Grinding to clean up the top edge of the shield with a high speed grinding tool.

The larger pieces of AHS-1/2-2 which were still intact were fired in order to gain experience with the use of the large furnace required for firing one-half scale and full scale heat shields. A photograph of this hevi-duty Lindberg Furnace is shown in Figure 4.2-12. The sections of AHS-1/2-2 were fired for five hours at 1230°C (2250°F) with a six-hour heat-up time. A total of six pieces were fired, the largest being about a 15 cm x 25 cm rectangular section.

Before firing, the parts were covered with a layer of Astroquartz cloth. Upon removal from the furnace, a black particulate contamination was present on the cloth and had also filtered through the cloth to the surface of the parts. The particles were apparently from the heating elements or the furnace roof. Additional protection was obviously needed for firing of future shields.
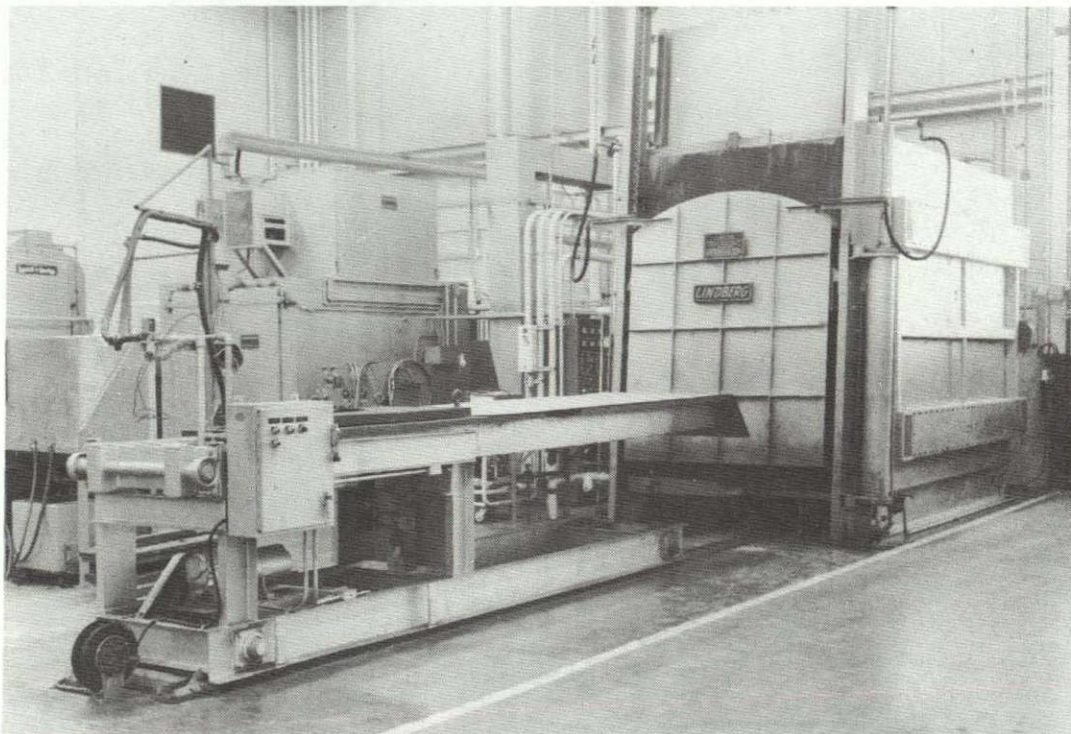
FIGURE 4.2—12 HEVI-DUTY LINDBERG FURNACE

ORIGINAL PAGE IS

Several new cracks were visible after firing, particularly starting from the inside surface of the shield. Most of these cracks appeared to be only a surface condition, although some extended nearly through the total thickness, indicating they might have been a result of repairing the inside surface.

Average firing shrinkages of about 4% were measured. The shrinkage was expected to be only 1.5 to 2%. The high firing shrinkage may have been due to the use of the reclaimed, contaminated slip or the long heat-up and cool-down times associated with the large Lindberg furnace. Prior to firing the next shield it was decided that extensive test runs would be made to determine the firing parameters required for controlled firing shrinkage.

4.2.4 ONE HALF SCALE AGGREGATE CAST HEAT SHIELD NO. 3

A new batch of aggregate slip for AHS-1/2-3 was milled for 72 hours in a 5 gallon container. It had the standard 10 μm average particle size distribution, as shown in Figures 3.1-2 and the pH was 3.9. The slip was aged and the pH lowered to 3.4 to acheive the desired thixotropic rheology. The aggregate particles were added to the slip one day before the heat shield was cast. Solids content of the slip was 77.7% and addition of the aggregate particles increased the content to 80.6%. The rheology of the aggregate slip as measured before AHS-1/2-3 was cast is shown in Figure 4.2-13 along with the rheology for the slip used for AHS-1/2-2 for comparison. The slip for AHS-1/2-3 was more fluid during pouring, even though the solids content was higher than AHS-1/2-1. High solids content is desirable in order to increase the casting rate, minimize the false setting and drying shrinkage.

Threaded rods were added to the mold frame to provide for controlled lowering and raising of the mandrel.

AHS-1/2-3 was poured in about 15 minutes and the mandrel lowered into position in 5 minutes. Additional slip was added to the top of the shield to assure a uniform thickness and to prevent premature drying. The wall thickness of the heat shield appeared to be completely cast within 25 minutes after the mandrel was in position. Damp cloths were immediately placed around the exposed lip of the shield in order to retard the edge drying rate. The mandrel was left in position for seven minutes and then slowly raised. When it was apparent that the heat shield was completely solidified and was not going to deform, the mandrel was rapidly removed. A layer of mylar was placed over the shield and the humidity drying chamber positioned over the mold and casting. The drying chamber was in place and sealed 15 minutes after casting was completed.

The relative humidity inside the drying chamber was raised by introducing water vapor from boiling water. The relative humidity was raised from the 60% ambient condition to 70% within 5 minutes to 88.5% within 70 minutes and 90% after 2 hours at which time water vapor addition was terminated. The day after casting the indicated humidity was 92.5%. The drying chamber doors were opened and the mylar, cheesecloth, and bladder were removed from the shield. The thickness of the shield was uniform except for a small rippled area caused by wrinkling of the bladder. Some small air bubbles were noted on the inside surface. A photograph showing AHS-1/2-3, the mold, and the relative humidity gauge in the humidity drying chamber is given in Figure 4.2-14.
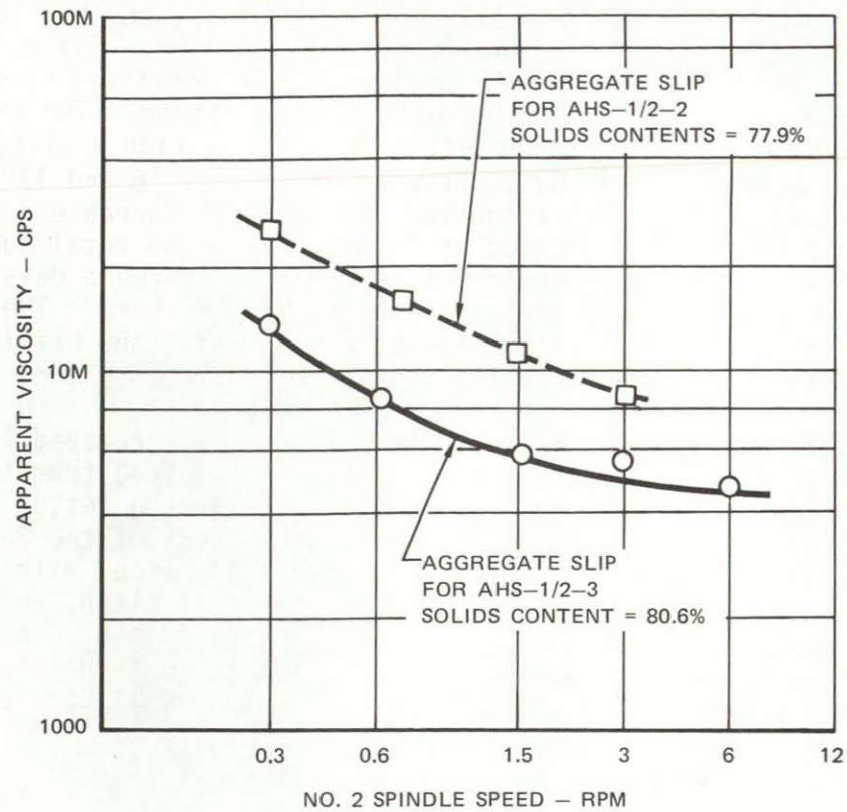
FIGURE 4.2–13 RHEOLOGY OF AGGREGATE SLIP USED FOR CASTING
1/2 SCALE HEAT SHIELD NUMBER 3
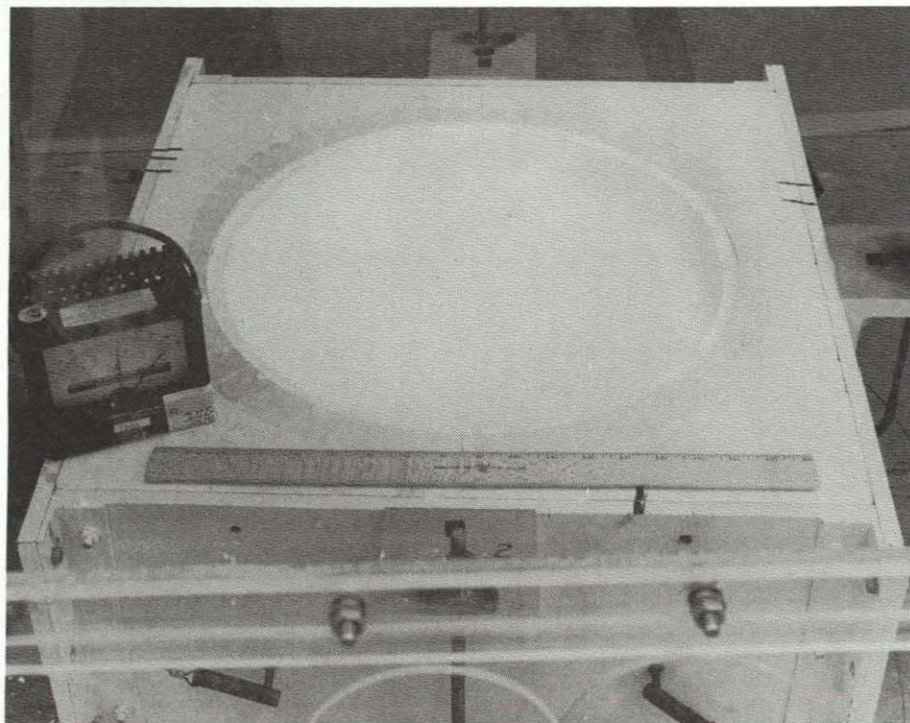
FIGURE 4.2–14 1/2 SCALE AGGREGATE CAST HEAT SHIELD DURING HUMIDITY DRYING

48

The drying chamber was completely sealed for a period of four days and the relative humidity remained at 92.5 to 93%. After four days, the baffles in the sides and top of the chamber were daily opened a small fraction. The rate of decrease in the indicated relative humidity in the chamber is shown in Figure 4.2-15 along with the distances which the breathing baffles were opened. The relative humidity in the room outside the chamber was checked daily with a sling psycometer and it remained between 53 and 59%. Between drying day 16 and 17 the room humidity increased to 73% which accounted for the 4.5% increase in chamber humidity at that time. As indicated in Figure 4.2-15 the total humidity drying cycle was 26 days. The drying could not be monitored between days 22 and 26, therefore the chamber was completely closed during this time. The chamber humidity climbed to 91%. Within 90 minutes of reopening the baffles on day 26 the chamber humidity dropped to nearly room condition.

On the 26th day of drying, the mold and heat shield were removed from the humidity drying chamber and the heat shield was manually lifted from the mold onto the silica firing setter (dome down position). The firing setter had been machined to a 30° contour to provide for maximum support of the 30° external surface of the shield. The machined firing setter was lined with 2 layers of 2mm (0.080") thick fiberfrax paper, 1 layer of Refrasil cloth, and 1 layer of No. 593 Astroquartz cloth to act as a cushion for the shield. The Superloid mold release coating adhered to a major portion of the external surface of the heat shield. This film is normally removed (though it will burn away during firing) because it may contain contaminates from the plaster mold. Because of the fragile heat shield, it was decided not to remove this alginate film. A photograph of AHS-1/2-3 after removal from the mold is shown in Figure 4.2-16.
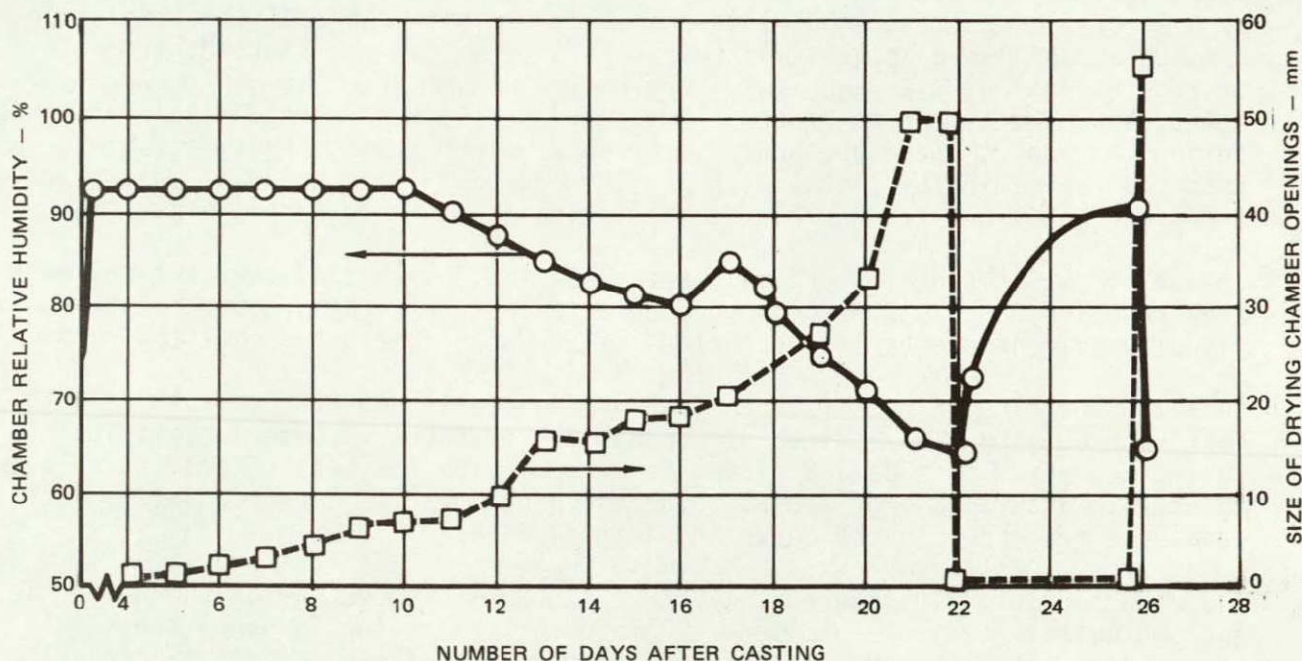
FIGURE 4.2–15 HUMIDITY DRYING RATE OF 1/2 SCALE HEAT SHIELD NO. 3
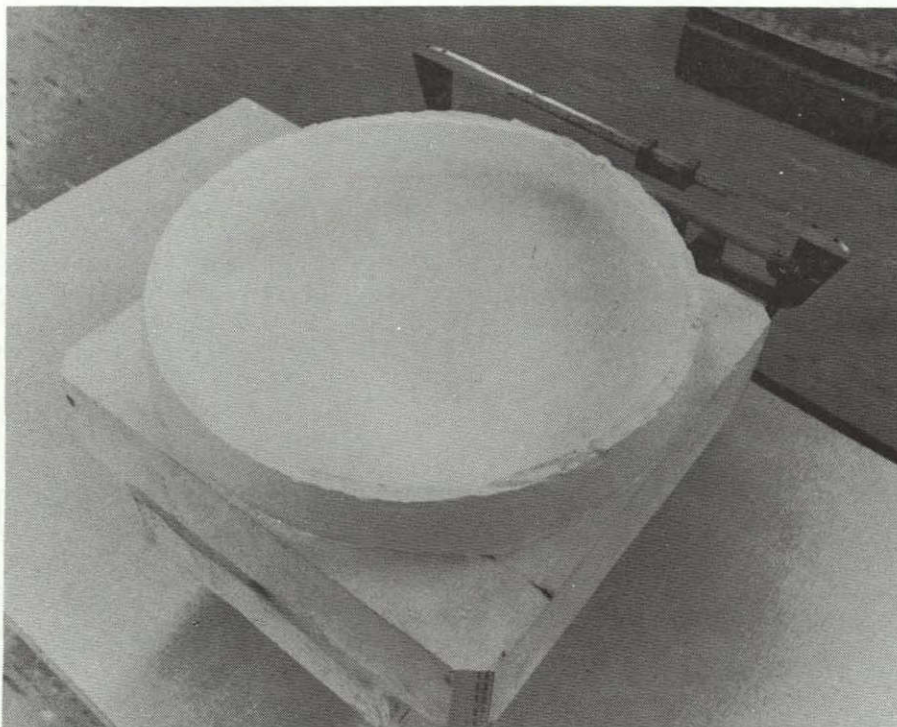
FIGURE 4.2–16 1/2 SCALE HEAT SHIELD NO. 3 AS REMOVED FROM CASTING MOLD

The weight of the heat shield after removal from the mold was 8.49 kg (18.7 lb). The shield drying was continued at room temperature for eight days and followed by oven drying at 121°C (250°F) to a constant weight. An additional moisture weight loss of 295 g or 3.5% was measured. The as cast moisture content of aggregate castings was about 16%. Drying in the humidity chamber therefore removed about 78% of the moisture in the casting, the remaining 22% being removed during the room temperature and oven drying. After drying, the heat shield was prepared for firing by lightly sanding the edge with fine grain SiC sandpaper. A photograph of AHS-1/2-3 prepared for firing is shown in Figure 4.2-17.

The shield was X-rayed extensively before firing. X-rays of the critical edge area revealed no cracks. Voids were detected on the X-rays, however, they were visually evident on the inside surface of the heat shield and could be removed.

Quality control specimens (3.8 cm (1.5") in diameter and 2.5 cm (1.0") thick) cast with AHS-1/2-3 were fired at various temperatures to determine firing shrinkage. From this data a firing temperature for the heat shield was selected to achieve a shrinkage of 1.5-2%. The shrinkage results for the quality control specimens are shown in the curve in Figure 4.2-18.

A firing schedule of 5 hours at 1190°C (2175°F) was selected for the heat shield and two quality control specimens. Before setting in the furnace, the shield was covered with one layer of Astroquartz cloth and three layers of Refrasil cloth. The temperature-time history for firing the heat shield is shown in Figure 4.2-19.
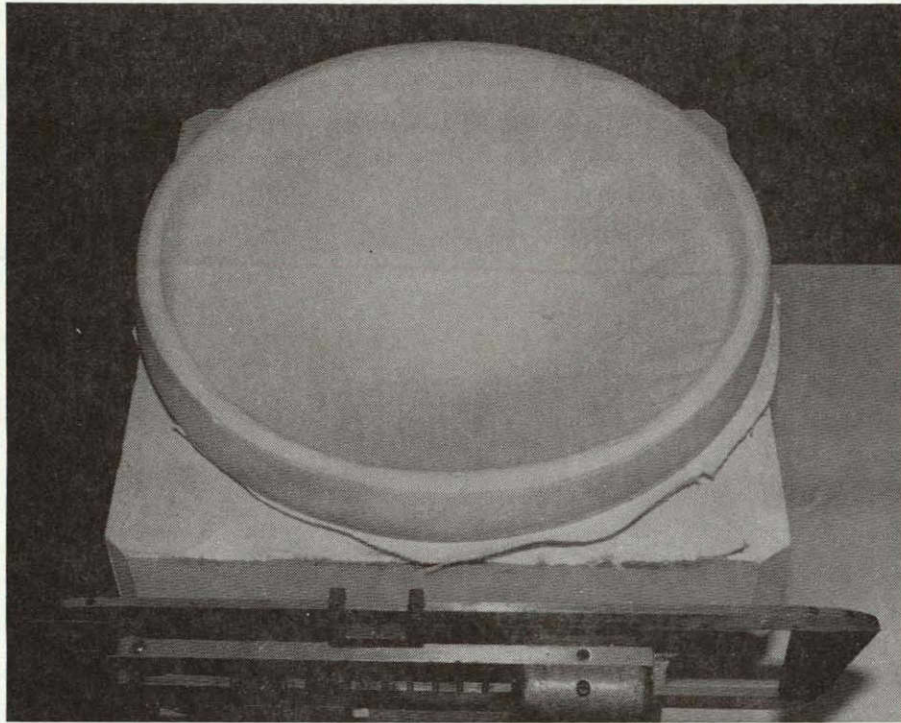
FIGURE 4.2—17 1/2 SCALE HEAT SHIELD NO. 3 PREPARED FOR FIRING

A photograph of AHS-1/2-3 and the firing setter upon removal from the furnace is shown in Figure 4.2-20. After firing, the shield was again x-rayed extensively and determined to be crack-free. Gas voids were again evident, virtually all of which were surface voids. The firing shrinkage of the heat shield was determined to be 1.6%, based on measurement of the diameter before and after firing. The quality control specimens had a 2.0% average shrinkage. Slightly lower shrinkage of the heat shield was expected because of its greater mass. The measured outside diameter of the fired shield was 44.25 cm (17.422") or 0.4% smaller than the intended diameter of 44.45 cm (17.50").

Examination of the external surface of the heat shield revealed the presence of surface voids which are patterned concentrically in three rows. The concentric nature of the voids and their location (near the point of the dome) indicated air entrapment during rapid casting. It is believed that these can be eliminated by introducing the slip into the mold at a slower rate and with a smoother flow. The absence of this type of void higher up on the external surface, or near the edge of the shield, indicated that the slow smooth immersion of the mandrel into the slip caused no air entrapment.

The external surface of the heat shield had a thin 0.1mm (.005") layer of surface devitrification. The devitrification resulted from the Superloid mold release coating which adhered to the heat shield surface when it was removed from the mold. The devitrification was somewhat heavier in three small localized areas. Final machining of the heat shield to remove this devitrification was not performed.

51
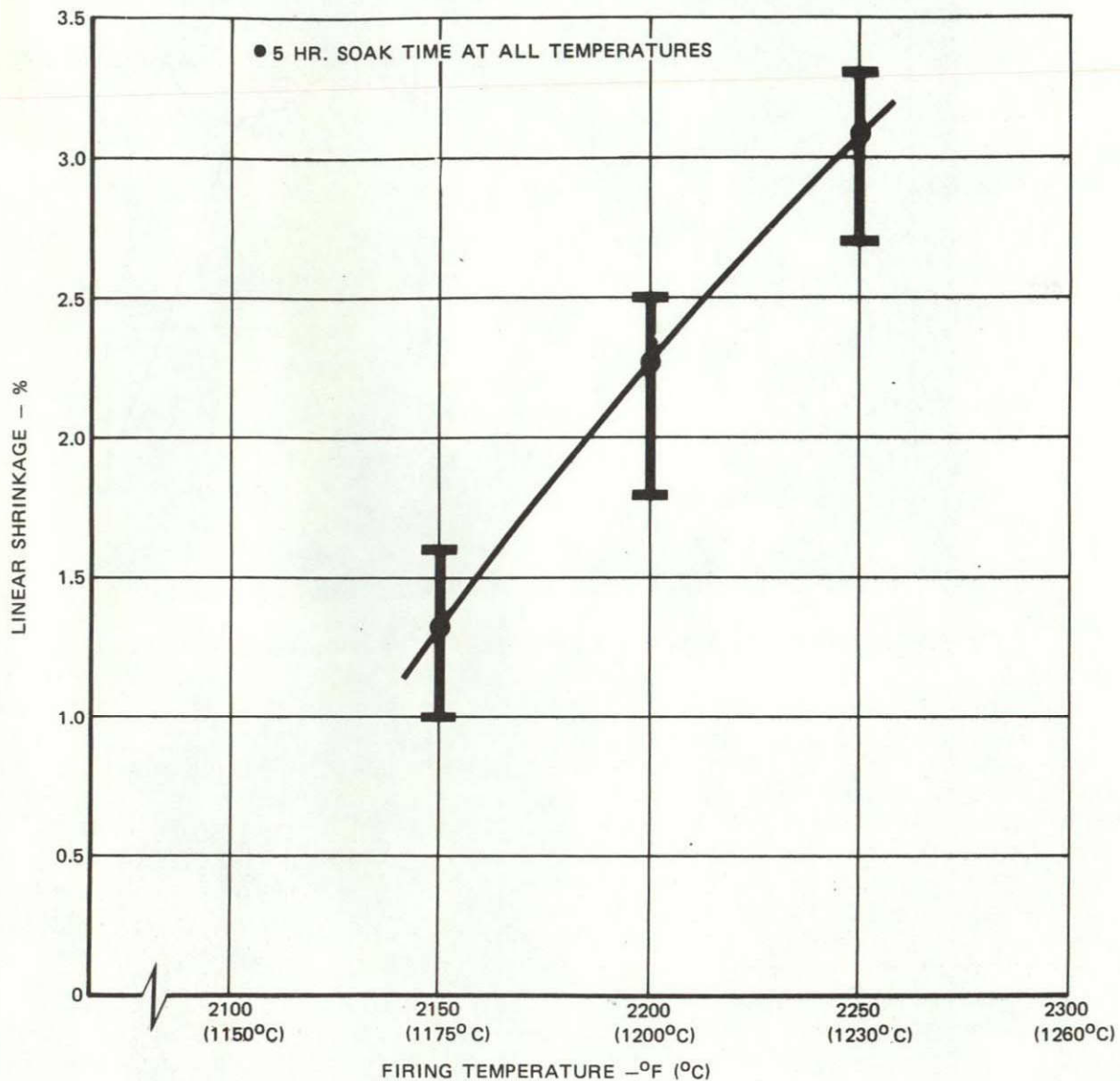
FIGURE 4.2—18 FIRING SHRINKAGE OF QUALITY CONTROL SPECIMENS
FOR ONE HALF SCALE HEAT SHIELD NO. 3
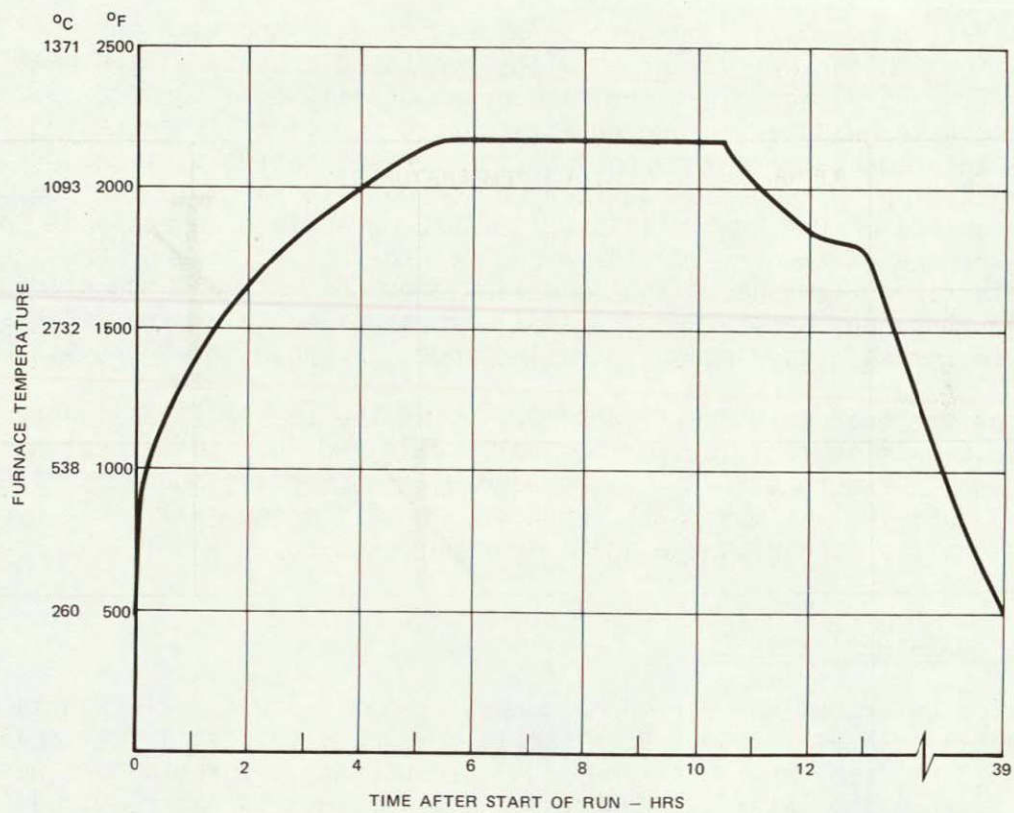
FIGURE 4.1—19 TEMPERATURE HISTORY FOR FIRING OF ONE HALF SCALE HEAT SHIELD NO. 3
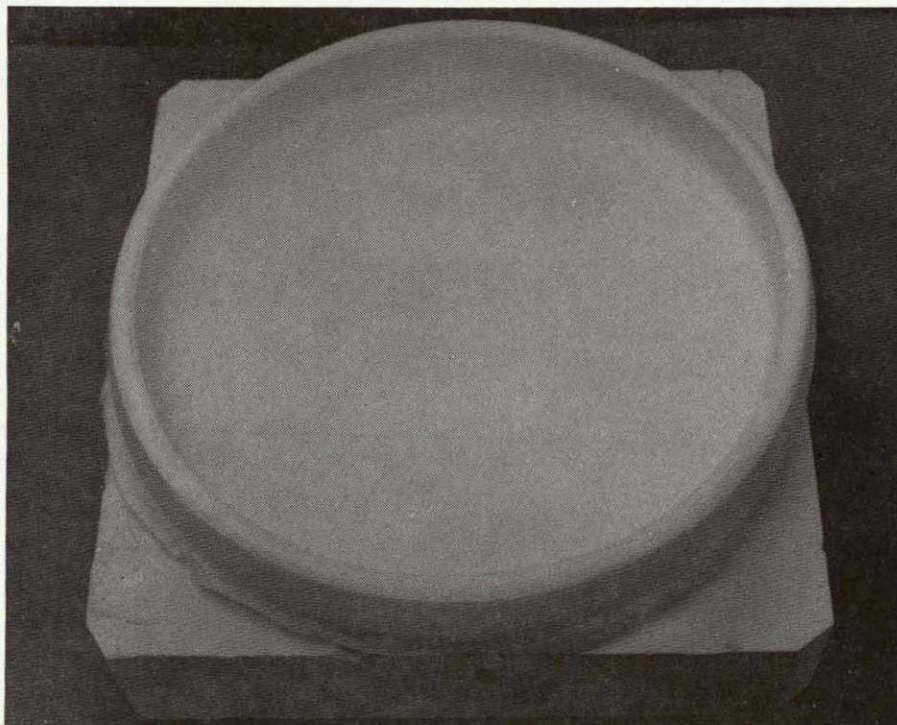
FIGURE 4.2—20 1/2 SCALE HEAT SHIELD NO. 3 AFTER FIRING

The density of both quality control specimens fired along with the heat shield was 1.63 g/cc (101.5 lb/ft^3), which means the fired density of the heat shield is 100 lb/ft^3 presuming it has the same green density of 1.53 g/cc (95.5 lb/ft^3). Reflectance data measured on one quality control specimen is presented in Figure 4.2-21. Measurements were made on both the top and bottom surfaces prior to any machining. The bottom surface corresponds to the mold surface or the external surface of the heat shield while the top surface corresponds to the internal surface of the shield. As expected, the reflectance of the as-processed surfaces is rather low due to contamination from the mold and the atmosphere in the firing furnace. Machining of a small amount of material from each surface resulted in a much higher measured reflectance, as shown in Figure 4.2-21.

The edge of the heat shield was machined, using the specially designed and fabricated machining facility for one half scale and full scale heat shields, and is shown in Figure 4.2-22. High speed diamond tooling and very high purity water (MMS 606) coolant was used. Photographs of the one half scale hyperpure heat shield after machining are shown in Figure 4.2-23.

4.3 FULL SCALE HEAT SHIELD

This section describes the work done toward casting a full scale aggregate cast hyperpure silica heat shield. No attempts were made to cast a full scale heat shield (89.8 cm diameter x 5.74 cm thick) because the program effort was redirected to improve the material toughness. However, 90% of the required tooling was completed including fabrication of the plaster of paris mold and enough hyperpure slip was prepared to cast one full scale heat shield.

BOTTOM SURFACE
EXTERNAL SURFACE OF HEAT SHIELD

TOP SURFACE
INTERNAL SURFACE OF HEAT SHIELD

FIGURE 4.2-21 REFLECTANCE DATA FOR QUALITY CONTROL SPECIMEN
PROCESSED WITH 1/2 SCALE HEAT SHIELD NO. 3

54

FIGURE 4.2—22 FACILITY FOR MACHINING 1/2 SCALE AND FULL SCALE
HYPERPURE SILICA HEAT SHIELDS

55

FIGURE 4.2–23   1/2 SCALE AGGREGATE SLIP CAST HYPERPURE FUSED SILICA HEAT SHIELD

4.3.1 TOOLING FABRICATION

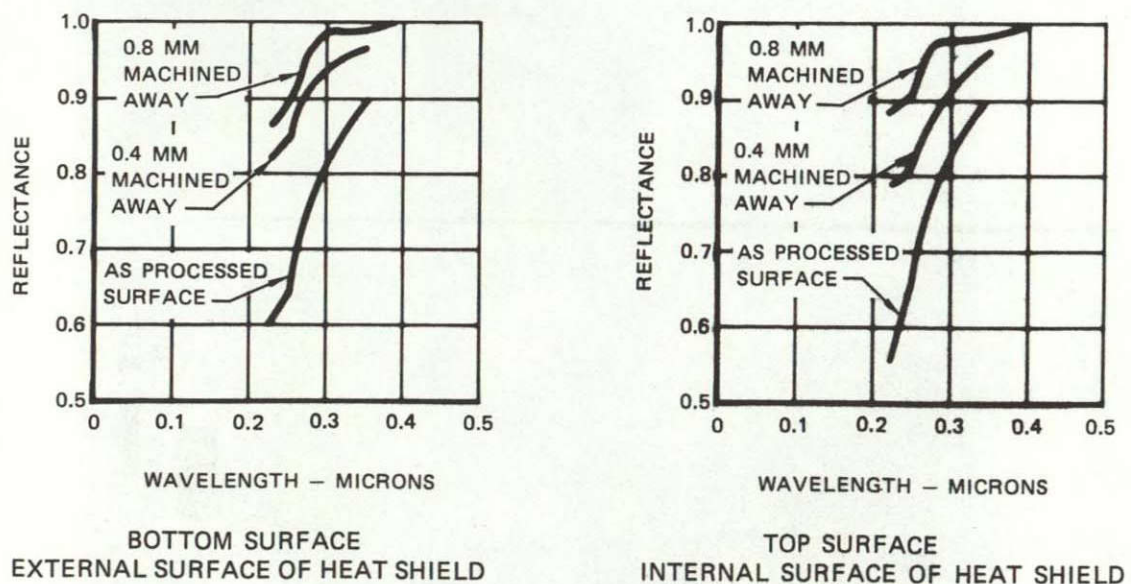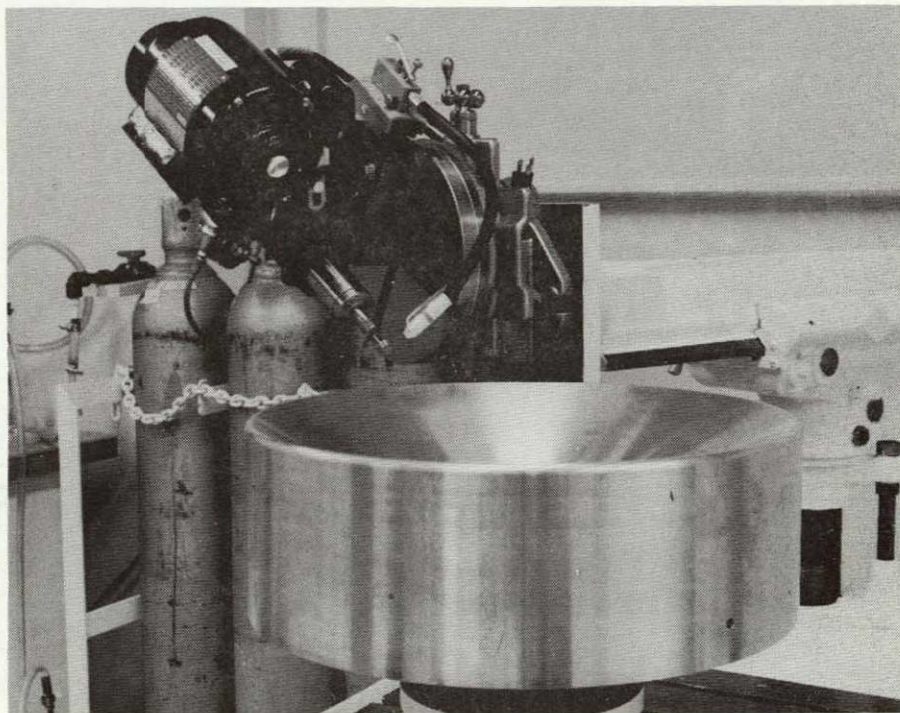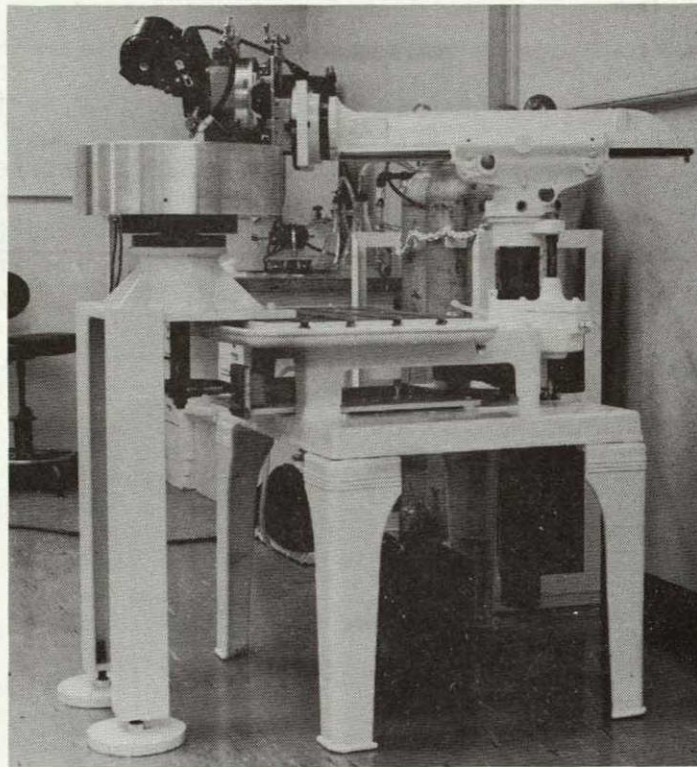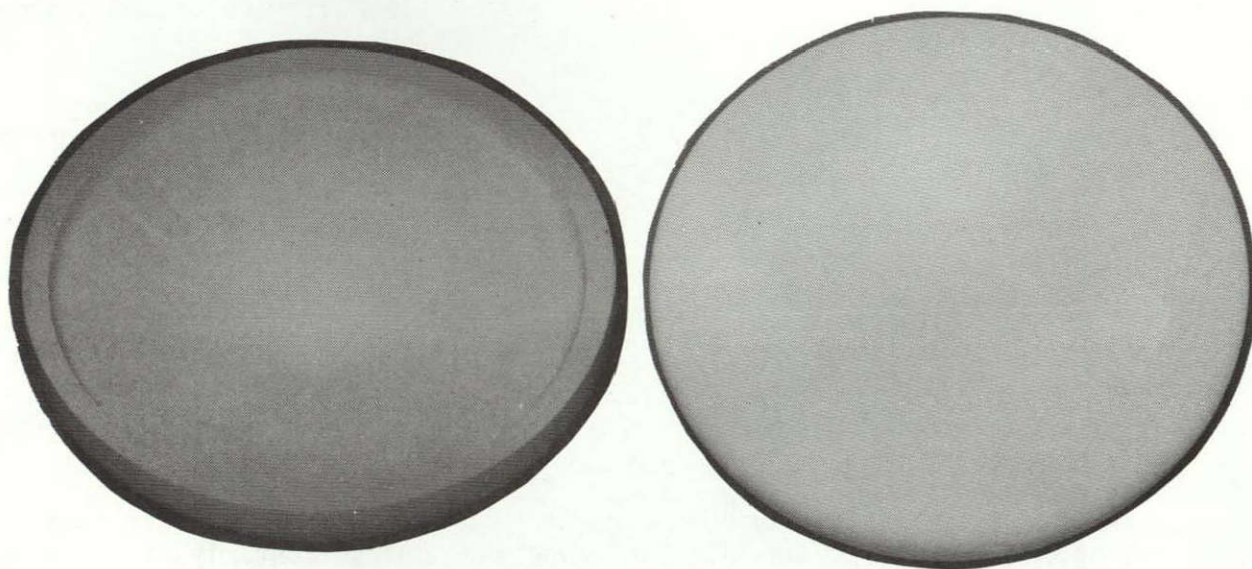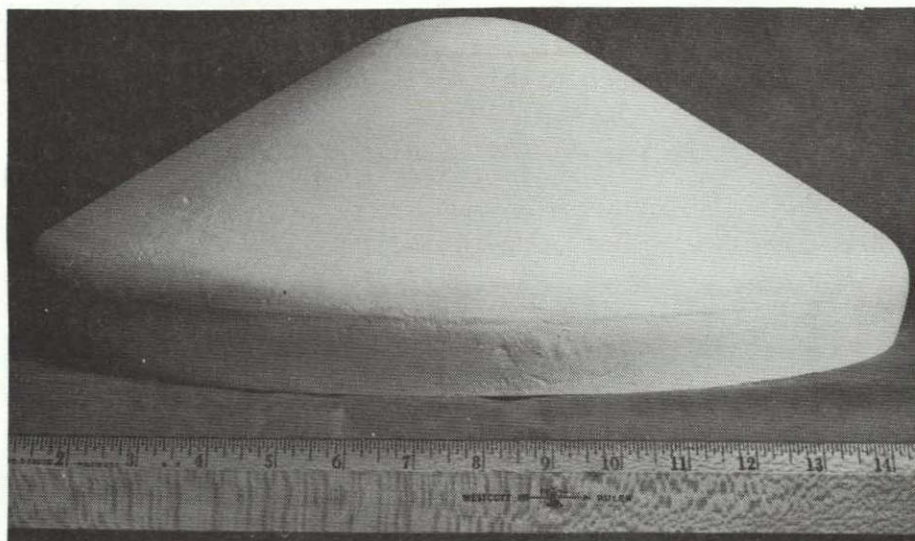The design of the casting mold and male mandrel for casting full scale shields were similar to the one half scale mold and mandrel design. The size of the aluminum mandrel was adjusted to allow for the use of the mandrel releasing materials (foam rubber, dry cloth layers, and nonpermeable bladder) used on the second and third one half scale shields. Also, the design of the mold and firing setter for the full scale heat shield was changed to provide for removal of the Superloid layer from the external heat shield surface prior to firing. Adherence of this material to one half scale shield number 3 resulted in surface devitrification. The full scale mold is an eight piece mold with four top sections which can be removed without moving the casting (See Figure 4.3-1). The bottom part of the mold is made in four quarter sections. The firing setter is also designed in four quarter sections. Therefore, one quadrant of the mold can be removed and replaced with a quadrant of the firing setter. This eliminates the need to manually lift the heat shield and provides for the removal of any Superloid material adhering to the heat shield surface.

Fabrication of the aluminum master model and male mandrel was done in a manner similar to that used for the one half scale master model and mandrel (see section 4.2.1). Aluminum rings were rough cut to a predetermined size and bonded together with American Cyanamid FM-123-2 adhesive. Design drawings showing the layout of the rings and the machining specifications for the full scale master model and mandrel are shown in Figures 4.3-2 and 4.3-3, respectively. Figure 4.3-4 shows a photograph of the full scale machined master model along with the master models for the one half scale and one sixth scale heat shields. A photograph of the full scale male mandrel is shown in Figure 4.3-5.

The full scale plaster of paris mold was cast from U.S. Gypsum No. 1 pottery plaster by methods as described in Section 4.2.1 and Reference 3. Photographs of the full scale mold are shown in Figure 4.3-1. As shown in these photographs the master model had been placed in the mold for storage purposes with a layer of mylar between the aluminum and the plaster to prevent contamination of the mold by aluminum corrosion.

4.3.2 RAW MATERIAL AND SLIP PREPARATION

At the outset of the program a total of 272 kg (600 lb) of high purity silica raw material was ordered. This was a conservative estimate of the total material requirement of the scale-up program. This material was ordered from Dynasil Corporation of America, Berlin, New Jersey. The order was for the scrap or "swiss cheese" material which was purchased at a considerably lower cost than the normal optical grade of Dynasil. Excluding the surface contaminants (refractory, machining waxes, etc.), the scrap material is chemically the same as the optical grade material. A process was developed for removing the surface contaminants. Even with this added process, the reduced material cost resulted in a 64% cost savings.

Of the 272 kg of material ordered, a total of 211 kg was cleaned, inspected and crushed to -40 mesh powder. The -40 mesh powder is the size of the ball mill charge for milling hyperpure silica slip and is also the size of the coarse

particles added to make aggregate slip. Of the 211 kg of -40 mesh hyperpure powder prepared, about 23 kg was used as hyperpure aggregate slip for casting the one-sixth scale shields, 24 kg was used as aggregate slip for casting the one-half scale heat shields and 97 kg of -40 powder was used to prepare hyperpure silica slip for use in casting a full-scale heat shield before the program effort was redirected as described in Section 5.0.
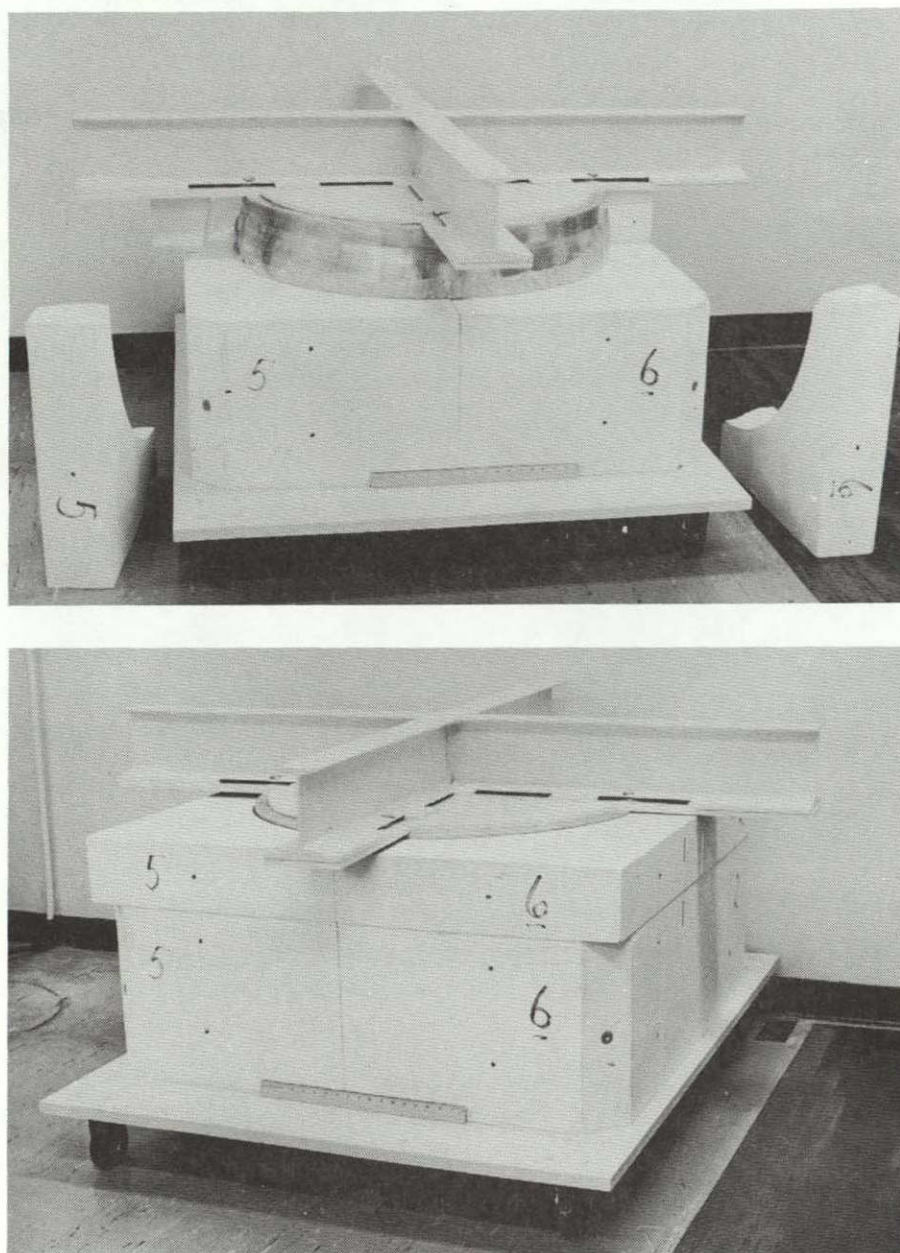
FIGURE 4.3—1 PLASTER OF PARIS MOLD (AND MASTER MODEL) FOR
AGGREGATE CASTING FULL SCALE SILICA HEAT SHIELDS

FIGURE 4.3—2   DESIGN DRAWING OF MASTER MODEL FOR FULL SCALE SLIP CAST SILICA HEAT SHIELDS

FIGURE 4.3—3   DESIGN DRAWING OF MALE MANDREL FOR FULL SCALE SLIP CAST SILICA HEAT SHIELDS

FIGURE 4.3—4   MASTER MODEL FOR 1/6 SCALE, ½ SCALE, AND
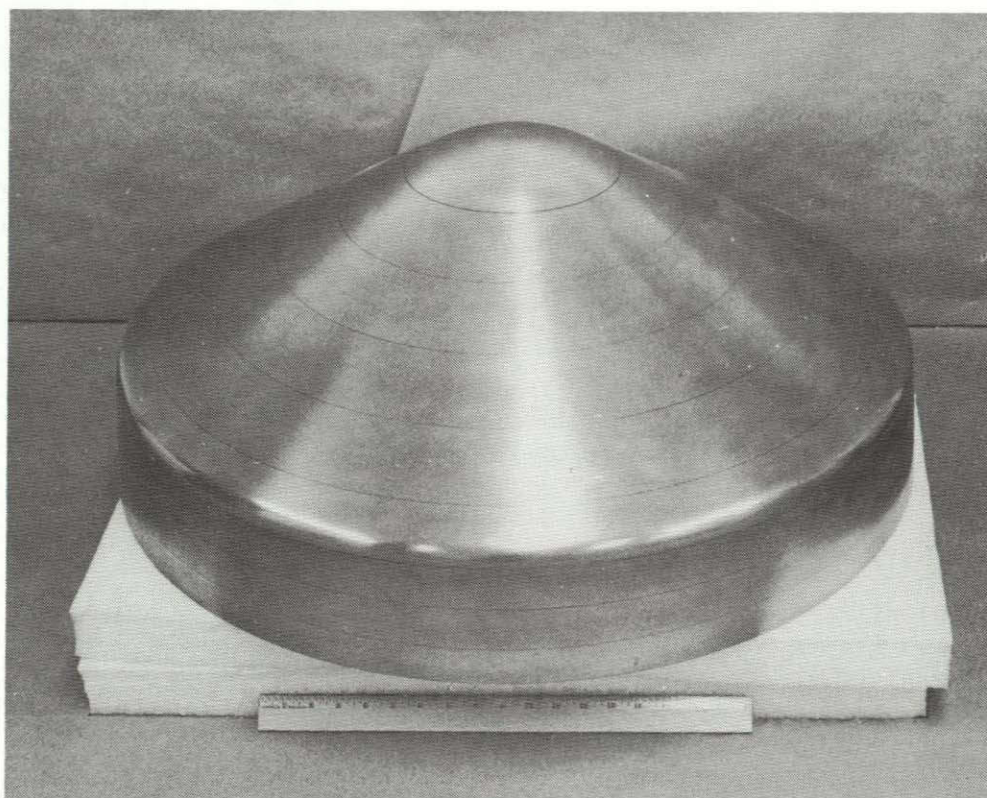FULL SCALE SILICA HEAT SHIELDS

FIGURE 4.3—5 MALE MANDREL FOR FULL SCALE SILICA HEAT SHIELD

4.4 STRENGTH ANALYSIS

Preliminary structural analysis of a silica heat shield was conducted to predict structural performance during an outer planet entry. Analysis was of a point design - a 2.54 cm (1.0 inch) thick solid silica heat shield configured to the Saturn/Uranus Atmospheric Entry Probe (SUAEP) baseline structure as identified in Figure 4.4-1. Variables in the analysis were: 1) silica mechanical and physical properties, 2) heat shield structural support stiffness and 3) thermal and mechanical loads.

CROSS SECTION VIEW
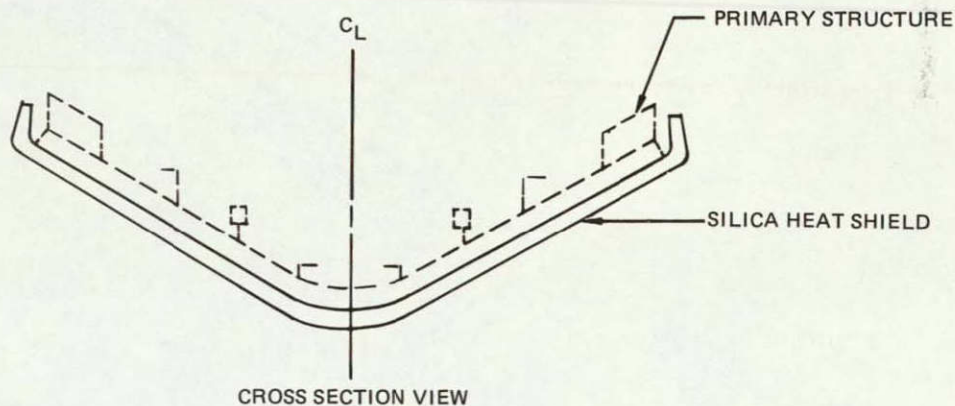
- AXISYMMETRIC — 88.9 cm DIAMETER — 2.54 cm THICK (35 INCH DIAMETER — 1 INCH THICK)
- ONE PIECE — SLIP CAST
- BONDED TO PRIMARY STRUCTURE WITH ELASTOMERIC STRAIN ISOLATOR

FIGURE 4.4—1 PROPOSED SILICA HEAT SHIELD DESIGN FOR THE SUAEP

An analytical model of the silica heat shield and the probe primary structure was built using the Structural Analysis of Axisymmetric Solids (SAAS) computer program. The model is illustrated in Figure 4.4-2 and contains elements for the silica heat shield, the adhesive bondline and for the honeycomb sandwich primary structure.

The complete parametric study utilizing this analytical model is summarized in Figure 4.4-3. Objective of the first two sets of analyses was to predict heat shield internal stresses due to thermal gradients for various heat shield support conditions from free to rigid. The last set of analyses was to aid in selection of a firing temperature for silica for specific use on the SUAEP configuration.

Thermal gradients (corresponding to the entry times of Figure 4.4-3) are illustrated in Figure 4.4-4. Mechanical properties of silica used in the analyses are given in Figure 4.4-5.

Mohr's failure theory for brittle materials was used to predict failure in the heat shield. A typical calculation is presented in Figure 4.4-6 for the critical location in the rigid supported heat shield for t = 23 seconds. A margin of safety of +0.04 results using a factor of safety of 1.25.
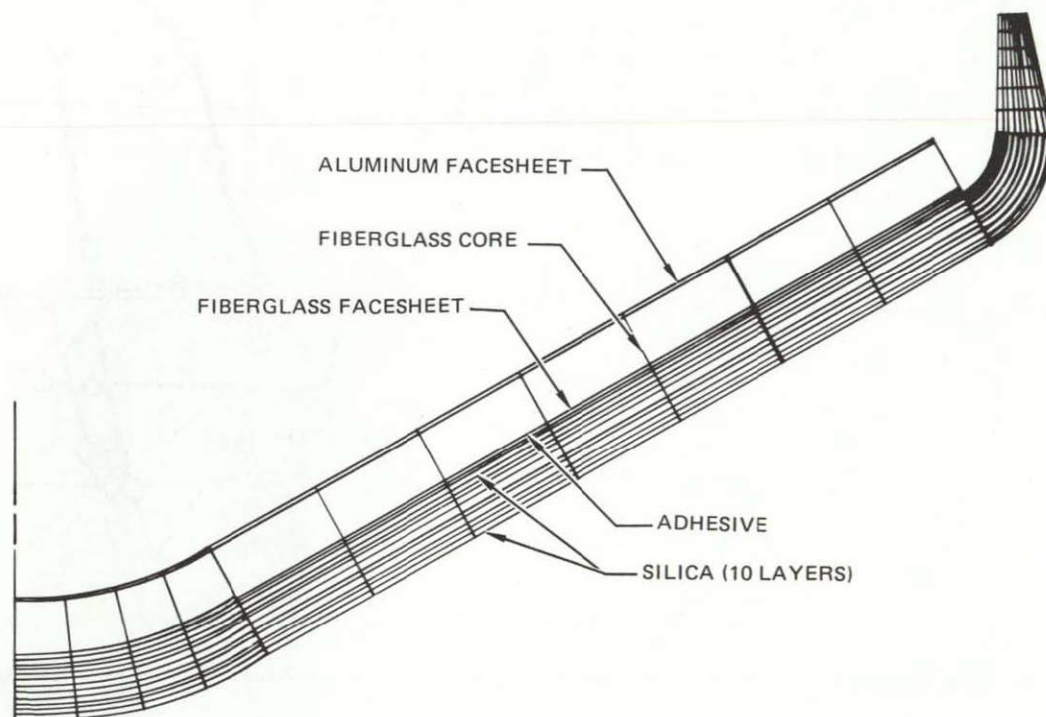
FIGURE 4.4–2 SAAS II ANALYTICAL MODEL
(CROSS SECTION VIEW)
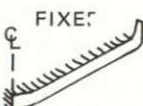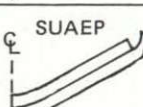
SET	CONFIGURATION	ENTRY TIMES ANALYZED	INERTIA LOADING	SILICA FIRING TEMPERATURE	RESULTS
1	℄ FREE	2 SEC 6 SEC 16 SEC	0	1202 °C (2200°F)	LOW THERMAL STRESSES ADEQUATE STRENGTH
2	℄ FIXED	2 SEC 6 SEC 16 SEC 23 SEC	0	1202 °C (2200°F)	MARGINAL STRENGTH MS = +.04 FOR t = 23 SEC (SEE FIGURE 4.4–6)
3	℄ SUAEP	2 SEC 16 SEC 16 SEC	0 1000 gE 1000 gE	1230 °C (2250°F) 1230 °C (2250°F) 1202 °C (2200°F)	1230 °C FIRED SILICA HAS HIGHER MARGIN OF SAFETY (MS = +.05) AT t = 16 SEC THAN 1202 °C FIRED SILICA (MS = –0.30) t = 2 SECONDS NOT CRITICAL

FIGURE 4.4–3 STRUCTURAL ANALYSIS MATRIX

62
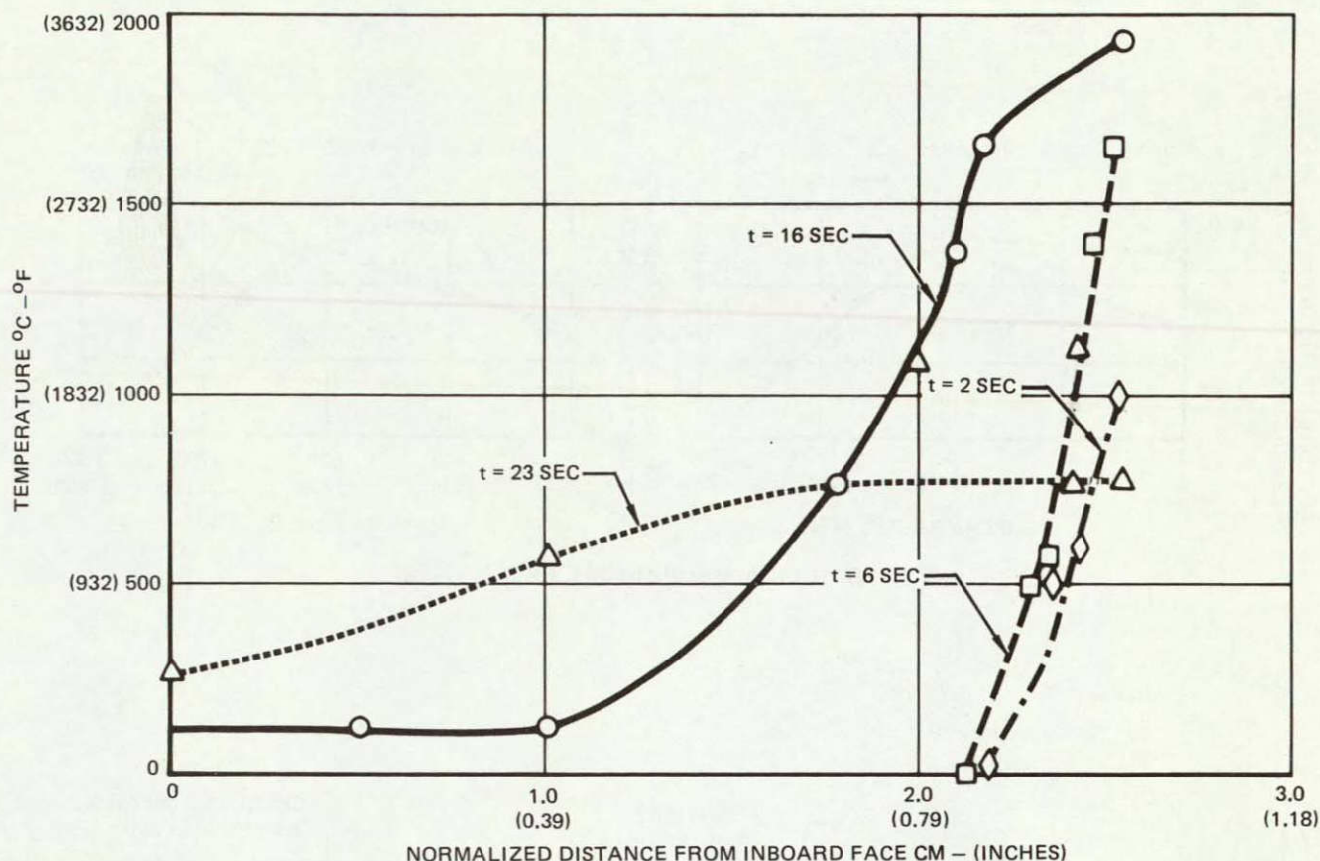
FIGURE 4.4—4 THERMAL GRADIENTS USED IN ANALYSIS

Mohr's theory predicted failure in the 2200°F fired silica heat shield attached to the SUAEP structure for t = 16 seconds. A margin of safety of +0.05 was predicted for the 1230°C (2250°F) fired silica heat shield for the same support and loading conditions.

The small margin of safety predicted for the silica heat shield indicates the criticality of having accurate silica mechanical properties. Estimated mechanical properties (as indicated in Figure 4.4-5) were used in this analysis.

In this analysis, (shown in Figure 4.4-6), the ultimate tensile strength was assumed to be about 80 percent of the flexure strength and the entire high temperature flexure strength curve was estimated based on measured flexure strength of three specimens tested at room temperature. Since actual mechanical properties could differ from these estimates, the effect of this change on structural margins of safety could be very significant. In addition, the probe baseline design changed from a three to a one ring design configuration (see 5.9-1). Therefore, the program was redirected to evaluate an alternate hyperpure silica material formulation to increase the material strength and toughness. This program redirection is discussed in the following section.

63
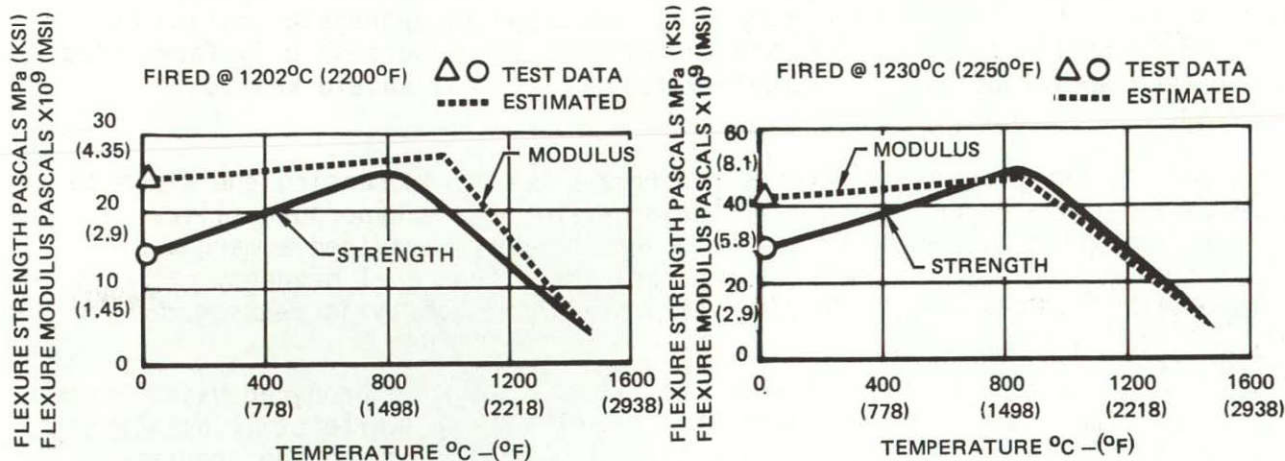
FIGURE 4.4–5 SILICA MECHANICAL PROPERTIES
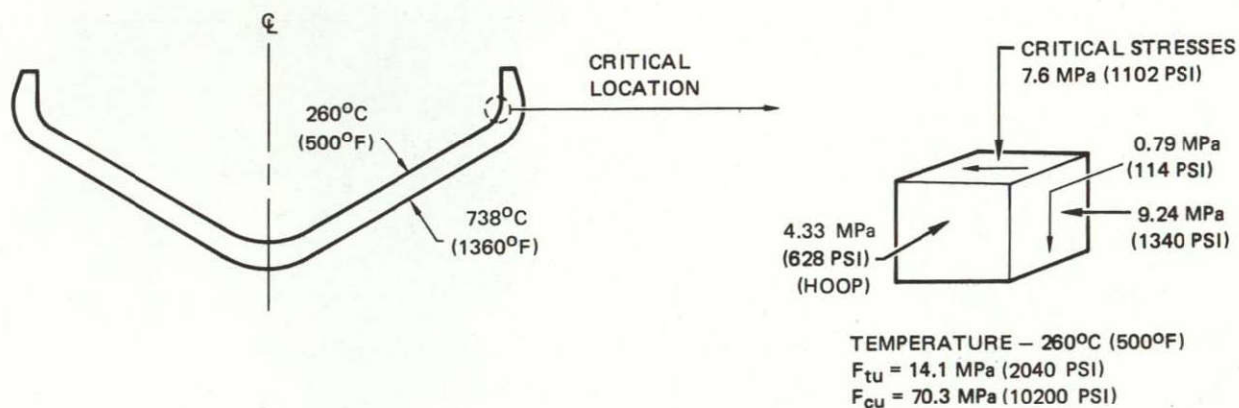
MOHR'S FAILURE THEORY YIELDS:

$$\sigma_b = \frac{1-m}{2}\,(\sigma_1 + \sigma_2) + \frac{1+m}{2}\left((\sigma_1 - \sigma_2)^2 + 4\,\tau^2\right)^{1/2}$$

$$\sigma_b = \frac{1-.2}{2}\,(1340 - 1102) + \frac{1+.2}{2}\left((1340 + 1102)^2 + 4\,(114)^2\right)^{1/2}$$

$\sigma_b = 1567$ PSI (LIMIT)

$\sigma_b = 1960$ PSI (ULT)

$$\text{MARGIN OF SAFETY} = \frac{F_{tu}}{\sigma_b} - 1 = \frac{2040}{1960} - 1 = \underline{+0.04}$$

NOTE: FACTOR OF SAFETY = 1.25

FIGURE 4.4–6 HEAT SHIELD MAXIMUM STRESSES AT
t= 23 SECONDS SET 2 – RIGID SUPPORT

64

5.0 PROGRAM REDIRECTION

The original program was to scale-up the process for slip casting hyperpure
fused silica. The slip casting process was modified to aggregate casting as
described in Section 3.3. A half scale heat shield was successfully fabricated
and the necessary tooling to fabricate a full scale heat shield was 90%
completed.

At this point, the program goals were redirected toward increasing the strength
and toughness (area under the stress-strain curve) of the hyperpure silica
material. Detailed stress analyses for a Jupiter entry provided a margin of
safety of only 0.04, using the latest mechanical and physical property data for
the aggregate slip cast material. A larger margin of safety is recommended for
a brittle material.

It was determined that a more reliable heat shield could be produced using hyper-
pure silica fibers as a reinforcement (See Figure 5.0-1), while still using the
slip casting technology and the tooling already produced during the program.

FIBER/GRAIN MIXTURE

ALL GRAIN MIXTURE
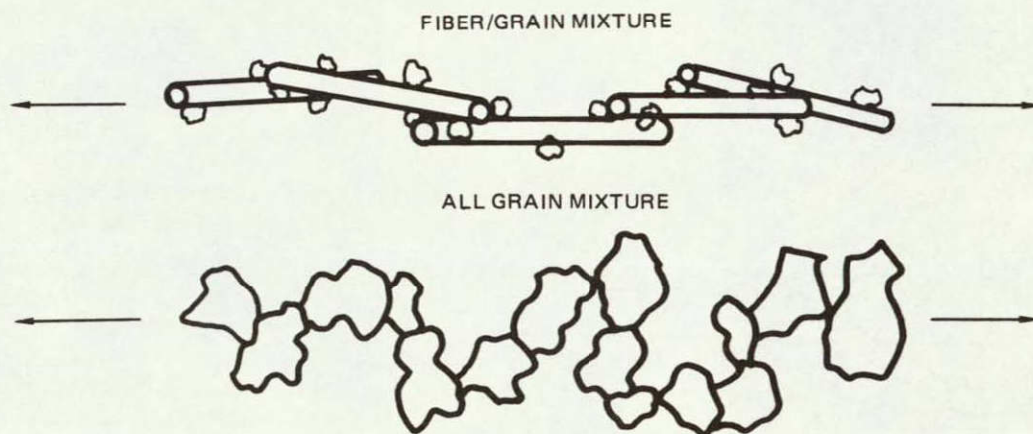
FIGURE 5.0–1 FIBERS PROVIDE BETTER MICROSTRUCTURAL CONTINUITY

5.1 DISPERSED FIBER SLIP PREPARATION

As previously stated, the goal of the redirected program was to develop a
fiber reinforced hyperpure silica material using the slip casting technology
developed under the program. A process was successfully developed for combin-
ing hyperpure silica fibers and hyperpure silica grains to yield a material
that can be slip cast by conventional means. During the course of the develop-
ment work continuous particle size grain suspensions having grain sizes from
10 µm average diameter, which is the grain size of our standard casting slip,
to as small as 3 µm average diameter were evaluated.

The hyperpure silica fibers (1 ppm total impurities) were received in the form
of loose wool, the individual fibers being extremely long. The fiber diameter
of this material ranged from 3 to 7 µm. This wool is made in France using
synthetic fused silica as a starting material, and is distributed in the USA by
J. P. Stevens, Aerospace Products Division under the name Suprasil. The Supra-
sil wool (99.9999% pure) is similar to J. P. Stevens Astroquartz wool (99.95%
pure) in texture and fiber diameter. SEM photographs of the hyperpure wool and
the Astroquartz wool are shown in Figure 5.1-1. During the initial stages of
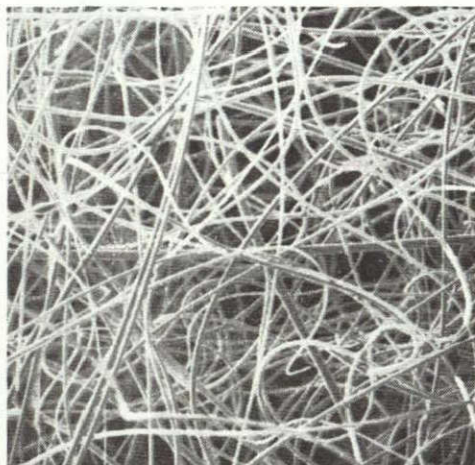
100X
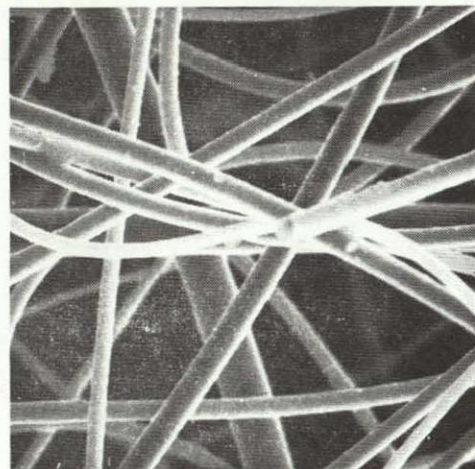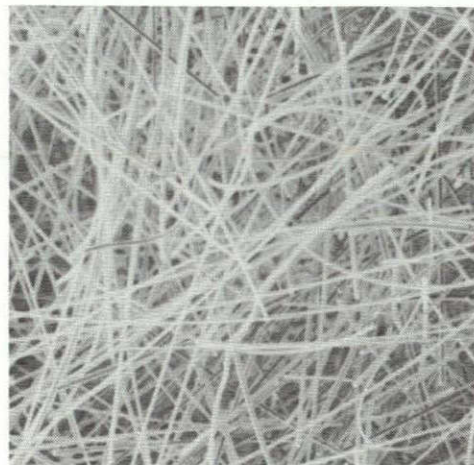
500X
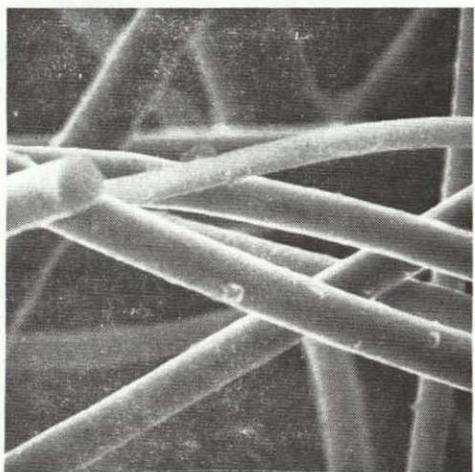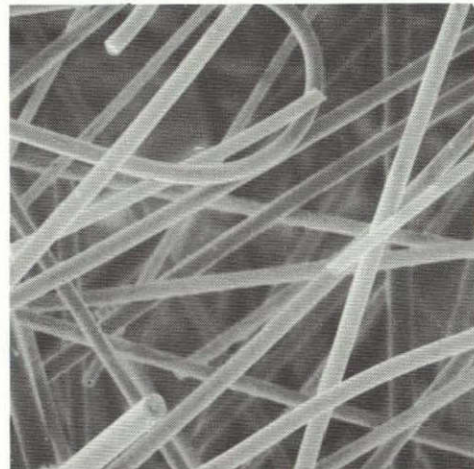
1000X
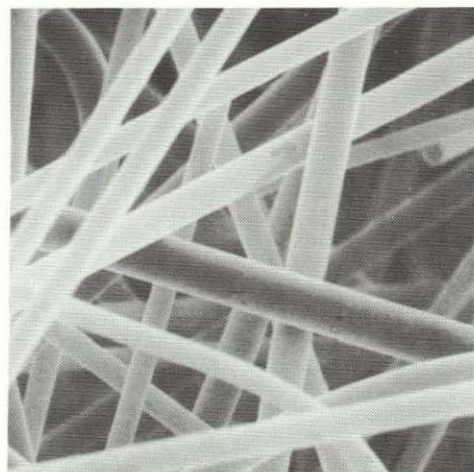
ASTROQUARTZ   SUPRASIL

FIGURE 5.1—1 99.95% PURE ASTROQUARTZ WOOL AND 99.9999% PURE SUPRASIL WOOL

fiber reinforced material development, the less expensive Astroquartz wool was used rather than Suprasil to establish processing procedures for preparing dispersed fiber casting slips.

The as-received wool fibers were reduced in length by wet chopping in a model CB-6 Waring blender. The Waring blender (Figure 5.1-2) was modified to prevent introduction of metallic impurities into the fibers. The inside surfaces of the stainless steel blender cup and lid are coated with Teflon (DuPont Teflon S) and the standard stainless steel blade is replaced with a plastic blade.

FIGURE 5.1–2 WARING BLENDER FOR WET CHOPPING HYPERPURE SILICA FIBERS

The as-received silica wool was chopped in the blender to an average fiber length of 0.127 cm (.050 in.). Batching for this wet chopping is 30 gm of fibers and 2000 gm of deionized water (MMS-606) with a chopping time of 20 seconds. The wet chopped fibers are vacuum felted on a nylon screen forming a wet cake which was dried and heated to 540°C (1000°F) to remove any organic contaminates.

The chopped fibers are dispersed into a previously prepared slip (continuous particle size grains in a water suspension). In order to facilitate wetting of the fiber addition, it was necessary to add the fibers in small increments ($\sim$ 5% of the grain solids weight) and a dilute (50%) water suspension of grains. The milling containers are slowly turned after each fiber addition to uniformly disperse and wet the fibers. This slow milling does not reduce the size of the silica grains because no grinding media is needed. The chopped fibers are very fluffy so that after each fiber addition the slip becomes extremely lumpy and viscous (like cottage cheese) until all the fibers are wetted, at which time it returns to a smooth, fluid state. When the desired amount of fibers have been added to the slip, the proper solids content ($\sim$ 78%) for casting is adjusted by water evaporation. The addition of fibers does not appreciably change the pH of the slip which remains at 3.4 to 3.9. The rheological properties of the fiber dispersed slips are similar to those without fibers and may be achieved to thixotropy or dilatancy by decreasing or increasing the pH respectively. Fiber dispersed slips have been prepared by these methods having grains as coarse as 10 μm average and as fine as 3 μm average diameter, and using fiber concentrations as high as 50% of the total solids weight of the slip.

5.2 HYPERPURE GRAINS 10 μm/ASTROQUARTZ FIBERS REINFORCEMENT

The initial work on fiber reinforced casting slip was accomplished with inexpensive Astroquartz fibers rather than the 99.9999% pure Suprasil silica fibers. The grains selected for the first fiber/grain casting slips was the standard 10 μm average diameter continuous particle size slip.

Dispersed fiber slips were made using 10 μm average size hyperpure grains and dispersed Astroquartz fibers having fiber concentrations of 10%, 17% and 25% of the solids weight of the respective slips. A rather small quantity of 10% fiber slip was prepared initially and was determined to have physical characteristics typical of normal casting slips. Several small ($\sim$ 3.8 cm x 0.64 cm thick) specimens were cast and determined to have characteristics typical of fused silica castings.

Specimens were prepared for strength testing from castings made with the 17% and 25% fiber slips, as well as slips without added fibers. Samples were cast in the form of test bars ($\sim$ 10 cm x 1.25 x 1.25 cm) so that a minimum of machining would be required to yield specimens suitable for flexural testing. These bars were cast by pouring the slip into plexiglass forms on a flat plaster of paris surface. Flexural test bars were also prepared from slip with identical sized grains without fibers added. The hyperpure slip used as a source for grains for the dispersed fiber slip was prepared in a 19 liter mill and was typically thixotropic. After the Astroquartz fibers were added and the slip was adjusted to the proper solids content for casting, it was dilatant rather than thixotropic. Castings made from the thixotropic slip produced green densities of 1.49 g/cc. Dilatant slips (with or without fibers added) produce higher density (1.62 - 1.65 g/cc) castings. In order to achieve the best comparison of the material strength with and without fibers, the slip without fibers was raised in pH to be dilatant so that its castings were similar in density to those cast from the fiber reinforced slips. The fiber reinforced slips were observed to be similar in consistency and to form castings at a similar rate to 100% grain slips having a similar solid content and rheology.

A series of test bars were prepared from each of the compositions described above (0%, 17%, 25% fibers) and fired at temperatures of 1150, 1180, 1200 and 1230°C. The soak time for each firing run was 5 hours at temperature. Each specimen was measured before and after firing in order to determine firing shrinkages and densities. The firing shrinkage and fired density data for the three (3) compositions are shown in Figures 5.2-1 and 5.2-2, respectively. The shrinkage figures shown in Figure 5.2-1 represent the average shrinkage for three (3) measurements (length, width, thickness) on each sample. The samples with dispersed fibers had a higher shrinkage ($\sim$ 25%) in the Z direction than the X-Y direction, indicating some nonrandom orientation of the fibers during casting. The lower overall shrinkage of the fiber reinforced materials was expected. The greater length of the chopped fibers with respect to the grain diameter was expected to retard drying and firing shrinkage. A lower drying and firing shrinkage offers processing advantages, particularly during scale-up and the casting of larger parts as was previously discussed.

68

In order to achieve flat and parallel surfaces for flexural testing, each test specimen was machined on the top and bottom surfaces using deionized water cooled, high speed diamond tooling. The final dimensions for each test specimen were about 0.80 x 1.25 x 10 cm long. The specimens were tested in four point flexural loading, as illustrated in Figure 5.2-3 to allow the midsection of the specimen to have a constant loading level without transverse shear load. A deflectometer measured midspan deflection as a function of applied load. All specimens were loaded at a rate of 0.127 cm head travel per minute. This procedure for casting, machining, and flexural testing was used for all fiber/grain test specimens discussed in this and subsequent sections.
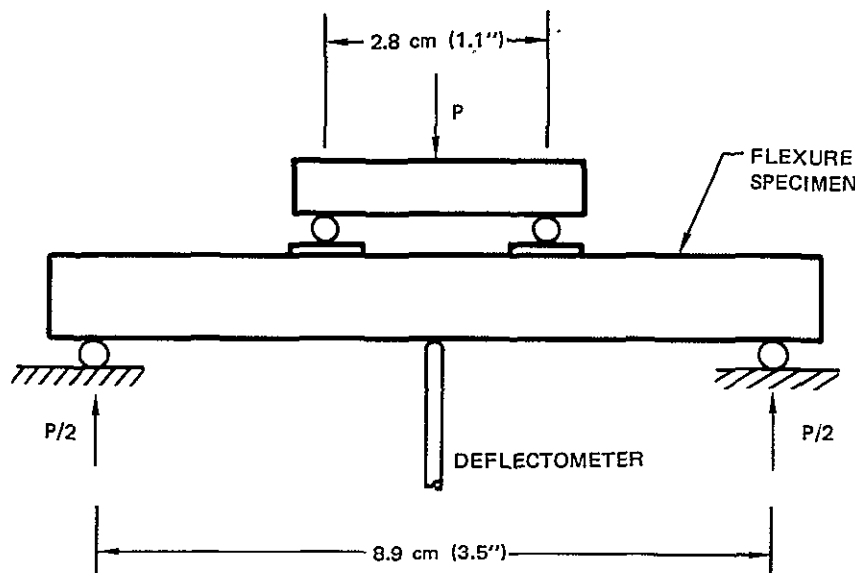
FIGURE 5.2—3 FOUR POINT FLEXURE TEST SET-UP

The strength and modulus test results for the 10 μm grains/Astroquartz fibers reinforced systems are shown in Figures 5.2-4 and 5.2-5 respectively. Since the objective of this effort is to produce a tougher material the test data was used to calculate an average toughness for each group of specimens. Toughness, which is equivalent to the area under the stress-strain curve, is defined by the equation:

$$T = \frac{F^2}{2E}$$

T = Toughness

F = Ultimate Flexural Strength

E = Flexural Elastic Modulus

70
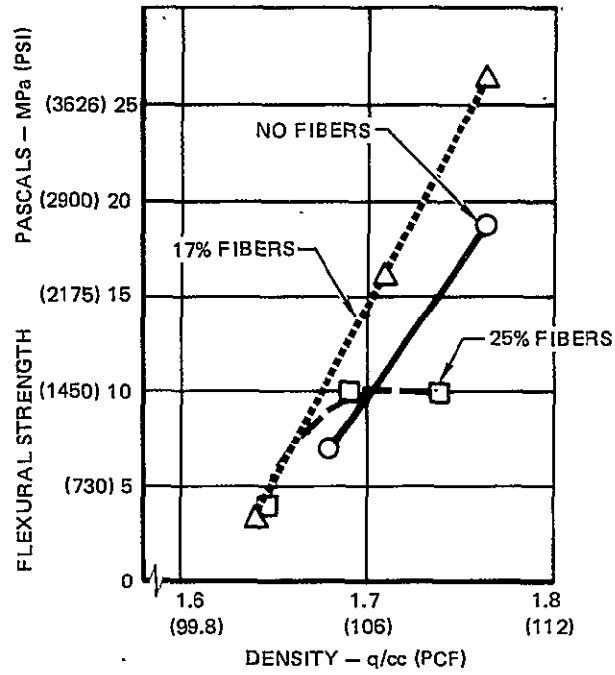
FIGURE 5.2–4 FLEXURAL STRENGTH OF SLIP CAST 10μm GRAINS
WITH ASTROQUARTZ FIBER REINFORCEMENT
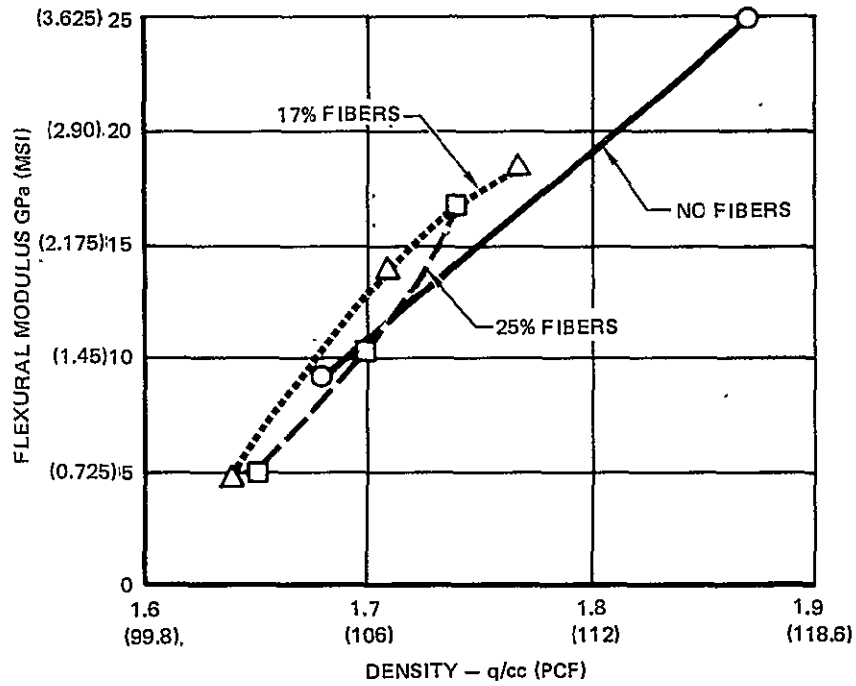
FIGURE 5.2–5 FLEXURAL MODULUS OF SLIP CAST 10μm GRAINS
WITH ASTROQUARTZ FIBER REINFORCEMENT

Figure 5.2-6 shows that the toughness was improved by adding 17% fibers to the 10 μm grains basic slip. The use of 25% Astroquartz fibers, however, showed no improvement in toughness and in the case of the higher firing temperature (1230°C), a toughness decrease occurred. It was concluded that the use of the lower purity Astroquartz (500 ppm impurities) caused devitrification of the castings in the 25% concentration. At this point dispersed fiber slips using the 99.9999% pure Suprasil fibers was initiated. No further work was done with Astroquartz fibers. All subsequent references to fibers or fiber reinforcement will refer to the very high purity Suprasil fibers.
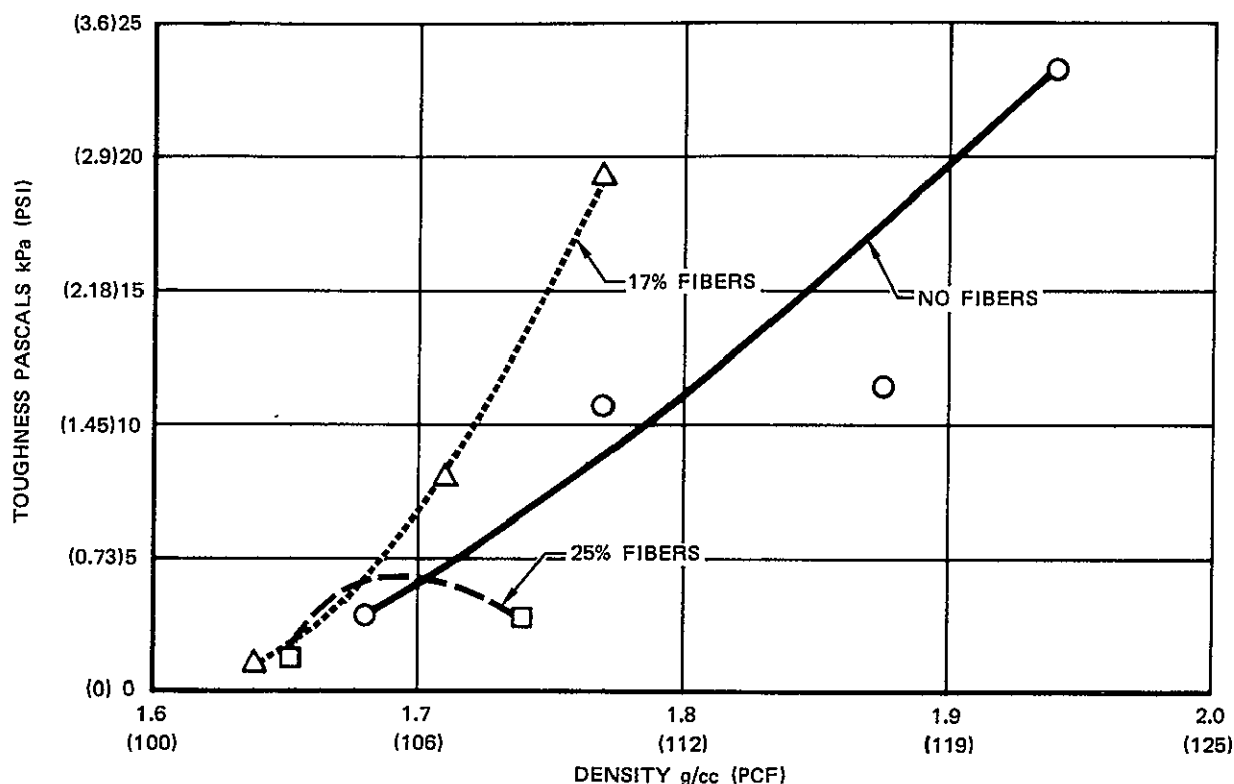
FIGURE 5.2—6 TOUGHNESS OF SLIP CAST 10 μm GRAINS WITH
ASTROQUARTZ FIBER REINFORCEMENT

5.3 HYPERPURE GRAINS 10 μm/SUPRASIL FIBERS REINFORCEMENT

Batches of casting slip were prepared using 10 μm average diameter grains and 99.9999% pure Suprasil fibers as reinforcement. The grains were from the same batch of hyperpure slip used for the work with the Astroquartz fibers reinforcement effort described in Section 5.2. Fiber concentration of 20% and 40% of the slip solids weight were evaluated.

Specimens were cast in the form of 1.25 x 1.25 x 10 cm long bars for flexural test specimens and 3.8 cm diameter x 0.635 cm thick discs for reflectance measurements. The reflectance specimens were fired at 1230°C. The bars for flexural testing were fired at 1170°C, 1200°C, and 1230°C. A total of twelve bars were processed for each formulation and four were fired at three selected temperatures. The firing shrinkage and density data obtained from these specimens are shown in Figures 5.3-1 and 5.3-2 along with the data for the basic slip cast grains without fibers reinforcement.
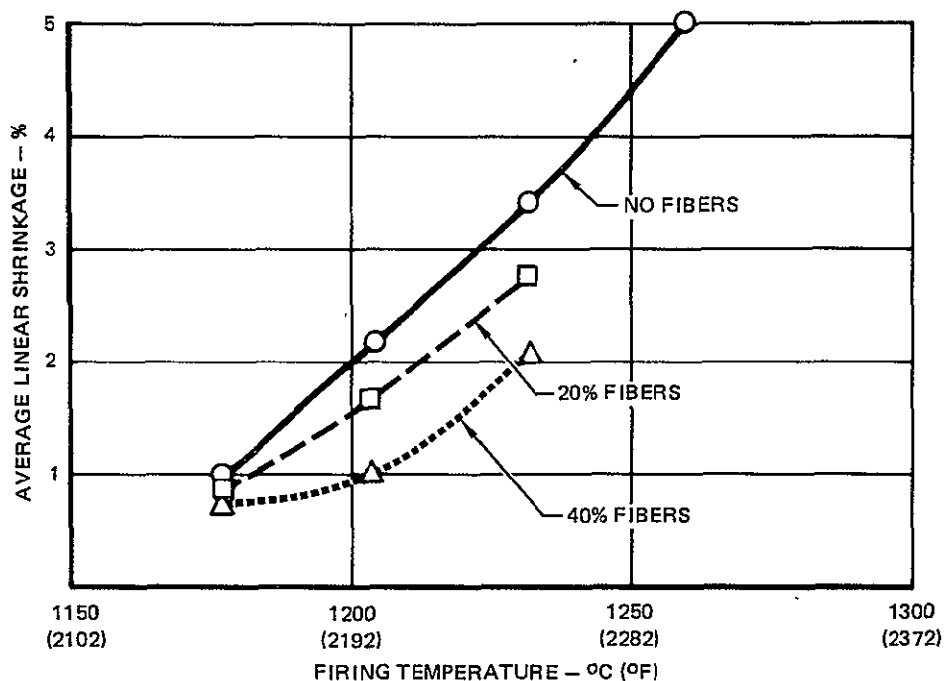
FIGURE 5.3-1 FIRING SHRINKAGE OF SLIP CAST 10 μm GRAINS
WITH SUPRASIL FIBER REINFORCEMENT

It was noted that the Suprasil fiber reinforced slip retained some of the natural thixotropic characteristics of the basic 100% grain slip. Slips made with dispersed Astroquartz fibers were very dilatant. Viscosity curves for the two types of slip are shown in Figure 5.3-3. The more thixotropic the Suprasil fibers reinforced slip, the faster the casting rate and the lower the "as cast" density. The lower "as cast" density is reflected in Figure 5.3-2 (as the fired densities are lower), since the slip used to make the 100% grain castings was adjusted in pH to be dilatant. Castings made with the Suprasil fibers reinforced slip showed no firing shrinkage difference in the Z and X-Y direction. This indicates a random fiber orientation which could result from the faster casting rate as well as the higher viscosity slip (retards movement of the fibers). SEM photographs, see Figure 5.3-4, show the microstructure of the Suprasil fibers reinforced material.

73
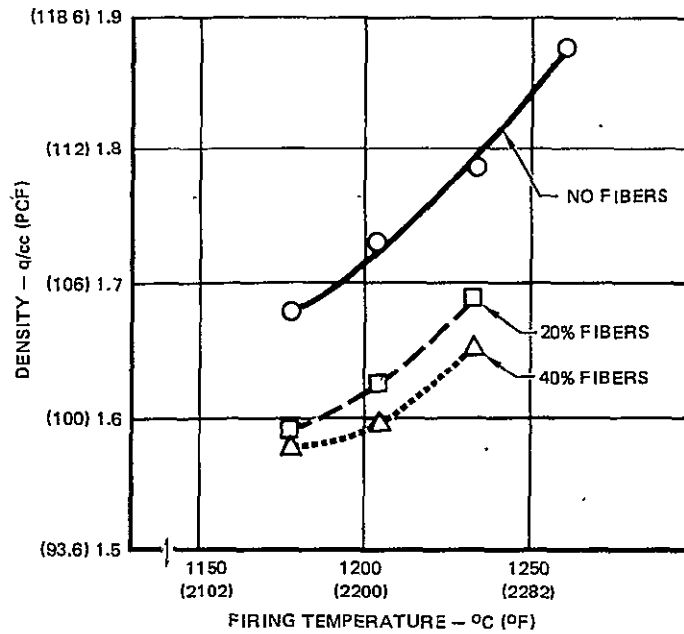
FIGURE 5.3—2 FIRED DENSITY OF SLIP CAST 10 μm GRAINS WITH SUPRASIL FIBER REINFORCEMENT

ASTROQUARTZ FIBER REINFORCEMENT	SUPRASIL FIBER REINFORCEMENT
VERY DILATANT SLIP	LESS DILATANT SLIP
SLOW CASTING RATE	FASTER CASTING RATE
GREEN DENSITY = (1.63 gm/cc)	GREEN DENSITY = 1 54 gm/cc
SOME PREFERRED FIBER ORIENTATION (HIGHER Z DIRECTION FIRING SHRINKAGE) DURING CASTING	NO PREFERRED FIBER ORIENTATION DURING CASTING
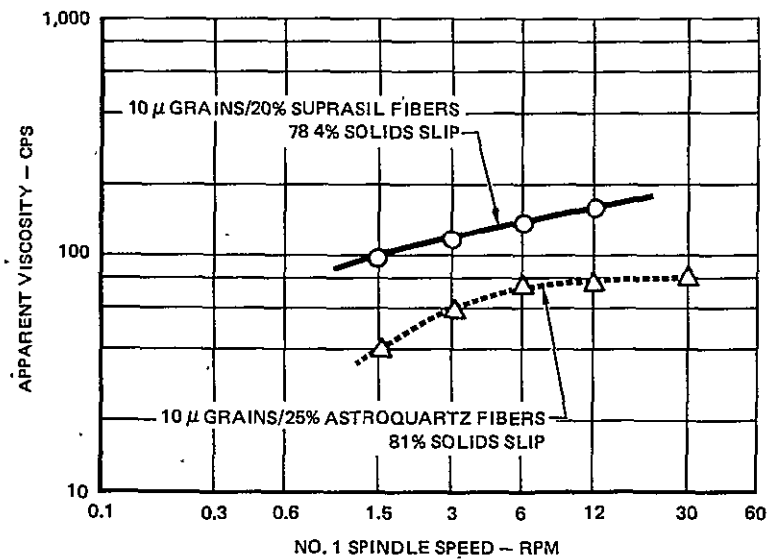
FIGURE 5.3—3 RHEOLOGY OF 10 μ GRAIN SLIPS WITH ASTROQUARTZ AND SUPRASIL FIBER REINFORCEMENT

74

1000X

NO FIBERS   20% FIBERS   40% FIBERS
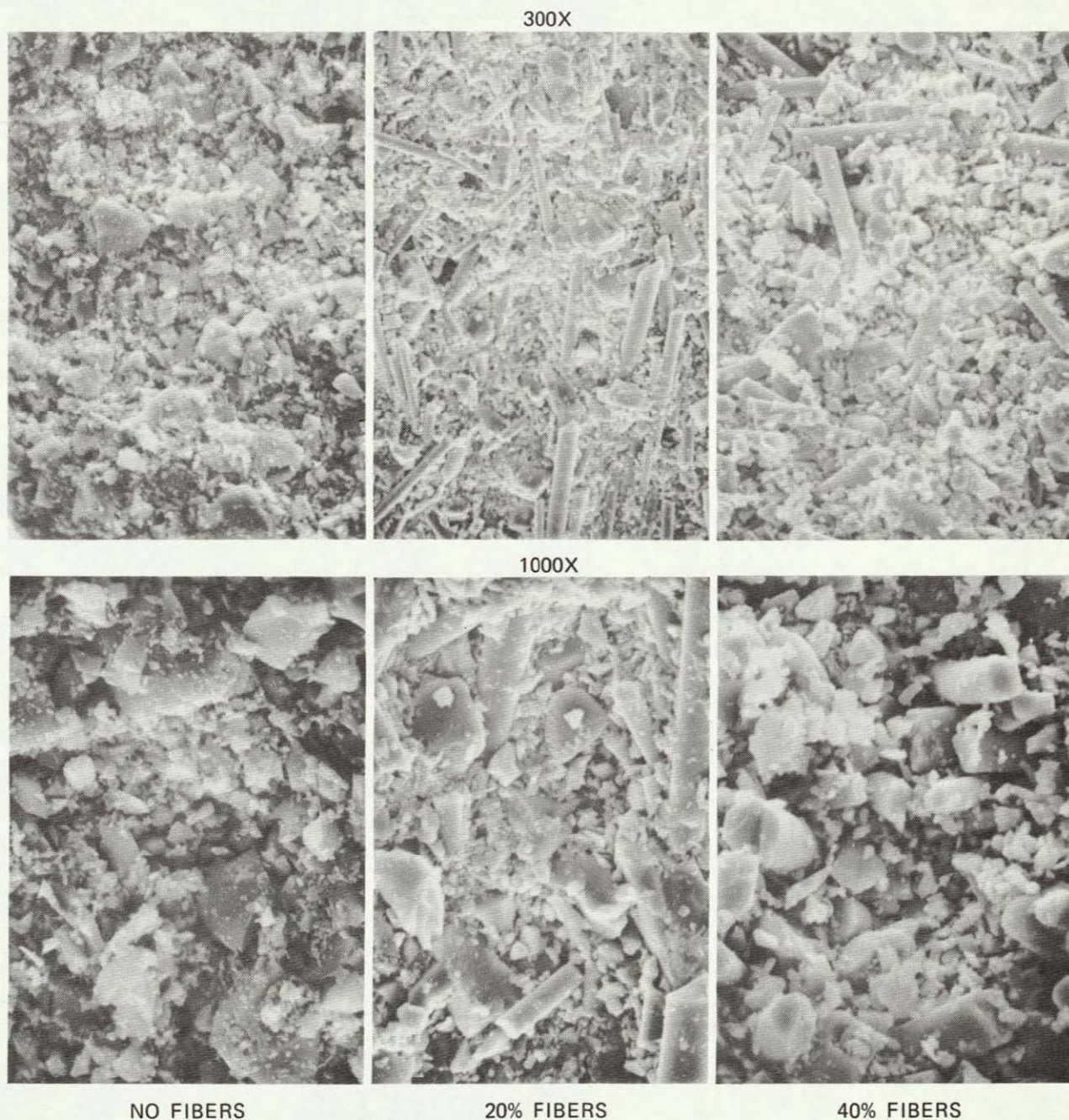
FIGURE 5.3—4 MICROSTRUCTURE OF HYPERPURE SLIP CAST 10 μm
GRAINS WITH AND WITHOUT SUPRASIL FIBER REINFORCEMENT

The ∿ 1.25 x 1.25 x 10 cm long specimen castings were machined and flexural tested. The test results are shown in Figures 5.3-5, 5.3-6 and 5.3-7. The data is plotted with respect to fired density, with the specimens grouped according to the average density in a given firing run. The use of the higher purity Suprasil fibers allowed the fiber reinforced specimens to be fired at 1230°C with apparently no devitrification. It is not known at what firing temperature devitrification would occur. Hyperpure slip cast materials without fiber reinforcement have been fired as high as 1320°C for 5 hours with no strength degradation due to devitrification (see Reference 2).
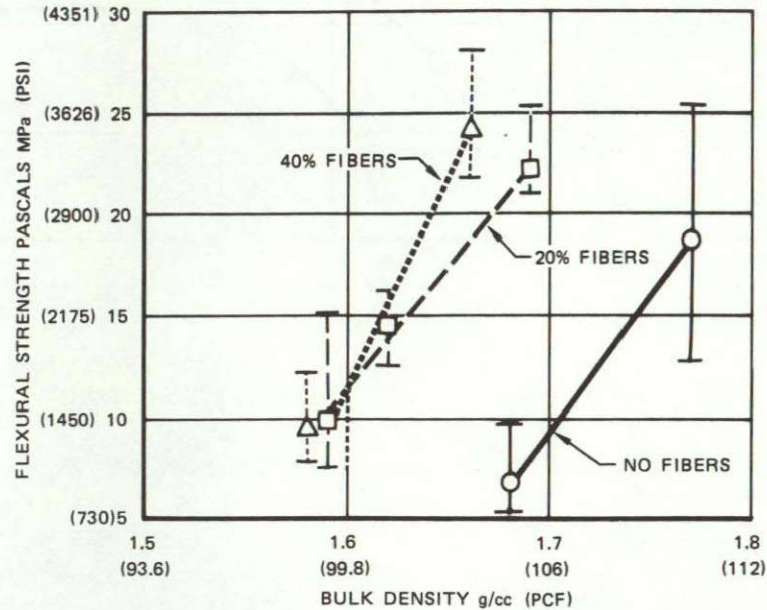
FIGURE 5.3—5 FLEXURAL STRENGTH OF SLIP CAST 10 μm GRAINS WITH SUPRASIL FIBER REINFORCEMENT
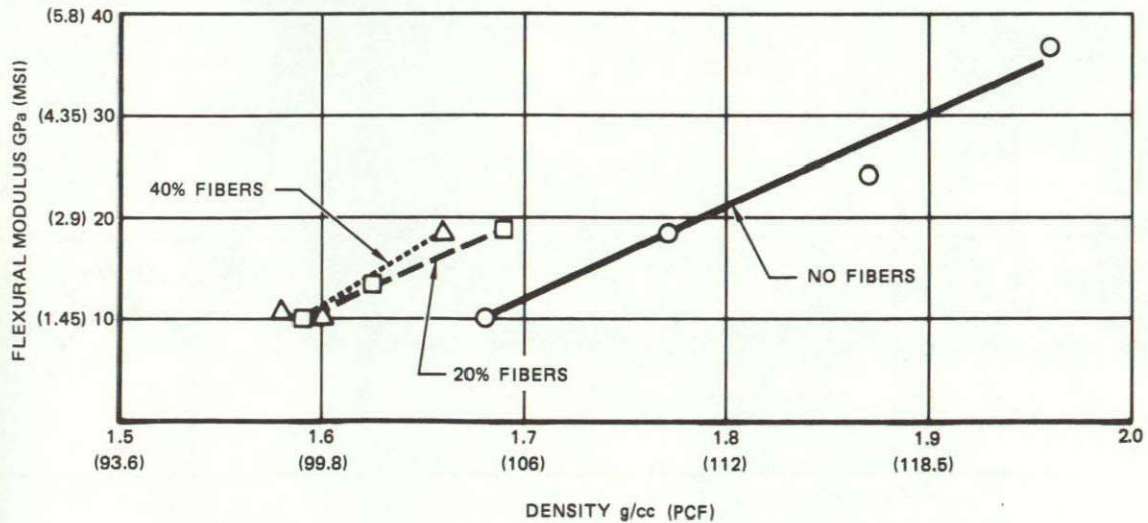
FIGURE 5.3—6 FLEXUREAL MODULUS OF SLIP CAST 10μm GRAINS WITH SUPRASIL FIBER REINFORCEMENT

76
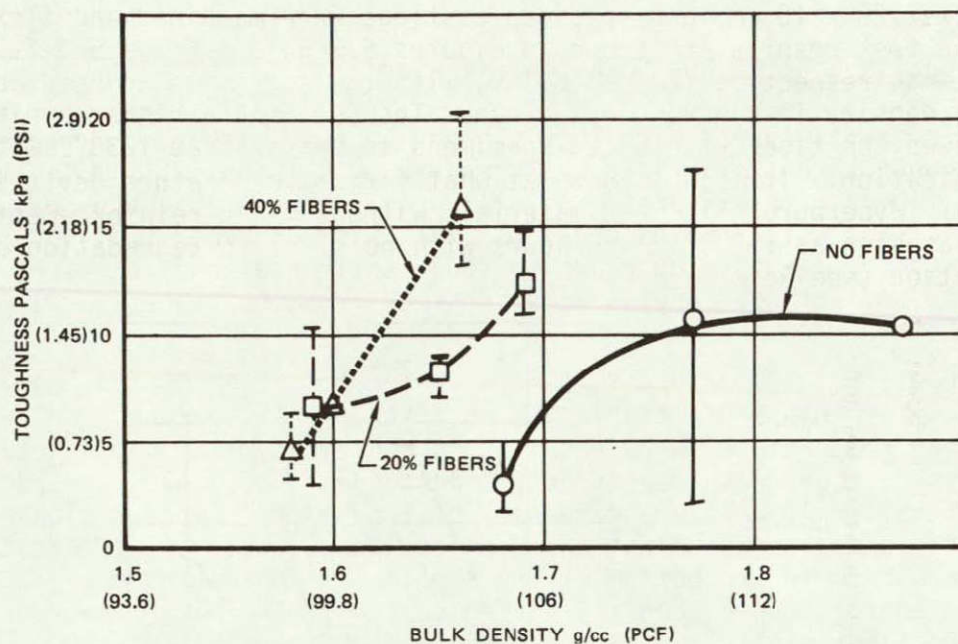
**FIGURE 5.3—7 TOUGHNESS OF SLIP CAST 10 μm GRAINS
WITH SUPRASIL FIBER REINFORCEMENT**

Density and reflectance versus wavelength were measured for specimens fired
for 5 hours at 1130°C. Reflectance curves for the Suprasil fibers reinforced
materials are shown in Figure 5.3-8. For comparison, a reflectance curve for a
typical 100% grain (10 μm average diameter) sample is also shown in Figure 5.3-8.
The reflectance data shows that up to 40% chopped Suprasil fibers reinforcement
for slip cast 10 μm hyperpure grains results in no penalty in reflective proper-
ties at wavelengths of .225 μm or above.
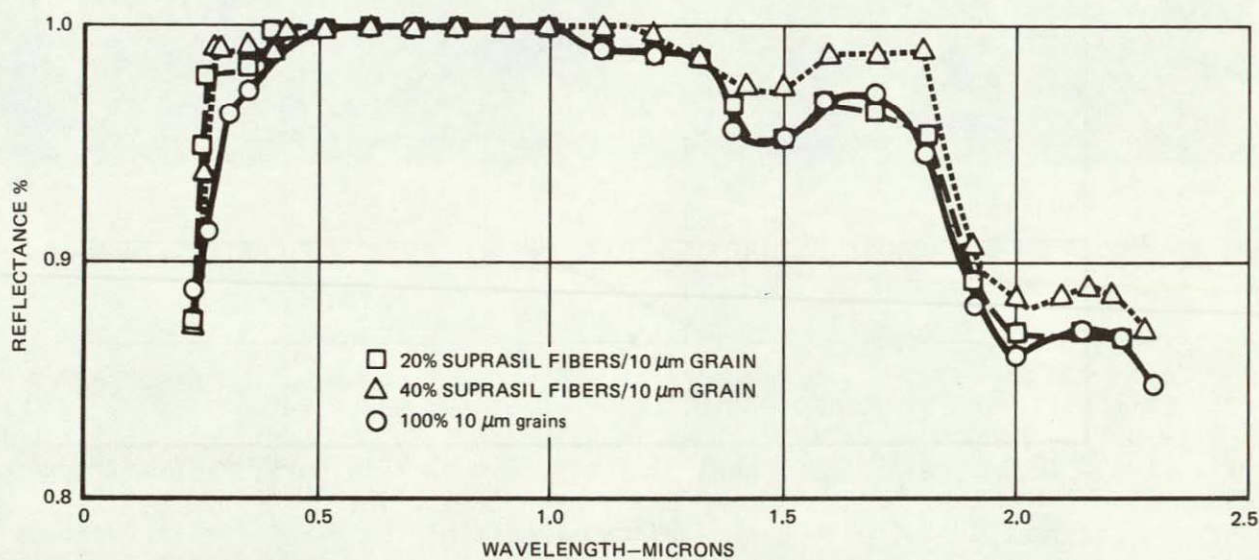
FIGURE 5.3—8 HYPERPURE SILICA REFLECTANCE WITH SUPRASIL REINFORCEMENTS

5.4 SLIP CASTINGS WITH 100% SUPRASIL FIBER

Evaluation of parts formed with 100% chopped Suprasil fibers (no hyperpure grains added) was undertaken. The slip was prepared by a technique similar to that described for fiber/grain mixtures. Several problems were encountered in processing this material and with limited development it was concluded that 100% fibers castings is not a feasible approach for full scale heat shield shapes. Limited strength and reflectance results were obtained from 100% fiber castings and are presented herein.

Specimens cast from 100% fiber slip were rather low in as casted density (1.35 vs 1.54 g/cc for 40% fiber material). As a result of the lower as cast density, higher firing temperatures were required to achieve similar densities. Firing at 1230°C for 5 hours resulted in an average density of 1.47 g/cc and firing at 1260°C resulted in an average density of 1.63 g/cc. Large shrinkage differences were encountered in X-Y and Z directions as well as differences in X-Y shrinkage from top to bottom of the specimens, indicating changes in fiber orientation and/or packing density during casting. The microstructure of a typical 100% fiber casting is shown in the SEM photographs in Figure 5.4-1.
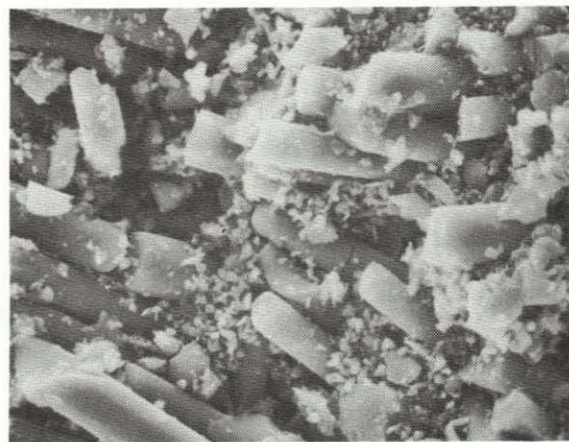
300X   1000X

FIGURE 5.4–1 MICROSTRUCTURE OF A 100% SUPRASIL FIBER SLIP CAST SPECIMEN

Flexural tests were performed on 100% fiber castings which were fired at 1230°C. The resulting toughness data is shown in Figure 5.4-2. For reference the toughness of 60% 10 μm grains/40% fibers is also shown on this curve. The firing temperatures for the specimens comprising each data point are shown on the curve. The fact that the toughness of the 100% fiber material is increasing indicates that processing of the 99.9999% pure Suprasil wool did not cause devitrification when fired for 5 hours at 1260°C.

5.5 HYPERPURE GRAINS 3 µm/SUPRASIL FIBERS REINFORCEMENT

The approach of mixing fibers and grains in a slip cast material was continued to increase the material toughness. It was believed that the toughness of the fiber grain system might be optimized by using smaller size grains to increase the bond area between fiber as illustrated in Figure 5.5-1.

Slips with 3 µm grains were prepared which had fiber concentrations of 25% and 50% of the total solid weight. Specimens were cast from the 3 µm grain suspension without fibers and from the 25% fiber formulation at 70% solids. The 3 µm slip with 0% fibers and 25% fibers were both highly thixotropic and suitable for casting at 70% solids. The 50% fiber formulation was raised in solid to 79% to make it suitable for casting. Viscosity measurements taken with the Brookfield LVT viscometer were similar for the three (3) formulations at the solids contents used for casting.

Specimens were cast in the form of ∿ 1.25 x 1.25 x 10 cm long bars for flexural tests. Rather long casting times were noted for these specimens; 180 minutes for a 0.197 cm thick specimen as compared to 25 minutes for the 10 µm grain formulations. Only a limited number of specimens were cast from the 100% grain formulation. These were fired for 5 hours at 1200°C. Specimens from the 25% fiber slip were fired for 5 hours at 1170°C and 1200°C. Specimens from the 50% fiber formulation were fired 5 hours at 1150°C (2100°F), 1175°C (2150°F), 1200°C (2200°F), and 1230°C (2250°F).
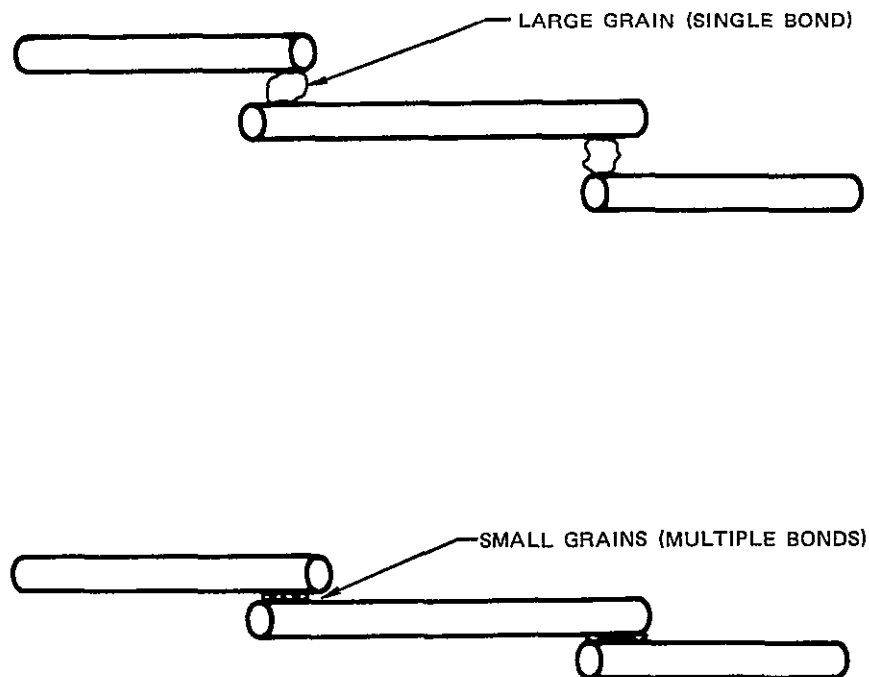
FIGURE 5.5—1 SMALL GRAINS MAY PROVIDE BETTER FIBER TO FIBER BOND

Firing shrinkage figures are shown in Figure 5.5-2. As expected, the 100% grain material had high firing shrinkage; 8% at 1200°C as compared to 2.5% for 10 μm

FIRING TEMPERATURE — °C (°F)
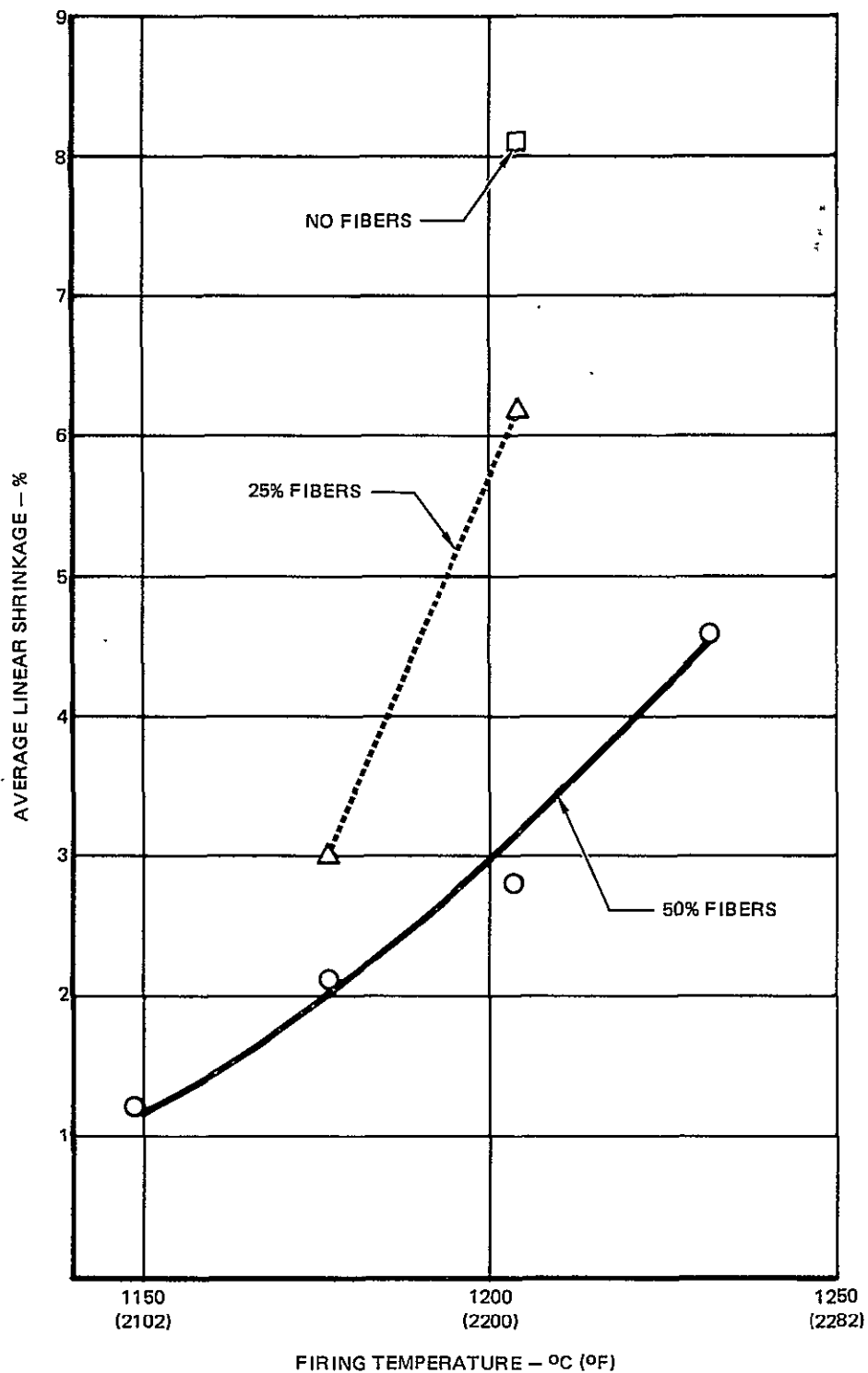
FIGURE 5.5—2 FIRING SHRINKAGE OF SLIP CAST 3μ GRAINS
WITH SUPRASIL FIBER REINFORCEMENT

grains. Very high drying shrinkages occurred for the 3 μm material although
no shrinkage cracks were observed. The fiber reinforcement 3 μm material had
considerably lowered drying and firing shrinkages. The shrinkage in all direc-
tions was similar, indicating no preferred fiber orientation. Fired density
data is shown in Figure 5.5-3. At the lower temperatures, the density of the
50% fiber material was higher than that of the 25% fiber material, even though
the firing shrinkages were lower. This is due to the fact that the green density
was higher (1.54 g/cc versus 1.43 g/cc) for the 50% fiber castings. The higher
green density is attributable to the fact that the slip was at 79% solids for
casting as compared to 70% solids for the 25% fiber slip.
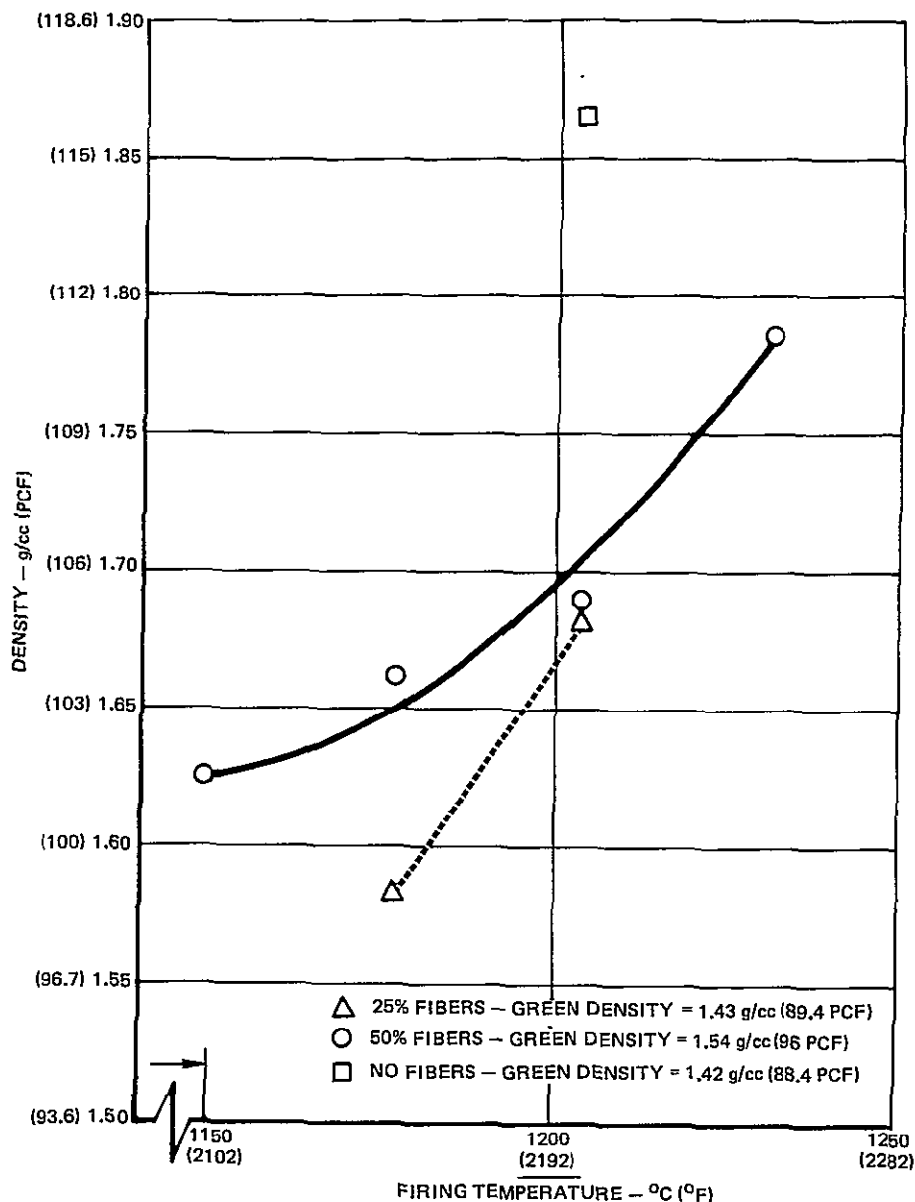
FIGURE 5.5–3 FIRED DENSITY OF SLIP CAST 3 μ GRAINS WITH
FIBER REINFORCEMENT

The flexural strength, modulus and toughness results in Figures 5.5-4 through 5.5-5 are shown with respect to specimen density with the data points grouped according to firing temperature. Figures 5.5-6 and 5.5-7 compare the toughness
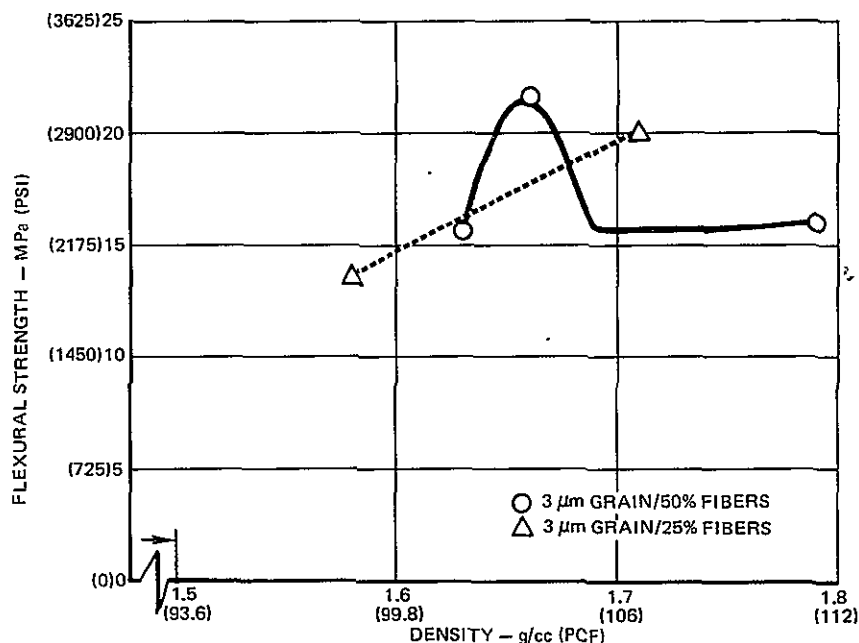
FIGURE 5.5-4 FLEXURAL STRENGTH OF SLIP CAST 3μm GRAINS WITH
FIBER REINFORCEMENT
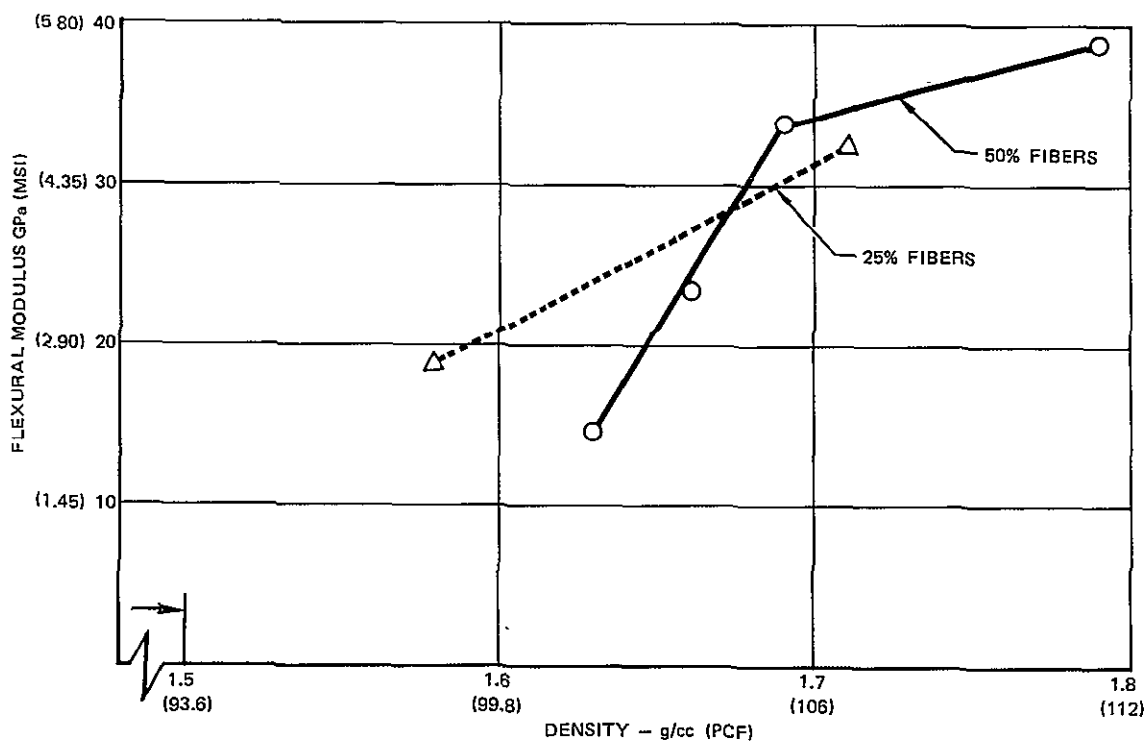
FIGURE 5.5-5 FLEXURAL MODULUS OF SLIP CAST 3μ m GRAINS
WITH SUPRASIL FIBER REINFORCEMENT
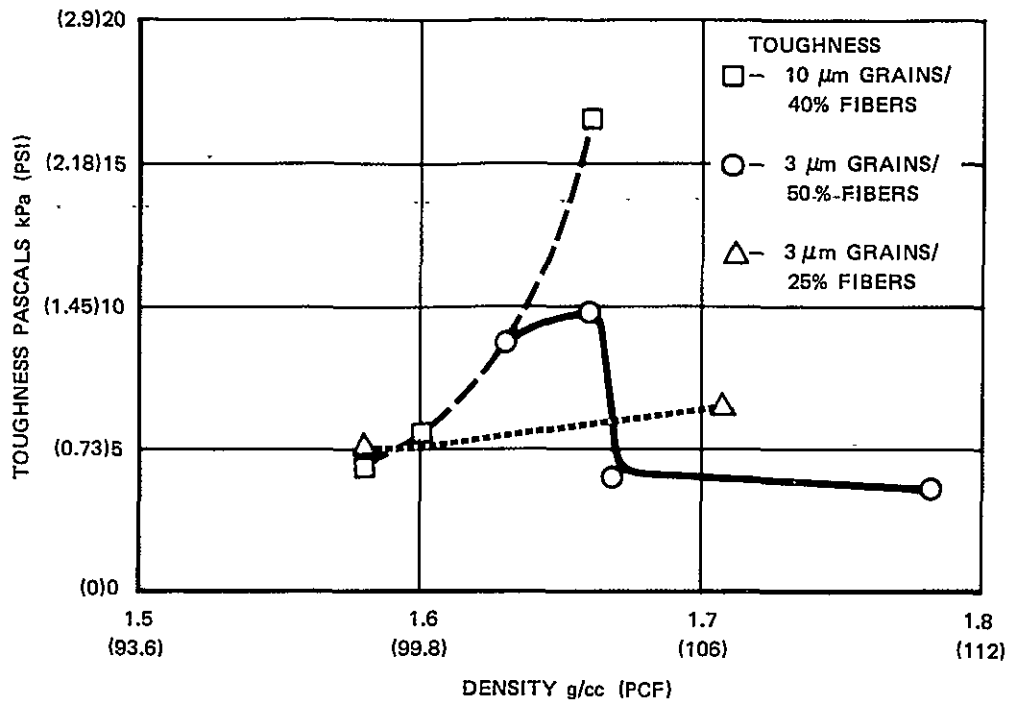
FIGURE 5.5—6 TOUGHNESS OF SLIP CAST 3 µm GRAINS WITH
SUPRASIL FIBER REINFORCEMENT
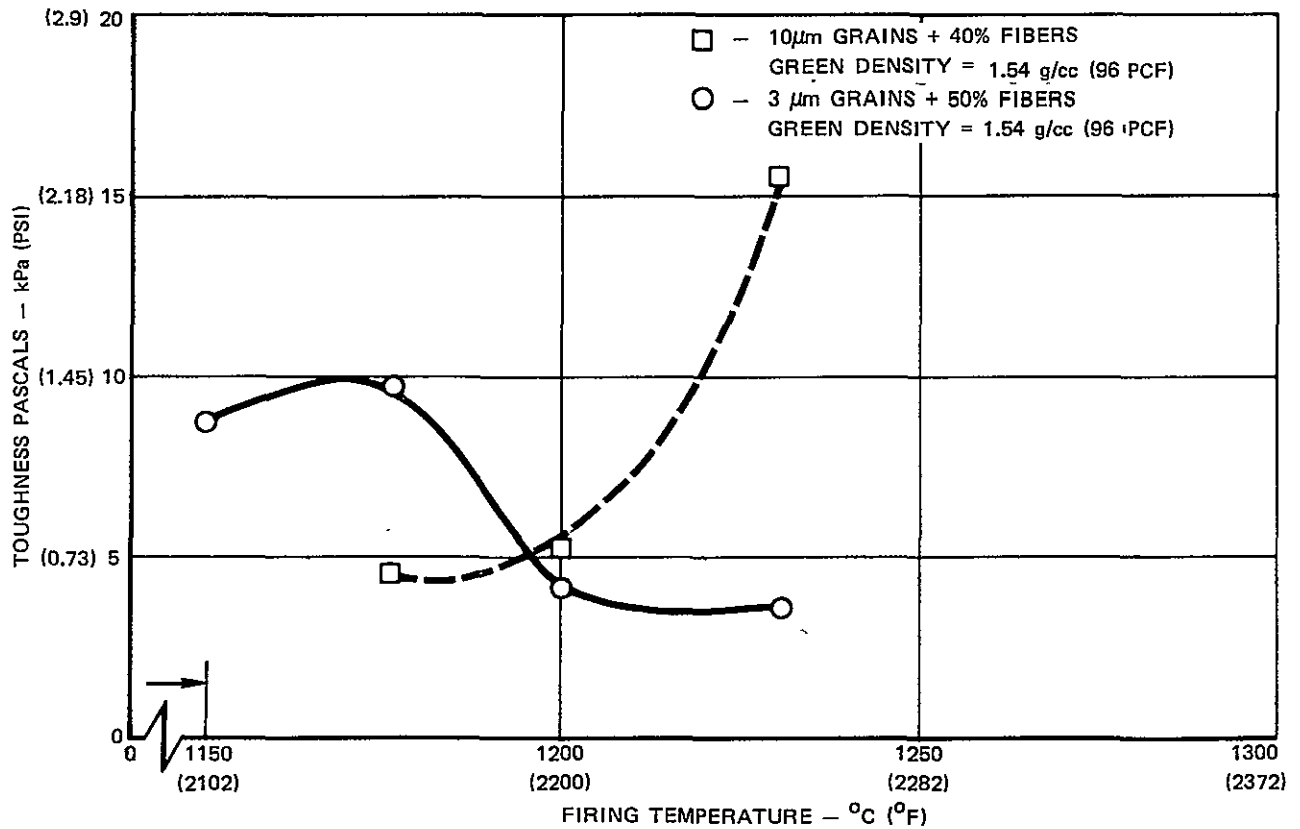
FIGURE 5.5—7 TOUGHNESS WITH RESPECT TO FIRING TEMPERATURE OF SLIP CAST 3µm
GRAINS & 10 µm GRAINS WITH SUPRASIL FIBER REINFORCEMENT

of the 10 µm grain/40% fiber and the 3 µm grain/50% fiber systems. Also shown is the toughness of the 10 µm grain/40% fiber formulation for reference.

The toughness of the fiber reinforced slip cast hyperpure silica was not improved by the use of 3 µm average diameter grains at firing temperatures of 1200°C and above. The flexural strength and toughness of the 3 µm grain/50% fiber material peaks out at a 1175°C firing temperature. Firing of the 10 µm grain/40% fiber material at 1230°C yields a material of similar density as the 3 µm/50% fiber system fired at 1175°C (due to lower shrinkage) but a much higher toughness, as shown in Figure 5.5-7. The effect of the embrittlement of the finely divided 3 µm grain material at the higher temperatures is shown clearly in Figure 5.5-7.

5.6 HYPERPURE GRAINS 5.5 µm/SUPRASIL FIBERS REINFORCEMENT

In an effort to find the optimum grain size for fiber reinforced hyperpure slip cast fused silica, a suspension of 5.5 µm average diameter grains was prepared. The particle size distribution of this suspension is shown in Figure 5.6-1.
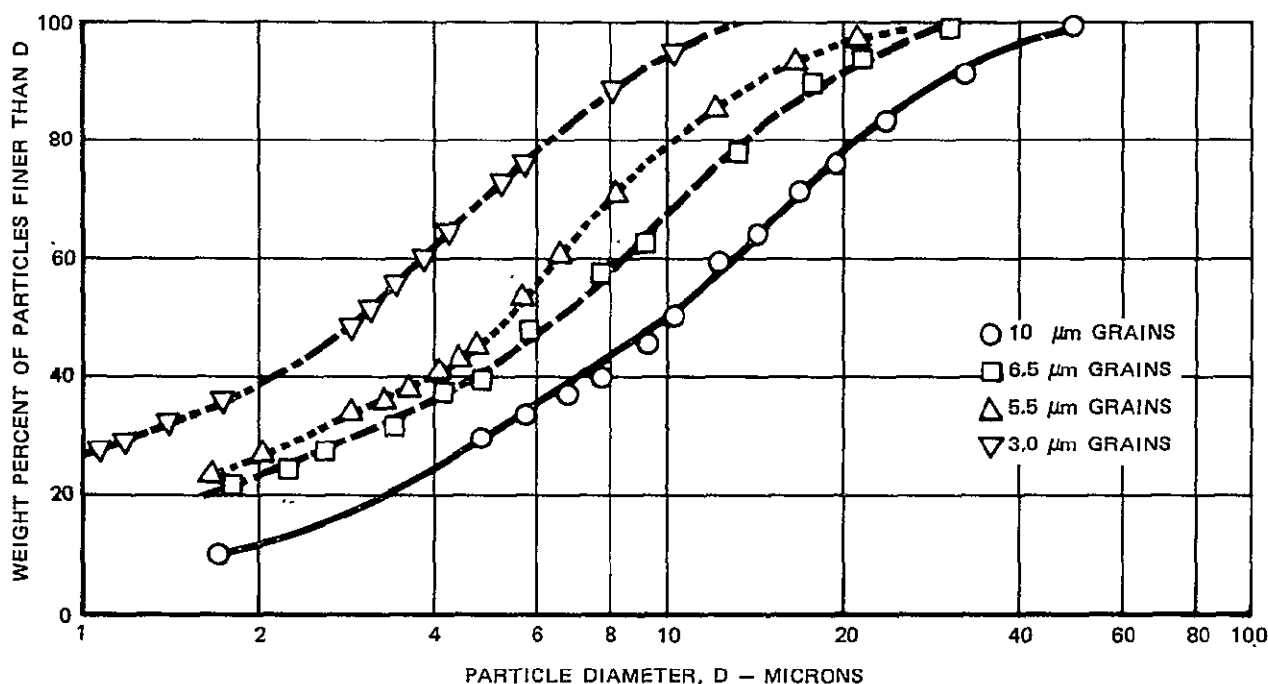
FIGURE 5.6-1 PARTICLE SIZE DISTRIBUTIONS OF VARIOUS GRAIN SUSPENSIONS

Dispersed fiber casting slips were prepared with the 5.5 µm material having fiber concentrations of 0%, 25%, and 50% of the total solids weight. The 5.5 µm grain slip without fibers was typically thixotropic and cast to a green density of 1.41 g/cc when used at 76% solids content. The 25% fiber slip retained the thixotropic qualities and was also used at 76% solids and cast to a density of 1.47 g/cc. The 50% fiber slip was observed to be very dilatant and cast to a

green density of 1.62 g/cc when used at 77.5% solids. Specimens were cast to this density and then the pH of the slip was lowered (from 3.7 to 3.4) to produce a thixotropic material, as shown in Figure 5.6-2. The solids content was maintained at 77.5% and specimens were cast having a green density of 1.41 g/cc.

Figure graph: APPARENT VISCOSITY - CPS (vertical axis, 10 to 10,000) vs NO. 1 SPINDLE SPEED — RPM (horizontal axis, 0.1 to 60). Labels: "77.5% SOLIDS PH = 3.4 CAST TO GREEN DENSITY OF 88 (PCF)" and "77.5% SOLIDS PH = 3.7 CAST TO GREEN DENSITY OF 101 (PCF)".
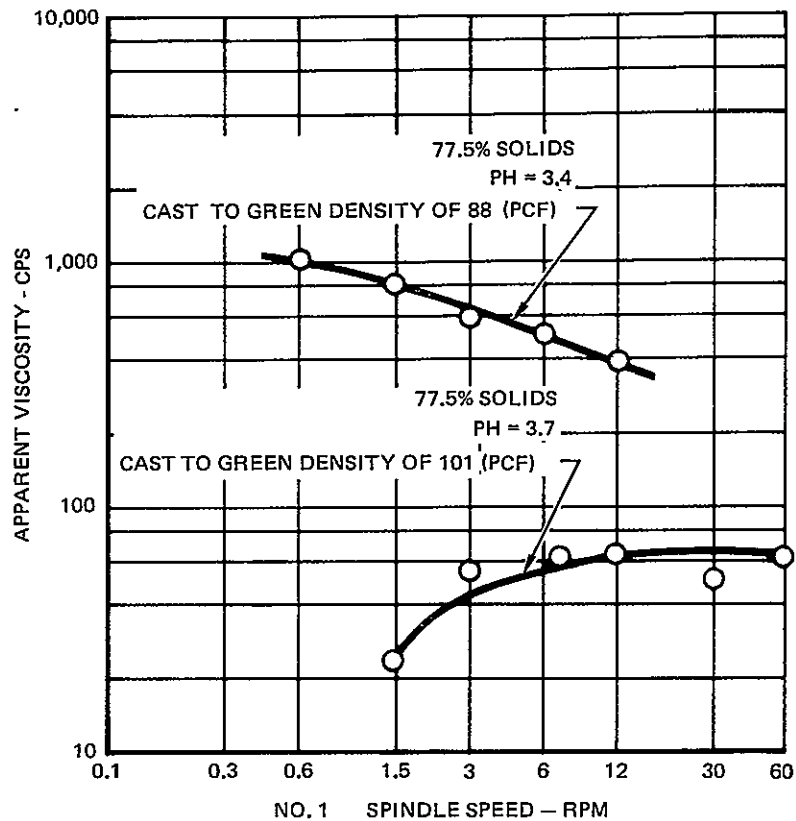
FIGURE 5.6—2 RHEOLOGY OF HYPERPURE SILICA SLIP WITH 5.5 μm GRAINS AND 50% FIBER REINFORCEMENT

Test bars ~1.25 x 1.25 x 10 cm for flexural tests were cast from 100% 5.5 μm grains and fired at 1175°C and 1200°C. Samples from the 25% fiber formulation were also fired at 1175°C and 1200°C. Firing temperatures of 1150°C and 1200°C were selected for samples cast from the 50% fiber - dilatant formulation (1.62 g/cc green density). The 50% fiber-thixotropic slip castings were fired at 1200°C and 1230°C. The resulting firing shrinkage and fired density data are shown in Figures 5.6-3 and 5.6-4.

The results of the strengh testing of the fiber reinforced 5.5 μm grain materials are shown in Figures 5.6-5 through 5.6-8. The rather large differences in green density and shrinkage of the materials makes the data difficult to interpret when plotted against either the single variable density or firing temperature. The toughness is therefore shown with respect to density in Figure 5.6-7 and firing temperature in Figure 5.6-8.
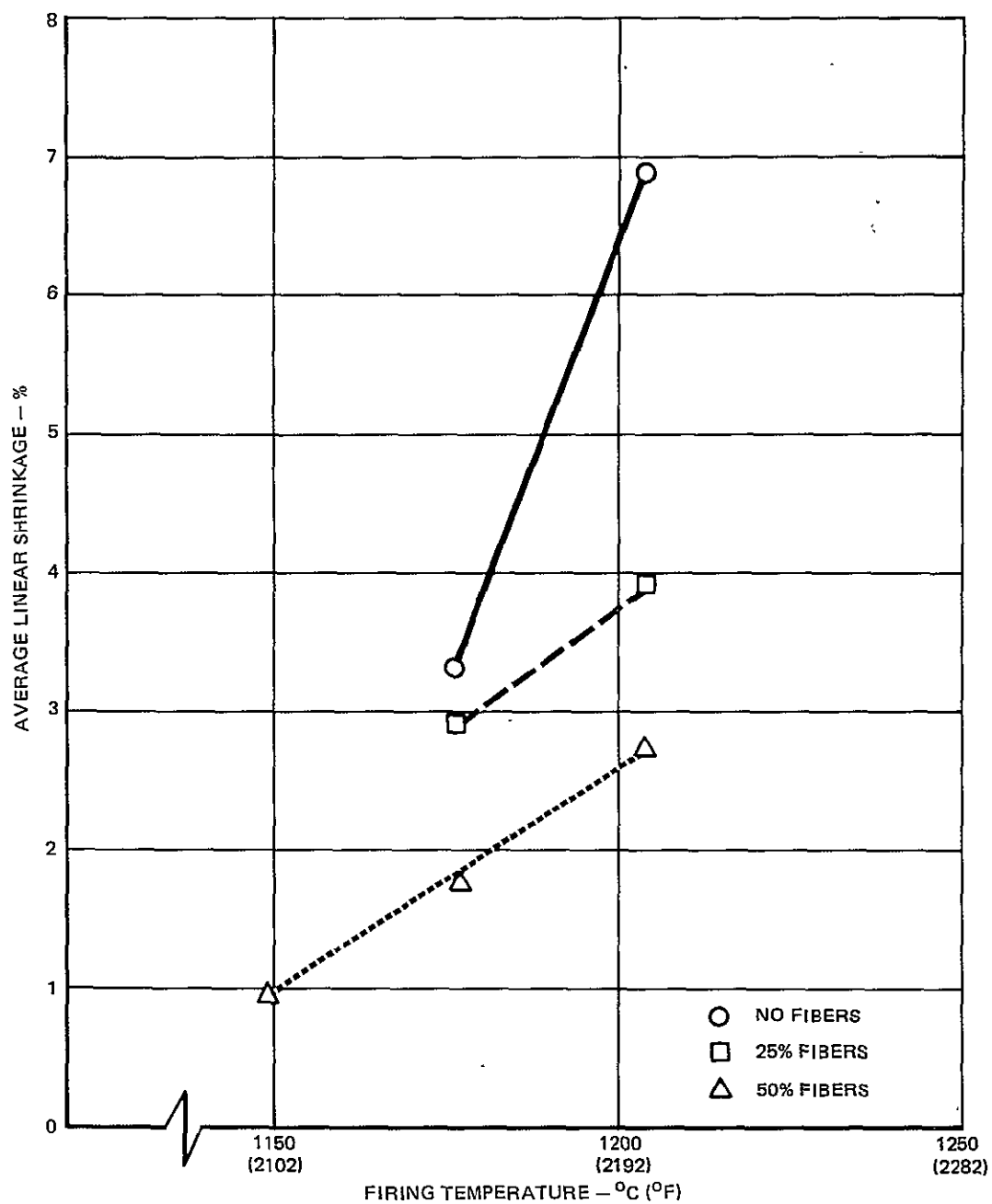
FIGURE 5.6–3 FIRING SHRINKAGE OF SLIP CAST 5.5 μGRAINS WITH FIBER REINFORCEMENT
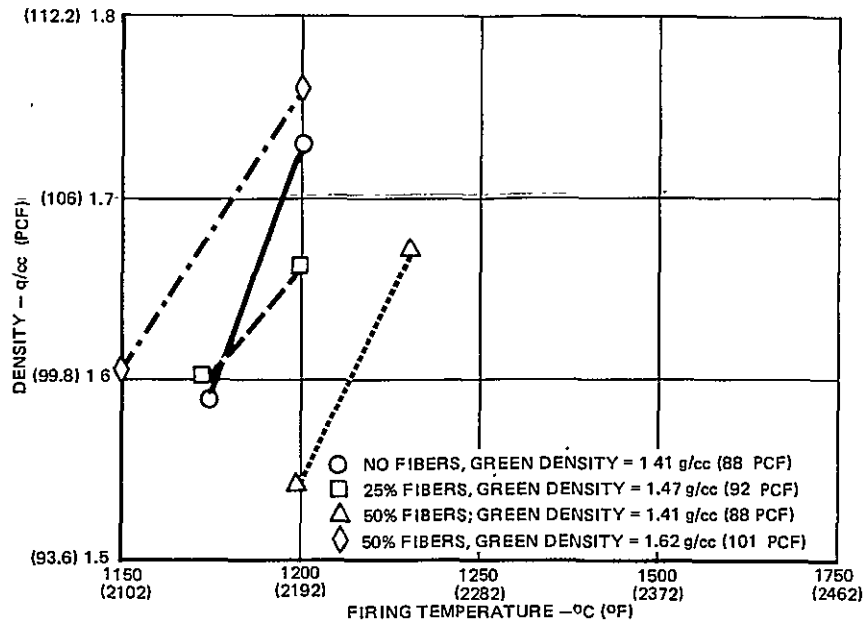
FIGURE 5.6—4 FIRED DENSITY OF SLIP CAST 5.5μ GRAINS
WITH FIBER REINFORCEMENT

Legend for Figure 5.6—4:
- ○ NO FIBERS, GREEN DENSITY = 1 41 g/cc (88 PCF)
- □ 25% FIBERS, GREEN DENSITY = 1.47 g/cc (92 PCF)
- △ 50% FIBERS; GREEN DENSITY = 1.41 g/cc (88 PCF)
- ◇ 50% FIBERS, GREEN DENSITY = 1.62 g/cc (101 PCF)

Legend for Figure 5.6—5:
- ○ NO FIBERS
  GREEN DENSITY = 1.41 g/cc (88 PCF)
- □ 25% FIBERS
  GREEN DENSITY = 1.42 g/cc (92 PCF)
- △ 50% FIBERS
  GREEN DENSITY = 1.41.g/cc (88 PCF)
- ◇ 50% FIBERS
  GREEN DENSITY = 1.62 g/cc (101 PCF)

FIGURE 5.6—5 FLEXURAL STRENGTH OF SLIP CAST 5.5 μm GRAINS WITH FIBER REINFORCEMENT

88

C — R

FIGURE 5.6—6 FLEXURAL MODULUS OF SLIP CAST 5.5 μm
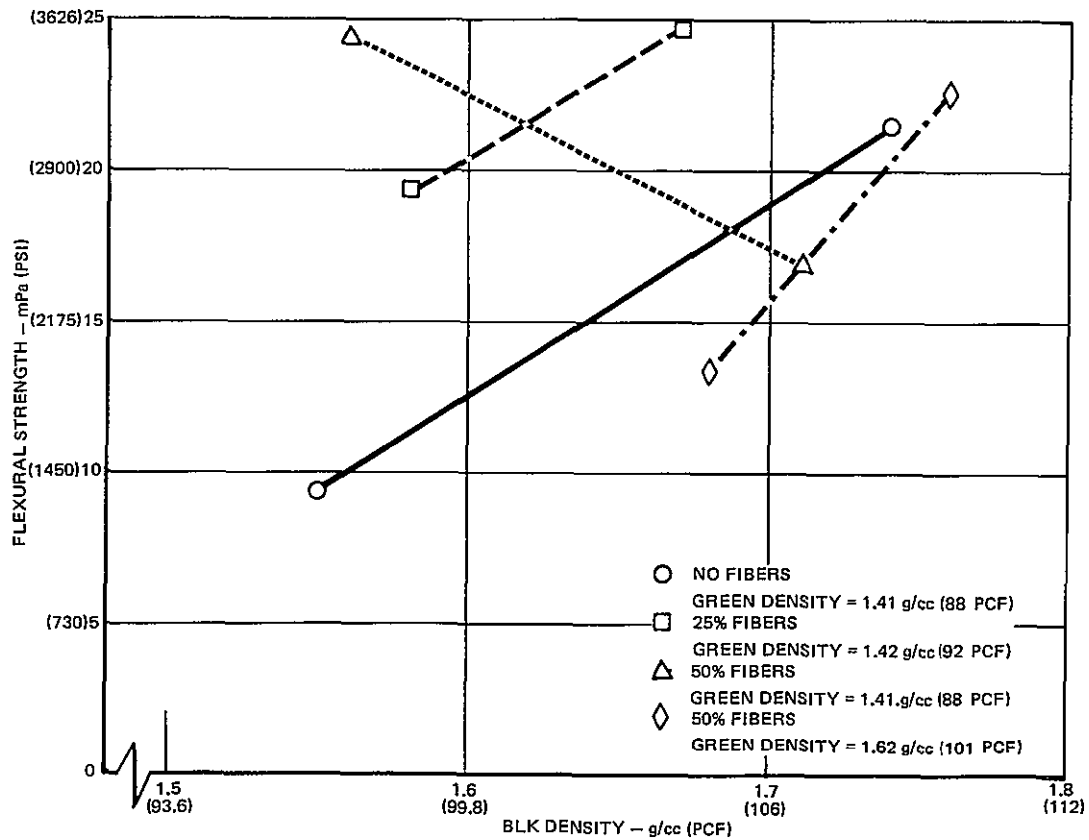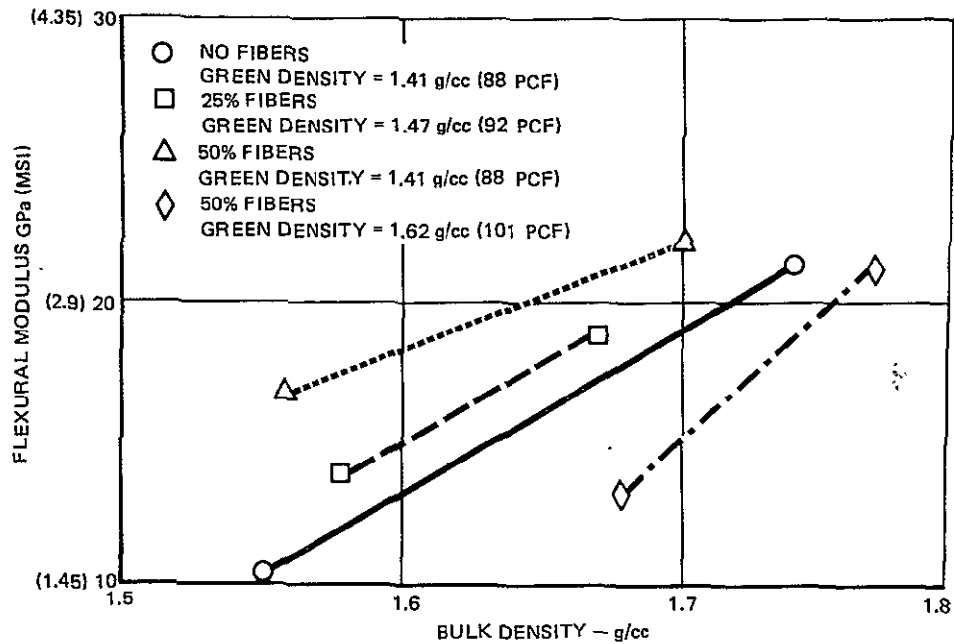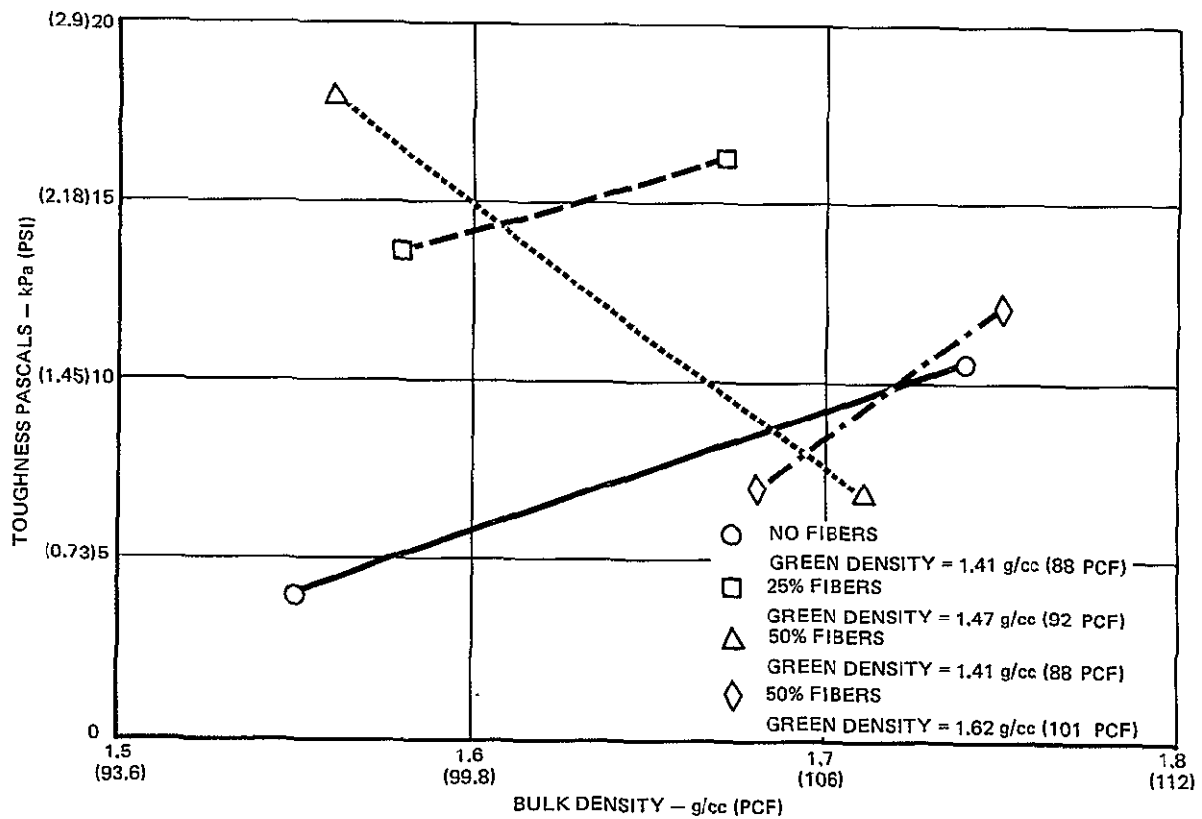GRAINS WITH FIBER REINFORCEMENT

FIGURE 5.6—7 TOUGHNESS WITH RESPECT TO DENSITY OF SLIP CAST
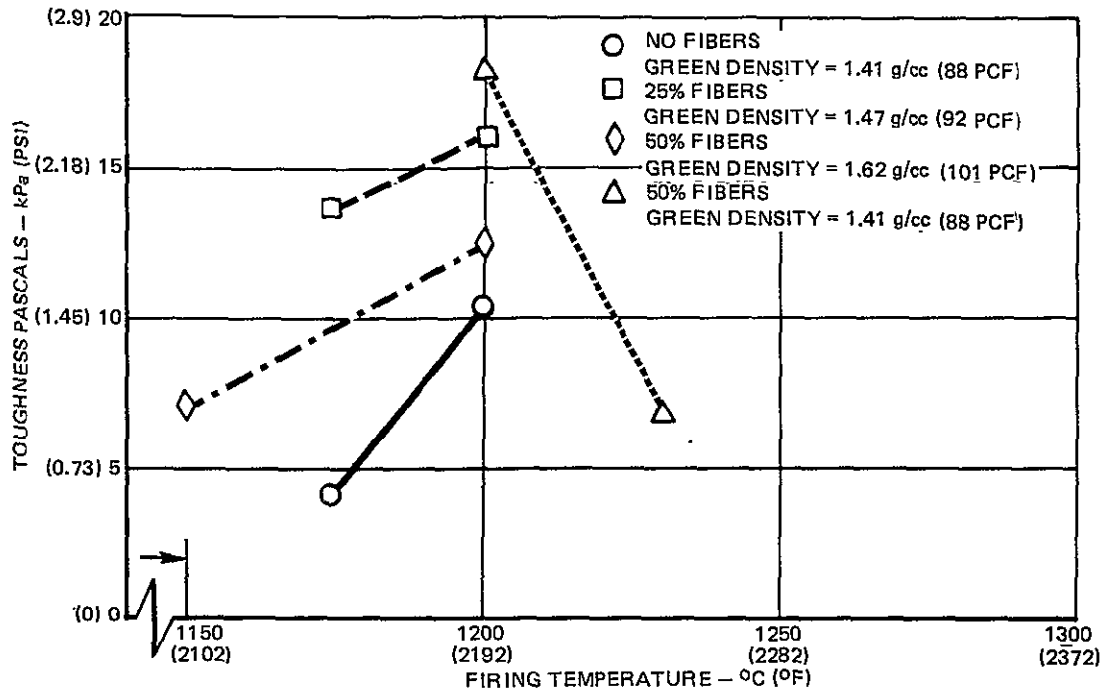5.5 μm GRAINS WITH FIBER REINFORCEMENT

FIGURE 5.6—8 TOUGHNESS WITH RESPECT TO FIRING TEMPERATURE OF SLIP CAST 5.5 μm GRAINS WITH FIBER REINFORCEMENT

Apparently the toughness of the 5.5 μm grain materials begins to degrade at firing temperatures above 1200°C in a similar manner to the 3 μm grain materials above 1175°C firing temperatures. This degradation will be described and discussed more fully in Section 5.8 which summarizes all of the strength results.

It appears from the toughness data that samples cast from slips which are thixotropic tend to have superior properties to materials cast with dilatant slips. The toughness of the 25% fiber reinforced material is higher than that of the 50% fiber (1.62 g/cc green density) material cast with dilatant slip. Previous results have indicated that the higher fiber concentrations generally provide tougher materials. Also, the higher density of these 50% fiber samples are expected to result in a higher toughness. The thixotropic nature of the 25% fiber slip resulted in more uniform castings and therefore superior strength results. This theory is supported by the results of the specimens cast with the thixotropic 50% fiber slip which were fired at 1200°C. The density of the specimens cast with the 50% fiber reinforced thixotropic slip was 15% less than the specimens cast with the 50% fiber reinforced dilatant slip, 1.54 versus 1.62 g/cc. The toughness, however, of the more uniformly cast specimens from the thixotropic slip was over 50% higher than specimens cast from the identical slip which was dilatant (17.9 kPa versus 12.2 kPa). It is important that both of these specimen groups were cast from the same batch of material, the only change being a slight adjustment in the pH.

Reflectance specimens were cast from the 50% fiber reinforced thixotropic slip and fired at the apparently optimum temperature for toughness of 1200°C. The resulting data is shown in Figure 5.6-8. The reflectance of this material is about 5% less in the extreme low wavelength regions than the reflectance for 10 μm grain material (Figure 5.3-9).

90

100X   300X   3000X

FIGURE 5.6—9   MICROSTRUCTURE OF SLIP CAST HYPERPURE 5.5 μm GRAINS WITH 50% FIBER REINFORCEMENT

SEM photographs showing the microstructure of the 50% fiber reinforced thixotropic slip cast material fired 5 hours at 1200°C are shown in Figure 5.6-9.

5.7   HYPERPURE GRAINS 6.5 μm/SUPRASIL FIBERS REINFORCEMENT

It was clear from the above data that the firing temperature of the 50% fiber reinforced 5.5 μm grain material needed to be optimized. It also seemed advisable to make a small change in the grain size in order to further optimize this variable. Accordingly, a 6.5 μm average grain size suspension was prepared and used to formulate a 50% fiber reinforced casting slip. Only one fiber concentration was used in order to concentrate the effort on the firing temperature variable.

Before any castings were poured, the fiber reinforced slip was adjusted in pH to be thixotropic. Castings which were prepared from this slip at 73% solids had green densities of $\sim$ 1.31 gm/cc ($\sim$ 82 lb/ft^3). The strength results for these specimens were poor as will be discussed below. Therefore, a similar batch of 50% fiber reinforced slip was prepared, made thixotropic and used for casting at 76.5% solids. The resulting specimens had a green density of $\sim$ 1.38 gm/cc. An additional set of specimens were vibration cast from this slip which yielded a green density of $\sim$ 1.41 gm/cc. The low green density $\sim$1.31 gm/cc specimens were fired at temperatures ranging from 1120°C (2050°F) to 1260°C (2300°F). The specimens of higher green density were fired at temperatures ranging from 1175°C (2150°F) to 1245°C (2275°F). The firing shrinkage and density data are shown in Figures 5.7-1 and 5.7-2.

91
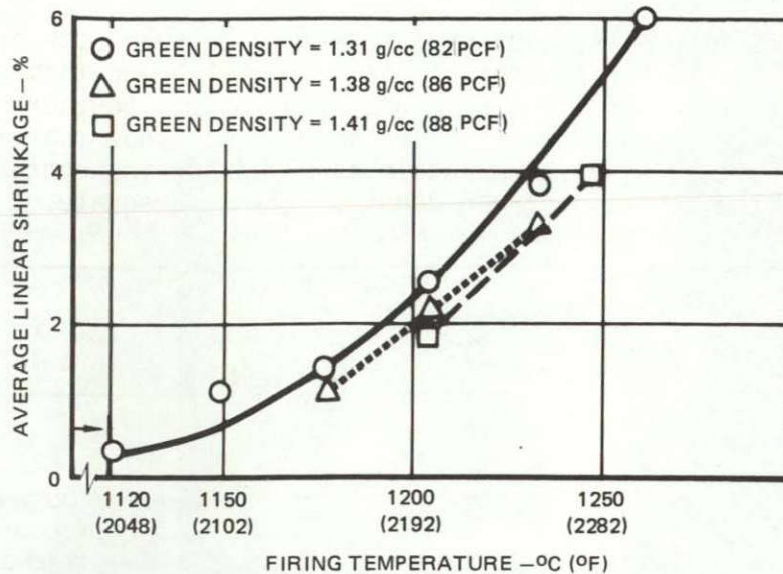
FIGURE 5.7—1 FIRING SHRINKAGE OF SLIP CAST 6.5μ GRAINS WITH 50% FIBER REINFORCEMENT
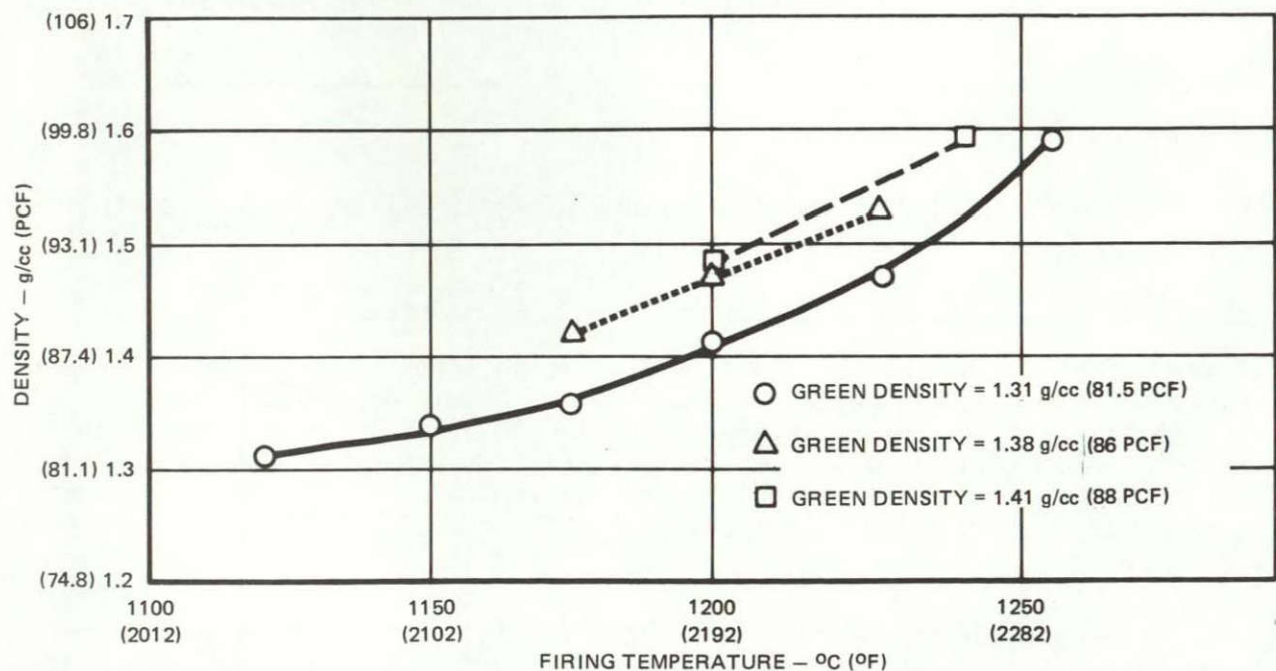
FIGURE 5.7—2 FIRED DENSITY OF SLIP CAST 6.5μ GRAINS WITH 50% FIBER REINFORCEMENT

Strength test results are shown in Figures 5.7-3 thru 5.7-5. Results are not shown for the specimens fired at 1120°C (2050°F) and 1150°C (2100°F). Testing of these groups was discontinued when the first specimen indicated the strengths were very low. The specimens which had the high green densities (1.38 gm/cc and 1.41 gm/cc or 86 PCF and 88 PCF, respectively) are shown as a single group with an average green density of 1.39 gm/cc (87 PCF). The test results indicate that the 50% fiber reinforced 6.5 μm grains may be fired up
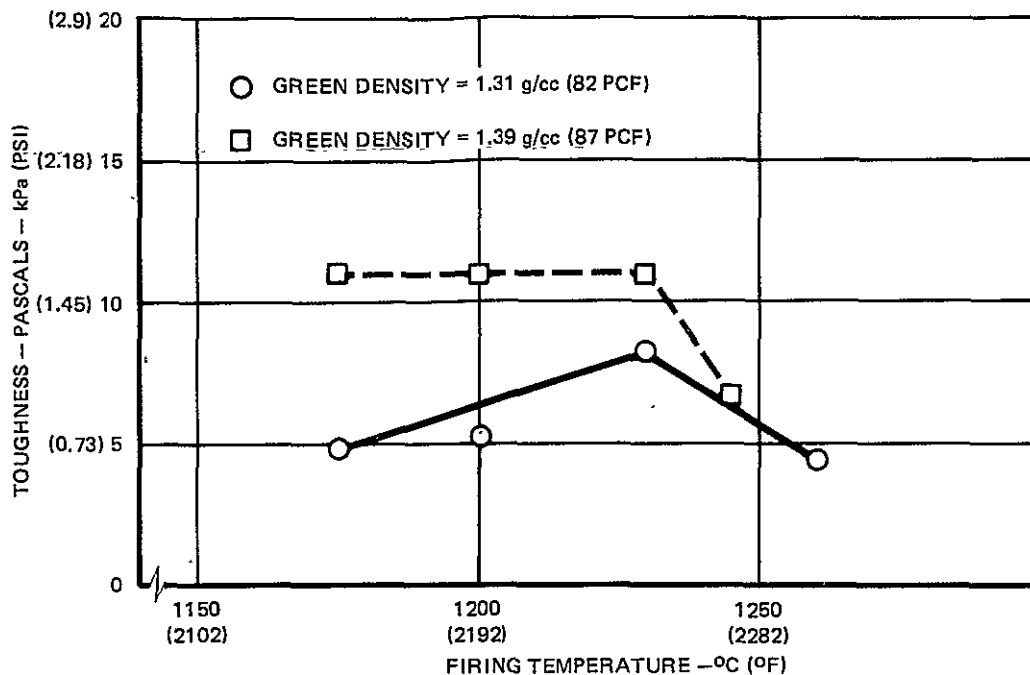
FIGURE 5.7–5 TOUGHNESS WITH RESPECT TO FIRING TEMPERATURE OF SLIP CAST 6.5 μm GRAINS WITH 50% FIBER REINFORCEMENT

5.8 SUMMARY OF STRENGTH IMPROVEMENTS RESULTS

The redirected goal of this program was to develop a tougher high reflective fused silica heat shield material which could be slip cast by conventional techniques. The concept of adding chopped fibers as a reinforcement for the hyperpure material was established and toughness improvements of 170% were obtained. It was determined that very high purity ($\leq$ 1 ppm total metal impurities) silica fibers were required for firing temperature >1204°C (2200°F) to achieve high strength without devitrification.

The initial fiber dispersed slips were prepared with the standard 10 μm average diameter hyperpure grains developed for slip casting. It was established that fiber reinforced slips with approximately 50% weight fibers provided an increase in toughness without presenting any processing problems during slip casting. In an effort to optimize the toughness of the fiber/grain material combination, various finer (<10 μm) grain sizes were evaluated. Particle size distribution curves for four different grain size distributions which were included in the evaluation are shown in Figure 5.6-1.

A large decrease in the drying and firing shrinkage occurred for all the fiber reinforcement grain mixtures. Firing shrinkage of the slip cast grains without fiber reinforcement having approximately 25% and 50% fiber reinforcement are shown in Figures 5.8-1, 5.8-2, and 5.8-3, respectively. The main variables controlling the shrinkage at a given firing temperature, were grain size and fiber concentration.

94

The use of finer grain materials did result in increased toughness at the lower firing temperatures due to improved sintering. The toughness of 50% fiber reinforcement material of various grain sizes fired at different temperatures is shown in Figure 5.8-4. Except for the 10 μm grains/40% fibers, the toughness of all these materials degraded at the higher firing temperatures. The firing temperature above which the material toughness decreased is generally proportional to the grain size, i.e., lower grain sizes degraded at lower temperatures. This effect, shown in Figure 5.8-5, may be due to embrittlement from sintering and/or from devitrification promoted by the very fine and highly reactive grains. The devitrification of fused silica is known to be promoted by increased surface area (Reference 2). The amount of devitrification, if any, in these materials could be evaluated by x-ray diffraction techniques as discussed in Reference 1. A study of this phenomina was beyond the scope of this program.

The fiber/grain material system with the most improved toughness is the 5.5 μm grain with 50% Suprasil fibers reinforcement, fired at 1200°C. The fiber dispersed 5.5 μm grain slip must be thixotropic in order to achieve a green density of 1.41 g/cc and a fired density of 1.55 g/cc. Figure 5.8-6 compares the toughness of this material to other candidate hyperpure silica slip cast materials of similar density and/or firing temperature.
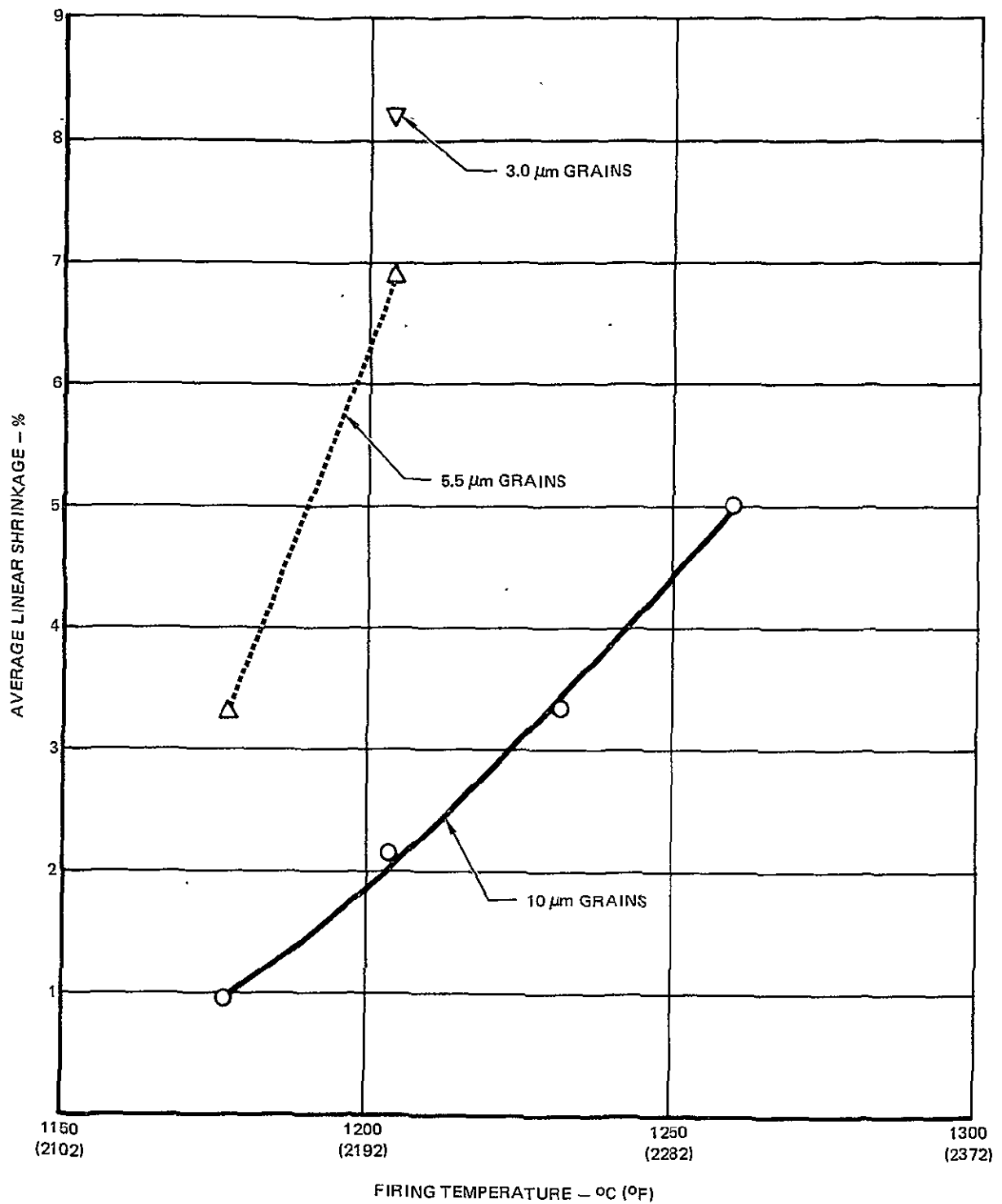
FIGURE 5.8–1 FIRING SHRINKAGE OF VARIOUS SIZE HYPERPURE SLIP CAST GRAINS WITHOUT FIBER REINFORCEMENT

96
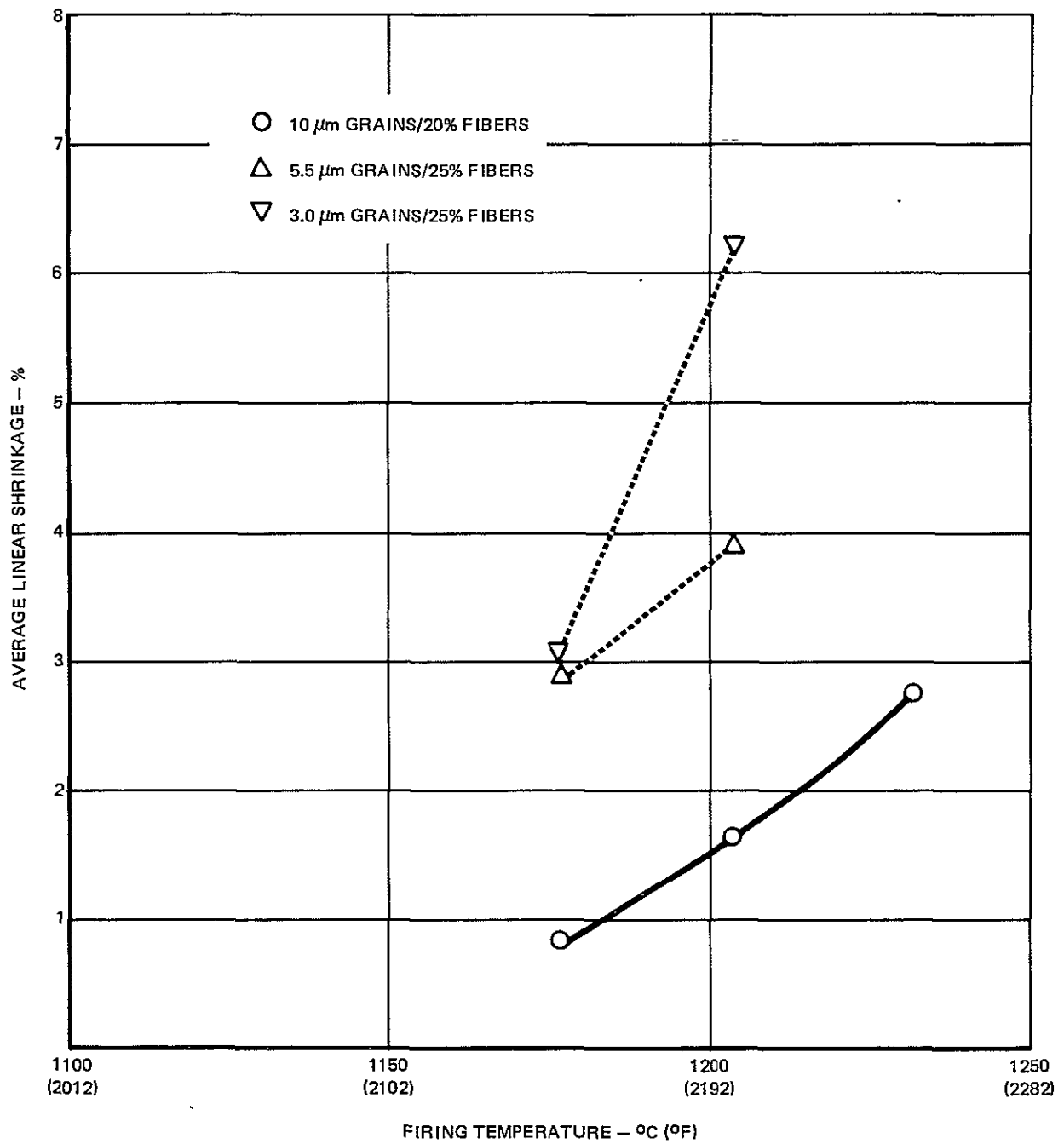
FIGURE 5.8–2 FIRING SHRINKAGE OF VARIOUS SIZE SLIP CAST
GRAINS WITH 25% FIBER REINFORCEMENT
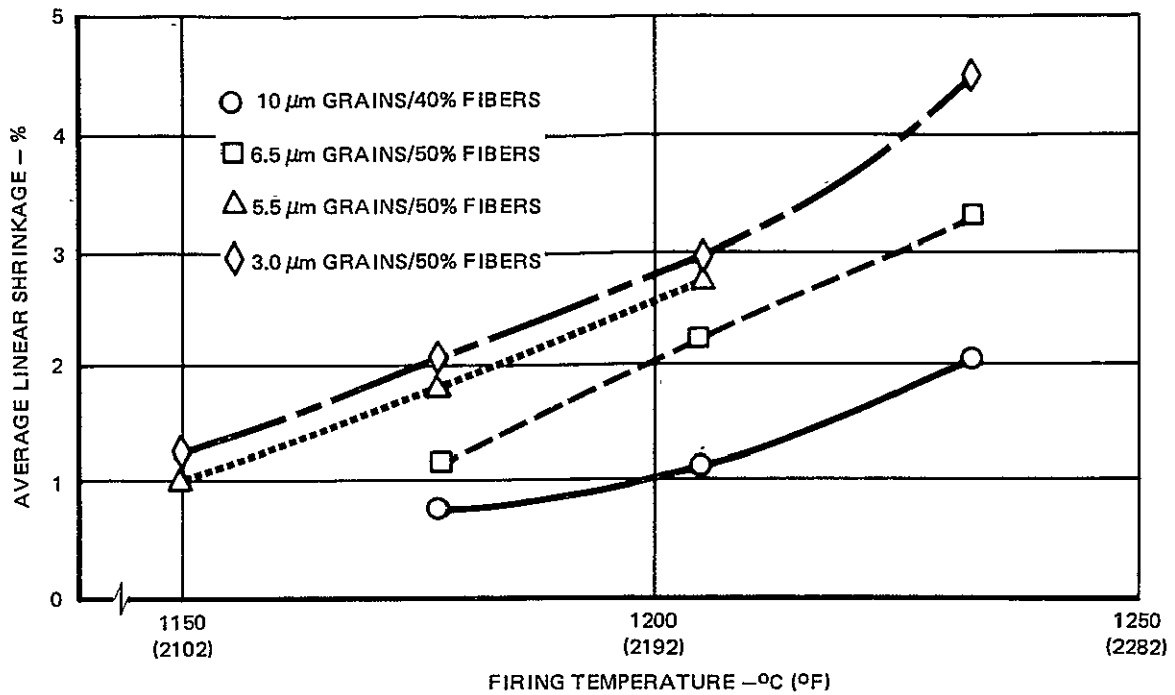
FIGURE 5.8–3 FIRING SHRINKAGE OF VARIOUS SIZE SLIP CAST
GRAINS WITH 50% FIBER REINFORCEMENT
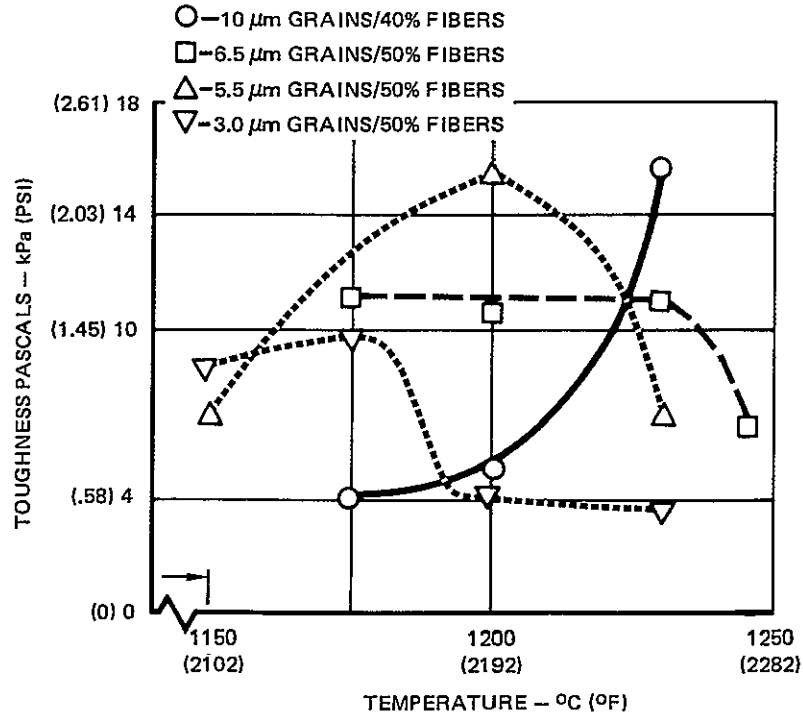
FIGURE 5.8–4 TOUGHNESS WITH RESPECT TO FIRING TEMPERATURE OF SLIP
CAST HYPERPURE GRAINS WITH 50% FIBER REINFORCEMENT
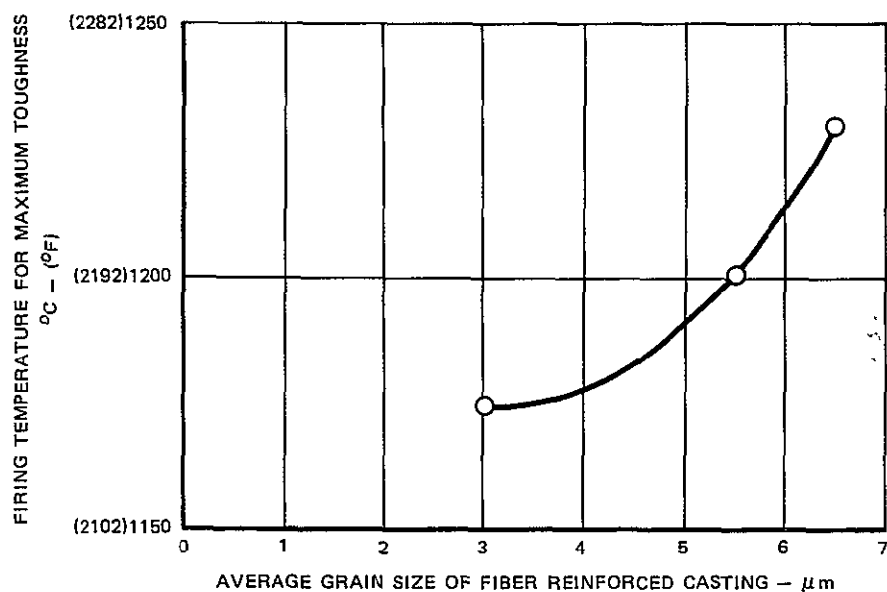
FIGURE 5.8—5 GRAIN SIZE EFFECT ON OPTIMUM FIRING TEMPERATURE
OF FIBER REINFORCED HYPERPURE SILICA

50% FIBER REINFORCED	AGGREGATE CAST	AGGREGATE CAST	STD. SLIP CAST
FIRED @ 1204°C (2200°F)	FIRED @ 1182°C (2150°F)	FIRED @ 1204°C (2200°F	FIRED @ 1204°C (2200°F)
DENSITY = 1.55 g/cc (97 PCF)	DENSITY = 1.55 g/cc (97 PCF)	DENSITY = 1.70 g/cc (106 PCF)	DENSITY = 1.59 g/cc (99 PCF)

FIGURE 5.8—6 TOUGHNESS OF HYPERPURE FUSED SILICA SLIP CAST MATERIALS

99

5.9 SUMMARY OF STRUCTURAL ANALYSES

As part of an MDAC-St. Louis Independent Research and Development (IRAD) activity, (Reference 6) additional efforts were directed toward the improvement and verification of our analytical modeling techniques to better predict structural performance of silica heat shield. After verification of the analytical modeling techniques, analytical model (SAAS III) of the silica heat shield was refined as shown in Figure 5.9-1.

FIGURE 5.9—1   AXISYMMETRIC STRUCTURAL MODEL WAS IMPROVED

Structural analysis of the silica heat shield was continued under IRAD with the aid of this improved SAAS III analytical model using the latest material properties presented in Figure 5.9-2. The results of this analysis determined the silica heat shield, Figure 5.9-3, is critical at peak deceleration with a maximum principal tensile stress of 28.3 MPa (4100 psi). This exceeded the allowable strength of 22 MPa (3200 psi). The critical stress is comprised of 30.8 MPa (4470 psi) mechanical and a -2.55 MPa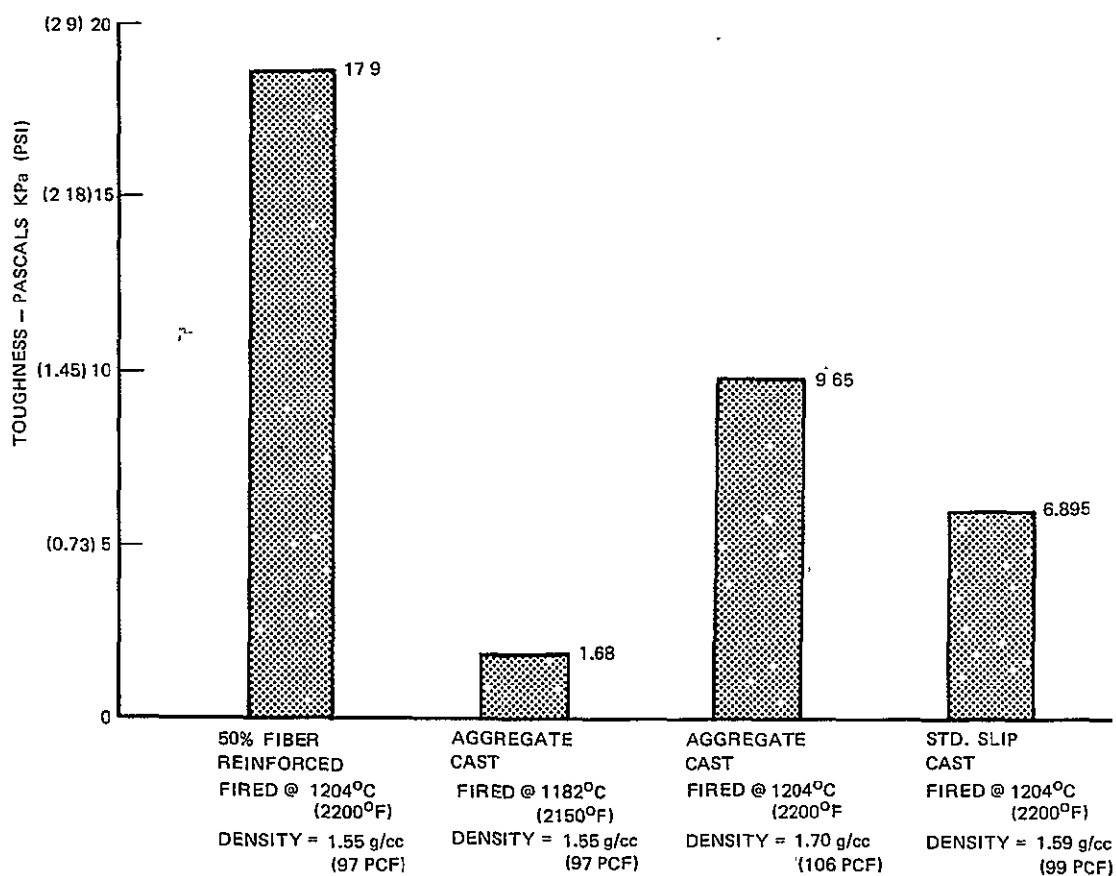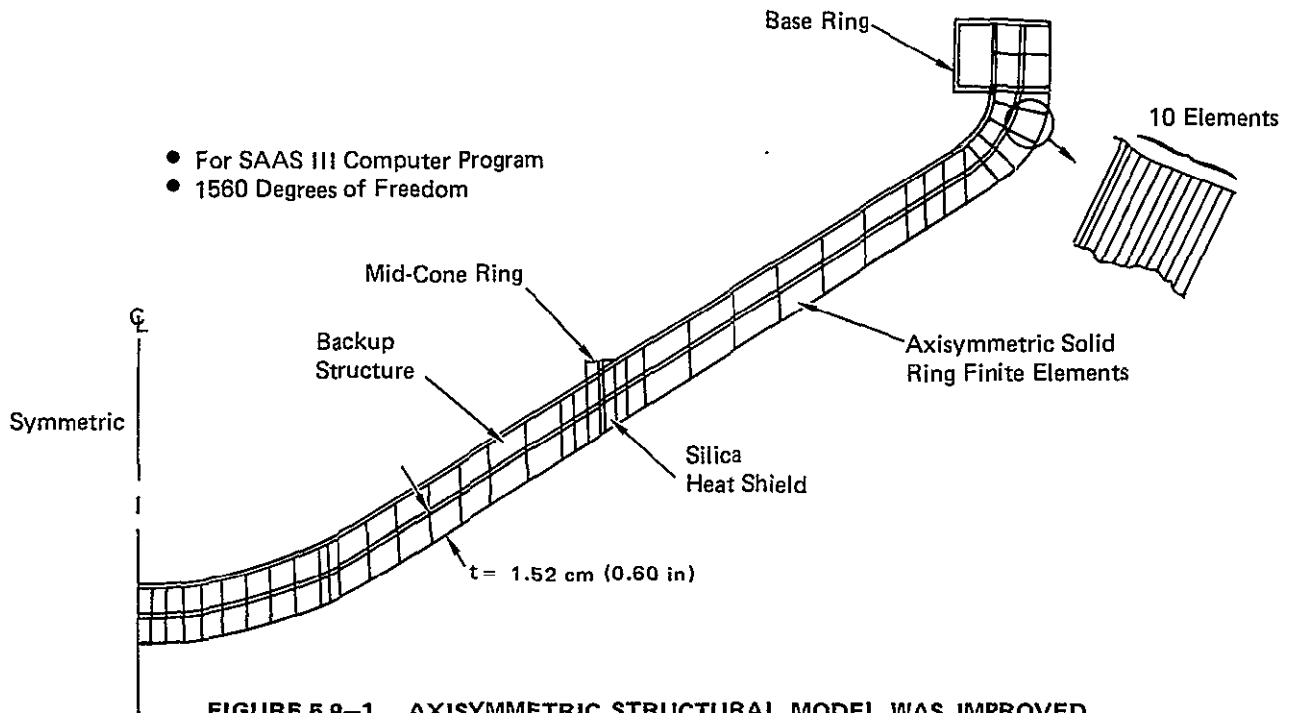 (-370 psi) thermal induced stresses. A plot of the maximum principal stress as a function of location on the heat shield is given as the dotted line in Figure 5.9-4. It was determined that by properly adjusting the probe structural stiffness the load distribution (P_1 and P_2, Figure 5.9-4) could be changed so that the silica heat shield design would show a positive margin of safety.

More recent structural analysis of silica heat shield with the current Jupiter probe backup structure indicates a maximum principal tensile stress of 41.9 MPa (6075 psi), which results from peak deceleration loads, is comprised of 44.4 MPa (6440 psi) mechanical induced stress and -2.52 MPa (-365 psi) thermal induced stress. This critical stress level of 41.9 MPa (6075 psi), which accounts for the nonuniform loading of the mid-cone ring determined by present analysis, signi-

ficantly exceeds (MS = -.47) the allowable strength of 22 MPa (3200 psi) for the material using silica grains reinforced with 50% fibers. Since aggregate silica without reinforcing fibers has even less allowable strength (MS = -.66), the silica heat shield development program has been evaluating methods of further increasing the strength and toughness of hyperpure silica heat shield material. Three dimensional (3-D) weaving of silica fibers shown in Figure 5.9-5 is scheduled for investigation. The 3-D woven silica heat shield material is recommended for further evaluation of fabrication processing and material characterization. A summary of mechanical property comparison of the three silica material formulations investigated is shown in Figure 5.9-6.

(ESTIMATED S VALUES)

Material	E_1 GPa (MSI)	E_2 GPa (MSI)	F_{TU_1} MPa PSI	F_{TU_2} MPa PSI	G 10^3 GPa (MSI)	F_{SU} MPa PSI	α $10^{-6}/^oC$ $10^{-6}/^oF$	ρ gm/ cm PCF	T^* KPa (PSI)	K Watts cm ^oK
Silica Grain +50% Fibers	16.69 2.42	16.69 2.42	16.0 (2320)	16.0 (2320)	6.90 1.00	76.0 (11,000)	0.54 (0.30)	1.65 (103)	7.7 (1.13)	0.0048

*Toughness (Area Under Stress-Strain Curve)

FIGURE 5.9-2 HEAT SHIELD MATERIALS PROPERTIES

$$\frac{P_1}{P_1 + P_2} = 0.44$$

● Mechanical Stresses Predominate
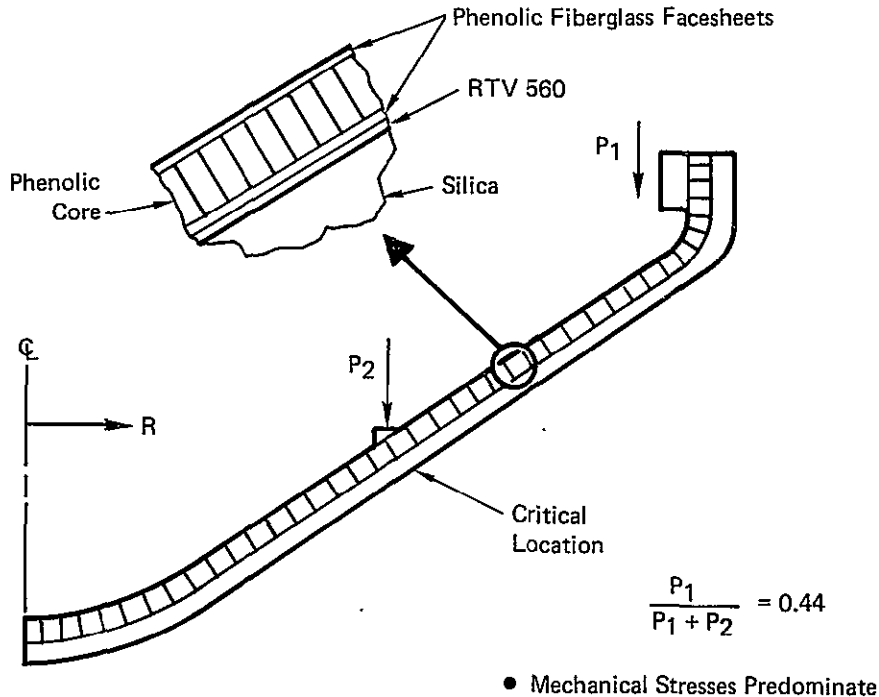
FIGURE 5.9-3   SILICA HEAT SHIELD CRITICAL AREA IDENTIFIED
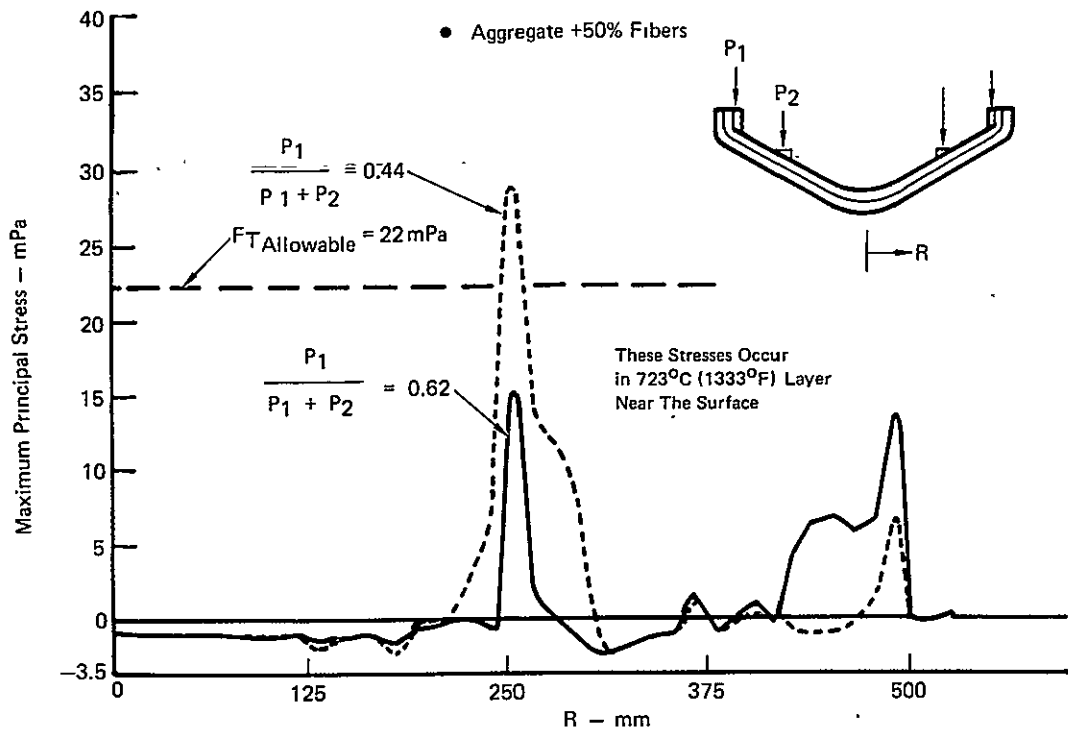
FIGURE 5.9—4 OPTIMUM LOADING OF SILICA HEAT SHIELD DETERMINED
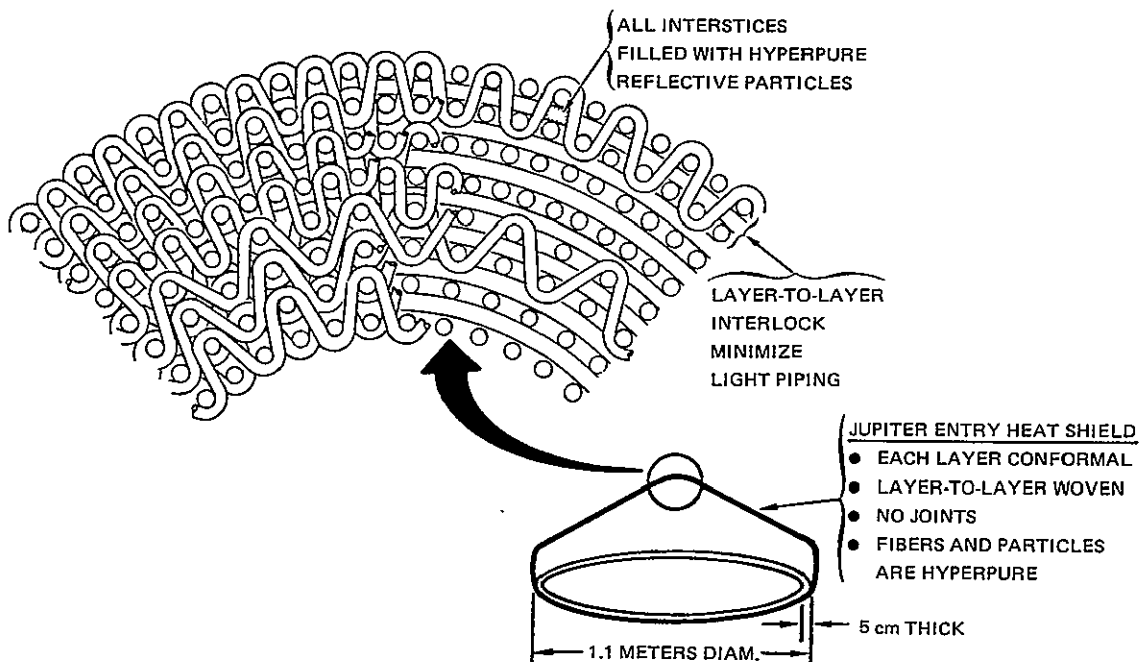
FIGURE 5.9—5 3D REINFORCED SILICA WEAVE PATTERN

Figure 5.9-6

Summary of Mechanical Property Comparison of Various Silica Materials

Material Formulation for Silica Heat Shield Fabrication	Flexural Strength MPa (KSI)	Flexural Modulus GPa (MSI)	Strain at Failure (%)	Material Toughness $10^3 \frac{m-n}{m^3}$ (in.-#/in.^{3})
Aggregate silica - no fiber reinforcement (baseline material)	13.3 (1.93)	14.3 (2.07)	0.093	6.62 (0.96)
Silica Grains with 50% reinforce fiber	23.8 (3.45)	15.8 (2.29)	0.150	17.9 (2.6)
3-D woven silica yarn densified with silica grains ⚠	44.1 (6.40)	14.1 (2.05)	0.313	69.0 (10.0)

⚠ Estimated values based on preliminary data.

6.0 CONCLUSIONS AND RECOMMENDATIONS FOR FUTURE WORK

This section contains the major conclusions of this program and the suggestions for future work for hyperpure silica reflective heat shield development and scale-up for the Jupiter Probe (Project Galileo).

The basic material conclusions based on the work performed during this program are as follows:

o The green strength of hyperpure silica castings increases by aging the hyperpure slip for 30 days after ball milling.

o The green strength of hyperpure silica castings is improved by increasing the very fine particles, <2 μm in a 10 μm average particle size slip.

o The addition of coarse aggregate particles (-40 mesh) in hyperpure silica slip (10 μm average particle size) results in a significant reduction in the drying and firing shrinkage of hyperpure silica castings.

o Large parts (>6 cm thick) cast from aggregate hyperpure silica slip can be processed without shrinkage cracks while nonaggregate containing hyyperpure silica castings of similar size develop severe shrinkage cracks.

o Aggregate hyperpure silica slip casts at a higher rate than nonaggregate hyperpure silica slip.

o The use of 15 weight percent of -40 mesh aggregate particles results in no decrease in reflectance of hyperpure silica castings at wavelengths as low as .225 μm.

o Milling efficiency was increased for 19 liters (5 gallons) milling containers versus 1.9 liter (1 gallon) milling containers.

o The 7.6 (2 gallon) and 19 liter (5 gallon) size milling containers result in silica slip which has thixotropic rheology after several days of aging.

o Hyperpure silica slips may be adjusted to be thixotropic or dilatant by lowering or raising the pH.

o Thixotropic hyperpure silica slip casts to an 8% lower green density than dilatant slip.

o Thixotropic slips reduce particle settling during slip casting.

o A high humidity drying cycle is required for thick (2.5 to 7.5 cm) slip cast silica heat shields to reduce shrinkage cracks.

o Aggregate casting of hyperpure fused silica has been scaled up to a
   one-half scale Jupiter Probe heat shield.

o Chopped high purity Suprasil fibers reinforcement for hyperpure silica
   results in a 2.5 psi increase in toughness and maintains a high
   reflectance.

o Astroquartz fibers are not a suitable reinforcing material for hyper-
   pure silica castings fired over 2200°F and for concentrations over 25%
   because of a strength reduction due to devitrification.

o Addition of up to 50% high purity silica fibers does not decrease
   reflectance of the 10 µm average grain size silica slip castings.

o Silica fiber reinforcement significantly lowers the drying and firing
   shrinkage of hyperpure castings.

o Fiber reinforced parts made from thixotropic slips have superior
   strength properties to those cast from dilatant slips.

o The use of finer mesh (< 5.5 µm average grain size) silica slip in fiber
   reinforced castings results in improved strength at lower firing temp-
   erature but a decrease in strength at higher firing temperatures.

o The most attractive fiber reinforced slip cast silica system for heat
   shield application is 5.5 µm average hyperpure grain size with 50%
   Suprasil fiber reinforcement fired at 1204°C (2200°F).

o Structural analyses, based on limited material property data, have
   revealed that the aggregate slip cast silica heat shield can survive a
   Jupiter entry with a safety factor of 1.25. It was desirable to have a
   higher margin of safety considering the brittleness of this material.

6.1 RECOMMENDATIONS FOR FUTURE WORK

This section contains recommendations for future work.

6.1.1 DEVELOPMENT OF FIBER REINFORCED SLIP CAST MATERIAL

As detailed in Section 5.8, the fiber reinforced slip cast material consisting
of 5.5 µm average grain size slip and 50% chopped Suprasil fibers is capable of
being scaled up. Very thick castings have been made with this material without
shrinkage cracks, and relatively thin-walled parts have been processed, indica-
ting adequate handling strength and resistance to deforming during drying and
firing.

It is recommended that the following steps be take to optimize the performance
of this material before final characterization and scale-up:

o Determine the effect of fiber length and diameter on processing, tough-
   ness, and reflectance. Suprasil fibers as small as 2 µm in diameter
   are available. Use of finer fibers could result in improved toughness.

o Further evaluate the effect of slip properties, i.e., solids content, pH and rheology, on unfired density and toughness of the fired material.

o Further evaluate and optimize the firing temperature from the standpoint of toughness.

o Measure the spectral absorption coefficients versus temperature for use in improved silica sizing analysis.

6.1.2 DEVELOPMENT OF 3D WOVEN SILICA DENSIFIED WITH SILICA GRAINS

A 3D woven silica structure would provide a heat shield material with a significant increase in strength and toughness. The toughness of 3D woven materials for antenna windows has been shown to be about 10 times that of slip cast grains with fiber reinforcement.

Recent in-house funded work has shown that suspensions of very fine (<1μm diameter) hyperpure silica grains may be prepared which have some colloidal properties and can be used to uniformly densify 3D woven silica structures by simple vacuum impregnation. The coarseness of the hyperpure silica material as compared to conventional silica colloids may be an advantage for reduced binder migration during drying.

A potential disadvantage of a 3D woven heat shield material densified with hyperpure silica grains is reduced reflective properties. This is because of the lower purity silica yarn used for weaving and because of transmission of energy from the surface into the material by light piping. However, the light piping problem may be minimized by using specially designed weave patterns in which the weaver yarns penetrate only one layer of the material thickness. Also, 3D weaving yarns may be fabricated from high purity Suprasil fibers at a cost increase.

The 3D woven approach needs to be developed by evaluating the following variables and properties:

o Weave patterns
o Yarn spacings
o Fiber purity
o Densification procedures
o Reflectance
o Transmission (light piping)
o Strength
o Toughness

6.1.3 SCALE-UP AND CHARACTERIZATION

Following evaluation of the 3D woven approach, either the fiber reinforced slip cast or the densified 3D woven material should be selected for final characterization and scale-up.

Final characterization would include:

o Plasma Arc Tests
o Mechanical Properties
o Physical Properties
o Thermal Properties
o Optical Properties

The scale-up of either of these approaches is necessary for full-scale heat
shield production. Much of the technology required for the fiber reinforced
slip casting has been developed during this program, but scale-up has not been
accomplished. Once it is established that three dimensional woven parts of the
required thickness can be uniformly impregnated, scale-up of this approach would
include fabrication of the required tooling.

7.0 REFERENCES

(1) Nachtsheim, P. R., Peterson, D. L., and Howe, J. T., "Reflecting Ablative Heat Shields for Radiative Environments," American Astronautical Socity, the 17th Annual Meeting, 28-30 June 1971.

(2) Blome, J. C., Drennan, D. N., Schmitt, R. J., High Purity Silica Reflective Heat Shield Development, Final Report, NASA CR 137617, October 1974.

(3) "High Purity Silica Reflective Heat Shield Development - High Temperature Reflectance and Strength Properties," Final Report, NASA CR 152118 May 1978 NAS 2-7897.

(4) Harris, J. N., and Welsh, E.A., Fused Silica Design Manual, Volumes I and II, Georgia Institute of Technology, Atlanta, Georgia, May 1973.

(5) Whiteside, E. L., "Quality Control in the Plaster Mold Shop," American Ceramics Society Bulletin, 4, No. 11, November 1966, pp 1022-1026.

(6) Independent Research and Development Project Number 72280 titled, "Heat Shield Integrity in Planetary Entry Environments", Dated 12 January 1978.